PETROLEUM RECOVERY INSTITUTE

TWO- & THREE- PHASE RELATIVE PERMEABILITY AT ELEVATED TEMPERATURES IN HEAVY OIL SYSTEMS

BY

BRIJ B. MAINI

PETROLEUM RECOVERY INSTITUTE

CALGARY, ALBERTA

SEPTEMBER 1989

TWO- and THREE- PHASE RELATIVE PERMEABILITY AT ELEVATED TEMPERATURES IN HEAVY OIL SYSTEMS

(Part of Energy Mines and Resources 50/50 Cost-Shared Energy Conversion Program and part of the Program of the Federal Panel on Energy R &D (PERD)

by:

Brij B. Maini
Petroleum Recovery Institute
Calgary, Alberta

Work on the project was conducted under the auspices of the Canada Centre for Mineral and Energy Technology, Energy, Mines and Resources Canada.

DSS File No. 030SQ.23440-8-9019
DSS Contract Serial No. 23440-8-9019/01-SQ
CANMET Scientific Authority: Dr. K.N. Jha

126 pp

September 1989

Table of Contents

	Page
Executive Summary	iii
Sommaire	iv
Nomenclature	v
Introduction	1
References	7
Part I. Two-Phase Relative Permeabilities	8
1. Objectives	9
2. Experimental Equipment and Procedure	10
3. Calculation of Relative Permeability from Displacement Data	11
4. Results and Discussion	12
4.1. Effect of Flow Rate on Relative Permeability Measurements by the Displacement Technique	12
4.1.1. Measurements at Room Temperature	12
4.1.2. Measurements at 100°C	15
4.1.3. Measurements at 200°C	16
4.2. Comparison of Steady-State and Unsteady-State Relative Permeability	17
4.3 Effect of Viscosity on Relative Permeability Measurements by the Displacement Technique	19
5. Conclusions	20
References	21
TABLES AND FIGURES FOR PART I.	
Part II. Three-Phase Relative Permeabilities	22
1. Objectives	23
2. Review of Three-phase Relative Permeability Techniques	24

2.1. Steady-State Methods 24

2.1.1. Capillary Pressure (Hassler) Method 26
2.1.2. Dynamic (Penn-State) Method 27
2.1.3. Use of High Flow Rates 28
2.2.4. Use of Long Cores 28

2.2. Unsteady-State Methods 28

2.3. Centrifuge Method 29

3. Experimental Equipment and Procedure 30

4. Results 33

4.1. Water Relative Permeability 34

4.2. Gas Relative Permeability 35

4.3. Oil Relative Permeability 35

5. Correlations for Estimating Three-phase Relative Permeabilities 36

5.1. Modification of Stones Method I 39

6. Comparison with Experimental Data 41

6.1. New Experimental Data 41

6.2. Corey et al. (1956) Data 41

6.3. Data of Donaldson and Dean (1966) 42

6.4. Data of Saraf and Fatt (1967) 43

6.5. Data of Dalton et al. (1970) 44

6.6. Data of Saraf et al. (1982) 44

6.6. Data of Oak et al. (1988) 45

7. Conclusions 46

References 47

TABLES AND FIGURES FOR PART II

EXECUTIVE SUMMARY

This report presents the results of experimental research aimed at improving the understanding of two- and three-phase relative permeability characteristics of heavy oil systems. The work was done at the Petroleum Recovery Institute under a cost-shared contract with CANMET.

Part I of the report deals with two-phase relative permeability measurements. A series of tests were conducted to evaluate the effect of flow rate on measurements by the displacement technique at three different temperatures. It was found that the relative permeability measured by the displacement technique in viscous oil system is affected by the displacement velocity. A combination of capillary end effects and viscous instabilities appear to be responsible for this problem.

The unsteady-state measurements of relative permeability were compared with steady-state measurements in the same rock-fluid system. It was found that the two techniques can provide very different results. Since, viscous fingering is not a problem in the steady state tests, it appears to provide more reliable results.

To evaluate the effect of viscosity ratio, relative permeability measurements were carried out with mineral oils of different viscosities. It was shown that at lower oil/water viscosity ratios, where the displacements are likely to be stable, the relative permeability was not affected by the oil viscosity. However, when the oil viscosity became high, as would be the case with heavy oils, relative permeability was affected by the oil viscosity.

Part II presents the results of three-phase relative permeability work. Three-phase relative permeability measurements were carried out at 100°C temperature and 3.5 MPa pressure using the steady-state technique. The system used in these measurements comprised clean silica sand, a viscous mineral oil (500 mPa.s at 20°C), de-ionized water and nitrogen gas. The three-phase water relative permeability was a function of water saturation only. Similarly, the gas relative permeability was a function of gas saturation only. However, the oil relative permeability was found to vary with all three saturations.

Stone's method I and II predictions of oil relative permeability were compared with the experimental data and were found to be unsatisfactory. The correlation suggested by Stone's method I was modified to obtain a better fit of the experimental data.

Data from six other sources were selected to test the modified Stone's method I. In all cases the modified correlation provided a better fit of the data.

Sommaire

Cette étude présente les résultats d'une recherche expérimentale, ayant pour but d'améliorer la compréhension de la perméabilité relative des huiles lourdes en système à deux et trois phases. Cette recherche à été complétée par: Petroleum Recovery Institute dans le cadre d'une entente ou les coûts étaient partagés avec Canmet.

La partie I de l'étude consiste à mesurer la perméabilité relative en système à deux phases. Une série de testes fut conduite afin d'évaluer les effets du débit sur la perméabilité relative, en utilisant la technique de déplacement roche-fluide et ce à trois températures différentes. Ainsi on trouva que la perméabilité relative mesurée avec la technique de déplacement, et en présence d'une huile visqeuse, est affectée par la vélocité du débit. Les effets capillaires joints à une instabilitée visqeuse semblent être responsables de ce problème.

Les données de perméabilité relative mesurées pour un régime non-permanent sont comparées avec celles d'un régime permanent, en utilisant le même système roche-fluide. Les deux techniques laisse voir des résultats très différents. Ainsi, la cannalisation due au rapport de viscosité, ne présente pas de problème dans un système à régime permanent, et donne des resultats plus fiables.

Pour évaluer les effets de rapport de viscosité, des données de perméabilité relative sont obtenues en utilisant des huiles minérales avec des viscosités différentes. On peut ainsi démontrer que lorsque le rapport de viscosité huile/eau est bas, donnant des déplacements qui sont plus stables, la perméabilité relative n'est pas affectée par la viscosité de l'huile. Cependant, lorsque la viscosité de l'huile est plus importante, ce qui est le cas des huiles lourdes, la perméabilité relative est alors affectée par la viscosite de l'huile.

La deuxième partie nous fait voir les résultats obtenus avec un système à trois phases. Les données de perméabilité relative, en système à trois phases, sont obtenus en tenant compte des paramêtres suivant: régime permanent, température de 100 degré celcius et une pression de 3.5 MPa. Les composantes du système sont: sable de silice, huile minérale avec une viscosité de 500 MPa.s à 20 degré C., eau déminéralisée et de l'azote. La perméabilité relative de l'eau, en système à trois phases, est en fonction de la saturation de l'eau. Egalement, la perméabilité relative du gaz est en fonction de la saturation du gaz. Cependant, la perméabilité relative de l'huile varie avec les trois saturations.

Les prédictions de perméabilité relative selon les méthodes Stone I et II furent comparées avec les résultats expérimentaux et furent jugées insatisfaisantes. La corrélation suggérée par la méthode Stone I à été modifiée afin de permettre une meilleure concordance avec les données expérimentales.

Des données, provenant de six sources différentes, furent sélectionnées afin de vérifier la méthode Stone I. Dans chaque cas, la corrélation modifiée concorde mieux avec les résultats expérimentaux.

NOMENCLATURE

α	Factor defined by equation 10
β_g	Factor to allow for oil blokage by gas in Stone's model
β_w	Factor to allow for oil blokage by water in Stone's model
ΔP_i	Pressure drop in fluid phase i
ϵ_o	Exponents of normalized saturation in the analytical expression for oil relative permeability
ϵ_w	Exponents of normalized saturation in the analytical expression for water relative permeability
θ	Angle of the displacement direction (measure from vertical)
μ_i	Viscosity of fluid phase i
μ_o	Oil viscosity
μ_w	Water viscosity
ρ_o	Density of oil
ρ_w	Density of water
A	Cross sectional area of the medium
d	Diameter of the core
k_{abs}	Absolute permeability
k_{oiw}	End point permeability to water
k_{ro}^o	End point relative permeability to oil
k_{rw}^o	End point relative permeability to water
k_{ri}	Relative permeability of fluid phase i
k_{ro}	Relative permeability to oil
k_{rw}	Relative permeability to water
k_{wor}	End point permeability to water.

L	Length of the porous medium
M	Mobility ratio defined by equation 4
N_s	Instability number defined by equation 2.
N_w	Wettability constant
Q_i	Flow rate of fluid phase i
S	Normalized saturation
S_g	Gas saturation
S_g^*	Normalized gas saturation defined by equation 8
S_o	Oil saturation
S_o^*	Normalized oil saturation defined by equation 6
S_{om}	Minimum rasidual oil saturation
S_w	Water Saturation
S_w^*	Normalized water saturation defined by equation 7
S_{wc}	Connate water saturation
S_{wi}	Irreducible water saturation
S_{wm}	Maximum water saturation
V	Displacement velocity
V_c	Critical Velocity defined by equation 3

INTRODUCTION

Production of oil and gas from petroleum reservoirs usually involves flow of two or more immiscible fluids through a porous rock. Multi-phase flow in porous media is a complex process that depends on a number of factors including the absolute permeability, pressure drop, capillary pressure, fluid viscosities, and relative permeability of each phase. Of these the relative permeability is probably the most important parameter in determining the reservoir performance. For modelling thermal recovery processes, one needs to know not only the relative permeabilities at the original reservoir conditions but also the effect of temperature on the relative permeability curves.

Relative permeability, by definition, is a measure of the ability of a porous medium to conduct a given fluid when one or more other immiscible fluids are present. The resistance to flow of a given phase in a multi-phase situation depends primarily on how this phase distributes itself within the porous medium in the presence of other fluids. The distribution of immiscible fluids within a porous medium, in turn, depends on a number of different factors, including pore structure and pore size distribution, wettability, saturation history, interfacial tension, viscosity ratios, density ratios and flow velocities. Because of the complex geometry of porous rocks, it is not possible to predict the fluid distribution and the resulting fluid conductivities from a knowledge of the above mentioned factors. It is therefore necessary to use experimentally measured relative permeabilities to represent the combined effects of these factors.

Much of the available information on relative permeability has come from measurements carried out on systems in which the fluid distribution within the

porous medium depends primarily on four factors; pore structure, pore size distribution, wettability, and saturation history. Most light oil systems fall within this category. As long as the other factors remain within certain limits they appear to have no influence on relative permeability in such systems. This invariance makes relative permeability a very powerful tool in describing multi-phase flow in porous media. As a result many workers in this field believe that relative permeability should always be independent of factors such as interfacial tension, viscosity ratio and flow velocity.

In recent years the quest for additional oil has lead to recovery techniques which involve multi-phase flow outside the range over which these factors have no influence on relative permeability. For example, when dealing with surfactant flooding, the influence of interfacial tension on relative permeability must be taken into account. Similarly, when dealing heavy oil recovery, the effects of viscosity ratio and flow velocity on relative permeability might become significant.

The available measurement techniques were also developed for conventional systems and present some difficulties when used with heavy oil systems. Maini and Okazawa (1987) have discussed many difficulties involved in using the displacement technique for measuring relative permeabilities in heavy oil systems. Though some of these problems have been solved with innovative improvements in equipment design, the measurement of relative permeability in heavy oil systems is far from becoming a simple and routine measurement.

Currently, the displacement technique (unsteady-state) is used in most of the routine laboratory measurements of relative permeability. This involves displacement of oil by water injection into a core which was initially at connate water saturation. The relative permeability is inferred from the

recorded history of oil production and pressure drop across the core. Several techniques are available for calculation of relative permeabilities from the displacement data. These include computer history match techniques reported by Sigmund and McCaffery (1979) and Batycky et al. (1981) as well as techniques based on the Buckley-Leverett theory such as Johnson et al. (1955) and Jones and Roszell (1977). These techniques for calculation of relative permeability from the displacement data are based on the assumption that the displacement is stable i.e. the fluid saturations at any cross section perpendicular to the direction of flow are uniform. This assumption is generally valid for conventional oil systems in which mobility ratio is never too adverse, however in heavy oil systems involving very adverse viscosity ratios, the displacement is often highly unstable and is characterised by presence of viscous fingers, i.e. channels containing high water saturation interspersed within areas of high oil saturation. The nature and extent of viscous fingering depends on several factors including physical dimensions of the core, the mobility ratio and the flood velocity. Although the presence of viscous fingering invalidates one of the important assumptions involved in measurement of relative permeability by the displacement technique (the uniform saturation distribution), in practice this conflict with theory is often ignored. It is readily possible to calculate relative permeabilities from such unstable displacements and very often these relative permeabilities when used in computer simulation will provide excellent history match of the displacement experiment. Since, the nature of viscous fingering is dependent on the experimental conditions, these relative permeabilities are strictly applicable only to the particular experiment and may not describe the general characteristics of the rock-fluid system. It is therefore important to

evaluate the sensitivity of measured relative permeabilities to factors which affect viscous fingering. Since the flood velocity and oil/water viscosity ratio have an effect on possible viscous fingering, it is of interest to investigate the contribution of these factors on relative permeability.

Often oil recovery processes involve simultaneous flow of three immiscible fluids. Examples of such processes include; alternating gas and water injection, steam drive, in-situ combustion, and immiscible gas injection in presence of mobile water. Thorough analysis of these processes is impossible without reliable three-phase relative permeability data. Although reservoir simulation programs incorporate one or several estimation techniques which permit three-phase simulation studies to be carried out with input of only two-phase relative permeabilities, such simulation studies can be no more reliable than the techniques for estimating three-phase relative permeabilities employed in them. Unfortunately, the reliability of these estimation techniques can not be tested without availability of extensive experimental data on three-phase relative permeabilities

Compared to the wealth of information available in the literature on two-phase relative permeabilities, there is a dearth of experimental studies on three-phase flow through porous media. The total number of reported experimental studies involving three-phase flow in porous media is smaller than 20. Not all of these provide sufficient data over a wide enough range of saturations to test available correlations. In a recent paper Baker(1988) reported that only eight data sets are complete enough for evaluating goodness-of-fit of various estimation techniques. All of these data sets involve strongly water-wet systems. There is virtually no information available on three-phase relative permeabilities in intermediately-wet or oil-

wet systems. Effects of variables such as; contact angles, viscosity ratios, interfacial tension, flood velocity and temperature on three-phase relative permeability have not been investigated. There is certainly a need for more experimental investigations of three phase relative permeabilities to resolve some of the uncertainties concerning effect of the variables mentioned above.

The main reason for the scarcity of experimental data on three-phase relative permeabilities is the effort and time required for such measurements. The only well accepted technique for such measurements is the steady-state method. Between 50 to 100 steady-state measurements are required to fully define the relative permeability characteristics of a given system for one direction of saturation change. It often takes 24 hours or more to reach steady state conditions for each such measurements. Combined with the time involved in core preparation and periodic extractions to overcome the problem of error accumulation the total effort involved is indeed formidable. If the hysteresis effects corresponding to various possible directions of saturation change are also to be evaluated, the task becomes so much more difficult. However, in view of the importance of three-phase flow in reservoir engineering studies, such experimental studies are necessary in spite of the time and expense involved.

Three-phase relative permeabilities play a central role in analysis of steam drive process for heavy oil recovery. Unfortunately, no experimental data is available on three-phase flow involving heavy oils at high temperatures. Several reported studies on the effect of temperature (Maini et.al., 1987 & 1985; Torabzadeh and Handy, 1984; Quitteier and Corre, 1986; Bennion et. al. 1985) on two-phase oil/water relative permeabilities show significant temperature effects. Similar effects can be expected in two-

phase oil/gas relative permeabilities also. The three-phase flow is a relatively more complex process. When considering the possible mechanisms of temperature effects on three-phase relative permeabilities, one has to deal with relative magnitudes of three contact angles (oil-water, oil-gas and water-gas), three interfacial tensions and two viscosity ratios. It is therefore probable that the effects of temperature on three-phase relative permeabilities will be more complex than the two-phase case. Whether or not this is the case can only be determined by experimental evaluations of the effects of temperature on three-phase relative permeabilities. Before this can occur the problem of developing techniques for reliable measurement of three-phase relative permeabilities at elevated temperatures and pressures has to be addressed.

This report presents the results of work done at the Petroleum Recovery Institute under a cost shared research contract with CANMET. The objective of this work was to answer some of the questions raised above. Two-phase relative permeabilities were measured in a silica sand - mineral oil - water system to evaluate the effects of flow rate, viscosity, temperature and the measurement technique (steady-state versus unsteady-state) on relative permeabilities. Three-phase relative permeabilities were measured using the steady-state technique and the available three-phase relative permeability correlations were tested against literature data as well as the new data measured in this work. The report is divided into two parts. The first part presents the results of two-phase relative permeability work which constituted the first three tasks in the contract. The second part presents three-phase relative permeability measurements and correlations which were the last two tasks in the contract.

REFERENCES

1. Batycky, J.P., McCaffery, F.G., Hodgins, P.K., and Fisher, D.B., "Interpreting Relative Permeability and Wettability from Unsteady-state Displacement Measurements", SPEJ, June 1981, pp. 296-308.

2. Bennion, D.W., Moore, R.G., and Thomas, F.B., "Effect of Relative Permeability on the Numerical Simulation of the Steam Stimulation Process," J. Can. Pet. Tech., March-Apr., 1985, pp. 40-44.

3. Johnson, E.F., Bossler, D.P. and Naumann, V.O., "Calculation of Relative Permeability from Displacement Experiments", Trans AIME 216, 370-372, (1955).

4. Jones, S.C. and Roszell, W.O., "Graphical Techniques for Determining Relative Permeability from Displacement Experiments" JPT, 807-817, May 1977.

5. Maini, B.B. and Okazawa, T., "Effect of Temperature on Heavy Oil-Water Relative Permeability of Sand," Jour. Can. Pet. Tech., May-June 1987, pp. 33-41.

6. Maini, B.B., and Batycky, J.P., "Effect of Temperature on Heavy-Oil/Water Relative Permeabilities in Horizontally and Vertically Drilled Core Plugs," Jour. Pet. Tech., August 1985, pp. 1500-1510.

7. Quitteier, L.R., Corre, B., "Hot Water and Steamflood Laboratory Experiments Under Reservoir Conditions," SPE 15650, presented at the 61st Annual Technical Conference of SPE, New Orleans, LA, Oct. 5-8, 1986.

8. Sigmund, P.M., and McCaffery, F.G., "An Improved Unsteady-State Procedure for Determining the Relative Permeability Characteristics of Heterogeneous Porous Media," Soc. Pet. Eng. J., Feb. 1979, pp. 15-28.

9. Torabzadeh, S.G., and Handy, L.L., "The Effect of Temperature and Interfacial Tension on Water/Oil Relative Permeabilities of Consolidated Sands," SPE 12689, presented at SPE/DOE Fourth Symp. on Enhanced Oil Recovery, Tulsa, OK, April 15-18, 1984.

PART I.

TWO-PHASE OIL/WATER RELATIVE PERMEABILITIES

1. OBJECTIVES:

The objectives of the two-phase oil/water relative permeability measurements presented in this part of the report were:

1. To determine the effect of flow rate on measurements of oil/water relative permeabilities by the displacement technique in heavy oil systems.

2. To determine whether or not the relative permeability measurements by the displacement technique are equivalent to the steady-state measurements in systems involving adverse viscosity ratios.

3. To evaluate the effect of viscosity ratio on measurements of oil/water relative permeabilities by the displacement technique.

A clean system consisting of silica sand, non-polar mineral oil, and de-ionized water was used to eliminate the complications of fines migration and wettability reversal. Oil/water relative permeabilities were measured at three temperatures (23°C, 100°C and 200°C). Effect of displacement velocity was determined by conducting several displacements at each temperature and varying the water injection rate. Relative permeabilities were also measured by the steady-state technique using the same rock-fluid system. The effect of viscosity ratio was evaluated by using similar mineral oils having different viscosities.

2. EXPERIMENTAL EQUIPMENT AND PROCEDURE

A schematic diagram of the experimental equipment is shown in Figure 1. The parts within the dotted enclosure were contained in a convection oven equipped with a temperature controller capable of maintaining constant temperature within 0.5°C. A triaxially loaded core holder shown schematically in Figure 2 was used for confining the test cores under simulated overburden pressure. In addition to the core holder, the oven accommodated a capillary viscometer, a pycnometer, a transfer vessel for injecting oil, a heat exchanger for heating the injection water, a hot water reservoir, and a number of valves most of which could be operated from outside the oven. A high pressure separator cell equipped with a glass window and volume graduations, a back pressure regulator, electronic differential pressure transducers, a chart recorder and the pumping system (consisting of a Ruska pump and a flow multiplier) were located outside the oven.

The cores were wet packed and then confined by application of triaxial stress using a technique described elsewhere (Maini et.al.,1985). Absolute permeability was determined by flowing water or brine at 100% saturation. Irreducible water saturation was established by injecting the oil at the test temperature. Higher injection rates were used at higher temperatures to obtain roughly the same pressure drop at the irreducible water saturation. After establishing the irreducible water saturation water or brine was injected at constant rate to displace the oil. The pressure drop across the core was recorded continuously on a chart recorder, and the volume of oil produced was recorded periodically by reading the level of oil/water interface in the accumulator cell. Water injection was continued until the volume fraction of oil in the produced fluid decreased to a value below 1%. The core

was then extracted by flowing hot toluene through it. It was cleaned further by flowing methylene chloride which was then evaporated out of the core by flowing hot nitrogen through it. The core was then evacuated and filled with deionized water or brine. Its absolute permeability was measured again to verify complete removal of oil. It was then ready for the next test.

The equipment used for steady-state measurements is shown in Figure 3. Both fluids were circulated in closed loops with HPLC type pumps (Beckman model 100A). The saturations were measured by reading the level of oil/water interface in the windowed cell placed in the circulation loop. Capillary end effects were minimized by using high flow rates and by measuring the pressure drop 2.5 cm away from the ends of the core. Relative permeabilities were calculated by applying Darcy's law to each fluid phase.

3. CALCULATION OF RELATIVE PERMEABILITY FROM DISPLACEMENT DATA

The production and pressure drop data recorded during the core floods were used to obtain relative permeabilities by a history match simulation approach based on the techniques reported by Sigmund and McCaffery (1979). This involved determining values for two unknown parameters, ϵ_w and ϵ_o, which reflect the shape of oil and water relative permeability curves as defined by the following equations.

$$k_{ro} = k^o_{ro} \frac{(1-S)^{\epsilon_o} + 0.01(1-S)}{1.01} \qquad (1a)$$

and

$$k_{rw} = k^o_{rw} \frac{S^{\epsilon_w} + 0.01S}{1.01} \qquad (1b)$$

where $S = (S_w - S_{wi})/(S_{wm} - S_{wi})$, S_{wi} and S_{wm} being the irreducible and maximum water saturations and k_{ro} and k_{rw} are the end point relative permeabilities to oil and water. The calculations were carried out with an automatic history matching program called PRISIM which varies the exponents ϵ_o and ϵ_w until the weighted least square error summation in both pressure drop and production history were minimized. The program uses a finite difference model of the displacement process and accounts for the presence of capillary pressure.

4. RESULTS AND DISCUSSION

The petrophysical properties of the silica sand core are listed in Table 1. All tests were carried out at 10.3 MPa confining pressure and 3.45 MPa back pressure at the core outlet. The porosity and absolute permeability of the core were measured before using the core for each relative permeability test and were found to remain constant. A non-polar viscous mineral oil (Shell Vitrea 150) was used as the oil phase. Its properties are listed in Table 2.

4.1 EFFECT OF FLOW RATE ON RELATIVE PERMEABILITY MEASUREMENTS BY THE DISPLACEMENT TECHNIQUE

4.1.1 Measurements at Room Temperature (23°C):

Five displacement tests were carried out at room temperature. Results of these tests are summarized in Table 3. Figures 4 to 13 show the computer history matches of production and pressure drop data for each of the displacements. Figure 14 compares the five sets of oil/water relative permeabilities corresponding to the five water injection rates used. The end

point oil relative permeability (at irreducible water saturation) was measured by first saturating the core with water and then displacing the water with oil to establish irreducible water saturation. The rate of oil injection was kept the same in all tests and both the irreducible water saturation and the relative permeability to oil at irreducible water saturation were found to be reproducible. It was evident from the figures showing history matches of the production data that the experiments were stopped before the oil production had completely ceased. Thus the true residual oil saturation was never reached in these displacements. This was necessary in order to complete the experiments in a reasonable length of time. At the lowest flow rate used it took about 55 hours for each pore volume injected. The true residual oil saturation was estimated from extrapolation of the production data for 0.5 ml/min displacement which was carried out to 16 pore volumes injected. The corresponding end point relative permeability was determined by iteration in the computer history matching process. As shown in Figure 14 the end point water relative permeability appeared to increase with increasing rate of water injection. The oil relative permeability also displayed significant sensitivity to injection rate. The curvature of the oil relative permeability curve decreased in going from 0.125 ml.min to 1.0 ml/min injection rate but then increased as the injection rate was increased further to 2.0 ml/min.

There are two possible reasons for the observed flow rate dependence of the relative permeability curves. Even though capillary pressure was used in the history matching for calculating relative permeabilities it is possible that due to the experimental errors in the capillary pressure curve the capillary end effects are not fully accounted for. However it should be stated that the flow rates used in these tests were high enough to make the

capillary end effects small even at the lowest flow rate. Kytes and Rapoport's (1958) scaling coefficient was 0.65 at the lowest flow rate and 10.3 at the highest. Therefore it is unlikely that the capillary end effects are the primary cause for the observed behaviour. It is more likely that the flow rate dependance stems from the effects of changes in extent of instability (viscous fingering) and the resulting fluid distribution with changing flow rate.

Figure 15 shows the recovery vs pore volumes injected curves near the breakthrough point for each displacement. Although it is difficult to precisely determine the breakthrough point it is apparent that the oil recovery at a fixed value of pore volumes injected increases with increasing flow rate. It also appears that the breakthrough recovery also increases with increasing flow rate. This type of behaviour would not be expected from the established theories of viscous fingering. For example, the theory of Peters and Flock (1981) and Bentsen (1985) leads one to expect decreasing breakthrough recovery with increasing flow rate for unstable displacements. The increasing breakthrough recovery with increasing flow rate would suggest that the capillary end effects were not insignificant at lower rates.

Peters and Flock defined a stability number which for a cylindrical system is given by:

$$N_S = \frac{(M - 1)(V - V_c)\,\mu_w d^2}{N_w\, K_{wor}\, \sigma} \qquad (2)$$

where:

$$V_c = \frac{K_{wor}\,(\rho_w - \rho_o) g \cos \alpha}{\mu_w\,(M - 1)} \qquad (3)$$

and

$$M = \frac{k_{wor}\,\mu_o}{k_{oiw}\,\mu_w} \qquad (4)$$

The critical value of the stability number for onset of viscous fingering was reported to be 13.56. That is, all displacements having a stability number higher than the critical value are likely to be unstable and the degree of instability increases with increasing stability number. The wettability constant, N_w, relates effective interfacial tension to the actual oil/water interfacial tension. Its value for the system used in this study was not measured experimentally. Since the rock/fluid system used in this study was similar to that used by Peters and Flock, their value of 306.25 was used for calculating the stability numbers. The value of oil/water interfacial tension was estimated to be 27 mN/m. With these values of N_w and IFT and using the steady state measurements for end point permeabilities the value of stability number was 125 for the lowest flow rate and 2000 for the highest flow rate used in these experiments (see Table 3). Therefore, all of the displacements were unstable according to the Peters and Flock criterion. However, the apparent increase in breakthrough recovery with increasing flow rate is not consistent with their instability analysis. It can be suggested that perhaps in the system used in our tests, viscous instabilities and capillary effects both play a significant role. The increasing flow rate simultaneously reduces the capillary end effects and increases viscous fingering.

4.1.2 Measurements at 100°C:

Four displacement tests were carried out at 100°C using water injection rates ranging from 1 ml/min to 8 ml/min. The results of these displacements

are summarized in Table 4. Computer history matches of production and pressure drop data for these displacements are shown in figures 16 to 23. The effect of flow rate on oil displacement at 100°C was similar to that observed at room temperature. Figure 24 compares the oil recovery versus pore volumes injected behaviour near water breakthrough at different flow rates. As the injection rate is increased from 1.0 ml/min to 4.0 ml/min, the breakthrough recovery and recovery at a fixed value of pore volumes injected (past breakthrough) increases significantly. At still higher displacement rates the breakthrough recovery appears to decrease. As shown in Table 4 the Peters and Flock instability numbers for these displacements were between 30 to 240. Therefore, it is possible that viscous fingering was involved in all of the tests at this temperature also. The relative permeability curves derived from these tests are shown in Figure 25. The water relative permeability curve shifts to higher values as the injection rate is increased from 1.0 ml/min to 4.0 ml/min. At still higher rate this trend is reversed. The oil relative permeability end points remain unchanged with flow rate but the curvature in the oil relative permeability curve decreases with increasing flow rate up to 4.0 ml/min and then decreases.

4.1.3 Measurements at 200°C:

Three displacements were carried out at 200°C using water injection rates ranging from 2 ml/min to 8 ml/min (measured at room temperature). The results of these displacements are summarized in Table 5. Figures 26 to 31 show the computer history matches of production and pressure drop data. The effect of flood velocity on oil recovery performance is shown in figure 32. At this temperature the recovery performance became more efficient at higher rates.

As shown in Table 5 the estimated values of Peters and Flock instability numbers for these displacements ranged between 13 to 52. Therefore the flood at the lowest injection rate would be stable while the other two would be unstable. The observed effect of displacement rate on recovery performance near water breakthrough suggests that the floods were stable and capillary effects were significant. Because of the uncertainty involved in estimating the wettability index and the IFT, it is possible that the actual instability numbers are considerably smaller and lie in the stable zone for all three displacements.

The effect of displacement rate on relative permeabilities is shown in Figure 33. Increasing displacement velocity reduces the curvature in the oil relative permeability curve. Water relative permeability curve shows very little effect in going from 4.0 m/d (2 ml/min injection rate) to 7.9 m/d (4.0 ml/min injection rate) but shifts downward at 15.8 m/d (8 ml/min injection rate). No steady-state measurements were not carried out at this temperature. If it can be assumed that the displacements were all stable, the relative permeability curves obtained at the highest rate would be the most reliable among the set due to reduced capillary end effects.

4.2 Comparison of Steady-State and Unsteady-state Relative Permeabilities:

Steady-state measurements of the oil/water relative permeabilities were carried out at room temperature and at 100°C. The rock-fluid system used in these measurements was identical to that in the displacement tests. A comparison of the oil/water relative permeabilities at room temperature measured by displacement technique with those measured by the steady-state method is shown in Figure 34. The steady-state values for water appear to

agree quite well with the low rate displacement tests but in the case of oil there are large differences. The steady state values of oil relative permeability are much higher than those obtained by the displacement tests. It is apparent that the two techniques vastly provide different sets of relative permeability curves.

Figure 35 compares the results of steady-state measurements at 100°C with the relative permeabilities calculated from 100°C displacement tests. The steady-state values of oil relative permeability at intermediate saturations are considerably higher than those determined by any of the unsteady-state tests. The water relative permeability shows better agreement between unsteady-state and the steady-state measurements and for the most part the steady-state values are close to those determined by the low rate floods.

The results of steady-state measurements at both temperatures show that the measurements of relative permeability in viscous oil systems by displacement technique do not agree with steady-state values. The unsteady-state measurements are subject to several experimental artifacts, the most troublesome of which appears to be viscous fingering. Measurements at low temperatures generally involve very adverse viscosity ratios and require extremely low flow rates to eliminate viscous fingering unless very small diameter cores are used (see equation 2). In real reservoir systems such small diameter cores would be impractical because of the inadequate representation of local heterogeneities and other experimental difficulties. Even if stable laboratory experiments can be carried out, the application of relative permeabilities derived from such experiments to field scale simulations would be questionable.

The problem is made even worse due to the large throughput required to

reach near residual saturations. This makes the use of low flow rates very time consuming. Other artifacts which can affect relative permeability measurements include migration of fines, inadequate suppression of capillary end effects or incomplete accounting of such effects and, at high temperatures, possible changes in rock and fluid properties.

It can be argued that the steady-state technique provides better results. While this is certainly true in heavy oil systems, the steady-state relative permeabilities may also fail to provide good history matches in computer simulations of field behaviour if the simulators are not capable of handling viscous fingering effects. The goal of research in this area should be to characterize the role of viscous fingering in reservoir scale displacements and to develop ways of duplicating such effects in the laboratory scale experiments. This would require determining the amount of instability that exists in field displacements, perhaps through the use of an appropriate scaling group. Scaled laboratory experiments can then be designed to represent the field behaviour. There is also a need to develop mathematical models to describe growth and propagation of viscous fingers in unstable displacements. If such models were available in computer simulation programs, the use of steady-state relative permeabilities would be strongly recommended.

4.3 Effect of Viscosity Ratio on Relative Permeability Measurements by the Displacement Technique:

The effect of viscosity ratio on oil/water relative permeability was investigated by changing the viscosity of oil in room temperature displacement tests. Normal octane was added to the viscous mineral oil to reduce its viscosity. The viscosity of the paraffinic mineral oil and octane mixtures

ranged from 10.5 mPa.s to 450 mPa.s. The viscosity of water remained constant at 0.99 mPa.s in all tests. The addition of octane to the mineral oil had very little effect on the interfacial tension and is unlikely to affect the wettability characteristics. Same water injection rate was used in all displacements. Therefore, the only factor changing in these displacements was the viscosity of the oil.

Figure 36 shows the effect of viscosity on measured relative permeabilities. For the two lowest viscosities of the displaced oil, the relative permeabilities were more or less unaffected by oil viscosity. At higher viscosities of oil the differences became significant. However, the trend of the changes observed was not consistent and additional tests are required to explain the behaviour. The relative permeabilities shown in Figure 36 were calculated by the history matching technique. The high viscosity runs required extrapolation of the experimental data to determine the end points. It is likely that this extrapolation introduced some errors in the calculated relative permeabilities.

5. CONCLUSIONS:

1. The displacement technique of relative permeability measurements provided flow rate sensitive results in viscous oil systems.
2. The steady-state relative permeability measurements did not agree with the unsteady-state results.
3. The relative permeability measurements by unsteady-state method were unaffected by oil/water viscosity ratio when the viscosity ratio was low.
4. At high oil/water viscosity ratios, the unsteady-state relative permeability changed with changing viscosity ratio.

REFERENCES

1. Bentsen, R.G., "A New Approach to Instability Theory in Porous Media", SPEJ (Oct. 1985) 765-779.

2. Kyte, J.R., and Rapoport, L.A., "Linear Waterflood Behaviour and End Effects in Water Wet Porous Media," Trans. AIME 213, 1958, pp. 423-426.

3. Maini, B.B., Singhal, A., Okazawa, T., Chu, Y., Batycky, J.P., and Nicola, F., "Measurements of Fluid and Rock Properties at Elevated Temperatures and Pressures," Report 1985-1, Petroleum Recovery Institute, Calgary, Nov. 1985.

4. Peters, E.J. and Flock, D.L., "The Onset of Instability During Two-Phase Immiscible Displacement in Porous Media" SPEJ (April 1981), 249-258

5. Sigmund, P.M., and McCaffery, F.G., "An Improved Unsteady-State Procedure for Determining the Relative Permeability Characteristics of Heterogeneous Porous Media," Soc. Pet. Eng. J., Feb. 1979, pp. 15-28.

Table 1: Properties of the Core Used for Relative Permeability Tests in Silica Sand.

Type of sand:	140-200 mesh silica sand
Core length:	46.7 cm
Cross-sectional area:	25 cm^2
Pore volume:	409 ml
Absolute permeability:	3.6 Darcy
Confining pressure:	10.3 MPa.
Pore pressure	3.45 MPa.

Table 2: Properties of the Mineral Oil used in Relative Permeability Measurements.

Temperature (^oC)	23	100	200
Density (g/ml)	0.877	0.828	0.767
Viscosity (mPa.s)	405.0	12.0	2.3

Table 3: A Summary of Displacement Results in Silica Sand Core at Room Temperature.

Temperature (^{o}C):	23	23	23	23	23
Water injection rate (ml/min)	0.125	0.25	0.50	1.00	2.00
Flood velocity (cm/hr)	0.84	1.67	3.34	6.69	13.4
End point rel. perm. to oil	0.85	0.85	0.83	0.75	0.85
End point rel. perm. to water	0.10	0.10	0.175	0.30	0.30
Break through recovery (percent PV)	10.5	12	14	17.5	14.5
Irreducible water saturation(% PV)	4	4	5	7	5
Experimental residual oil saturation (% PV)	64	56	47	45	48
Estimated true residual oil saturation (% PV)	30	30	30	30	30
Mobility Ratio based on steady-state end points.	51	51	51	51	51
N_w (Estimated from work of Peter and Flock)	300	300	300	300	300
N_s (from eq. 2)	125	250	500	1000	2000

Table 4: A Summary of Displacement Results at 100 C.

Flood velocity (cm/hr)	7.2	14.4	28.8	57.6
End point rel. perm. to oil	0.74	0.74	0.74	0.74
End point rel. perm. to water	0.25	0.30	0.42	0.36
Break through recovery (percent PV)	26.7	34.2	33.0	23.8
Irreducible water saturation(% PV)	9	9	9	9
Experimental residual oil saturation (% PV)	38.5	34.0	32.0	33.0
Estimated true residual oil saturation (% PV)	30	30	30	30
Mobility Ratio based on steady-state end points.	15.4	15.4	15.4	15.4
N_w (Estimated from work of Peter and Flock)	300	300	300	300
N_s (from eq. 2)	31	61	123	245

Table 5: A Summary of Displacement Results at 200°C.

Flood velocity (cm/hr)	15.9	31.8	65.8
End point rel. perm. to oil	0.75	0.75	0.75
End point rel. perm. to water	0.40	0.45	0.35
Break through recovery (percent PV)	35	37	38
Irreducible water saturation(% PV)	9	9	9
Experimental residual oil saturation (% PV)	38	32	20
Estimated true residual oil saturation (% PV)	25	25	20
Mobility Ratio	8	8	8
N_w (Estimated from work of Peter and Flock)	300	300	300
N_s (from eq. 2)	13	26	52

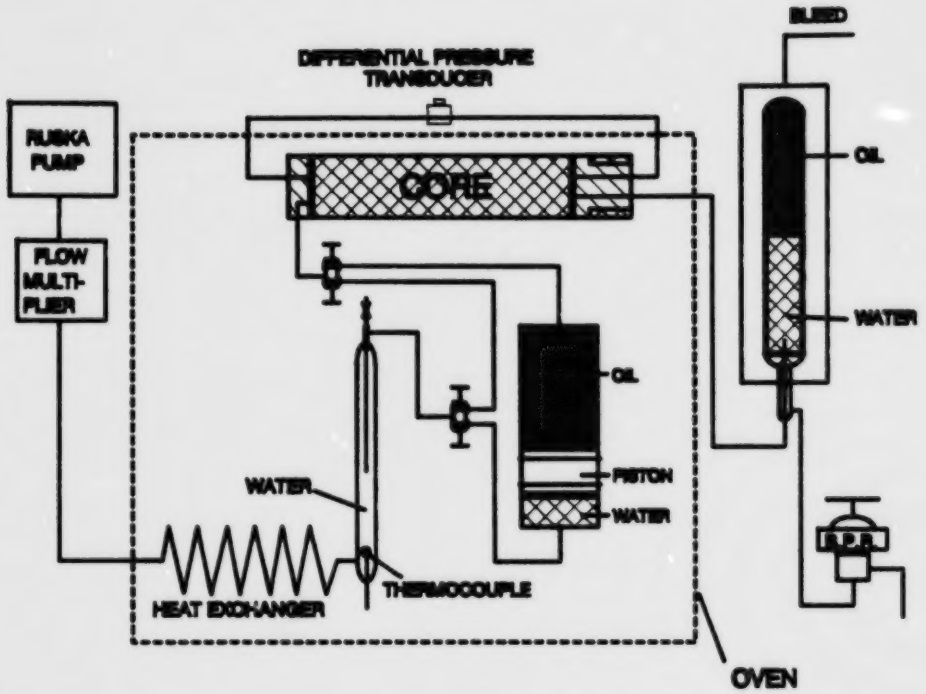

Figure 1. Schematic Diagram of Displacement Apparatus

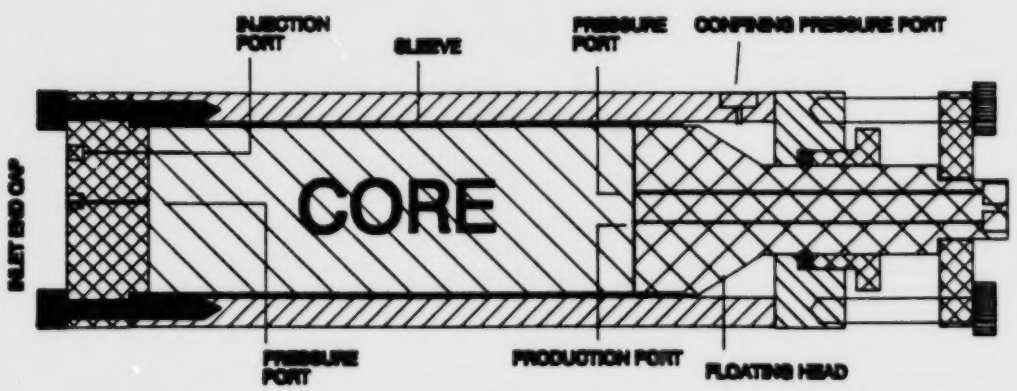

Figure 2. Schematic Diagram of Core Holder

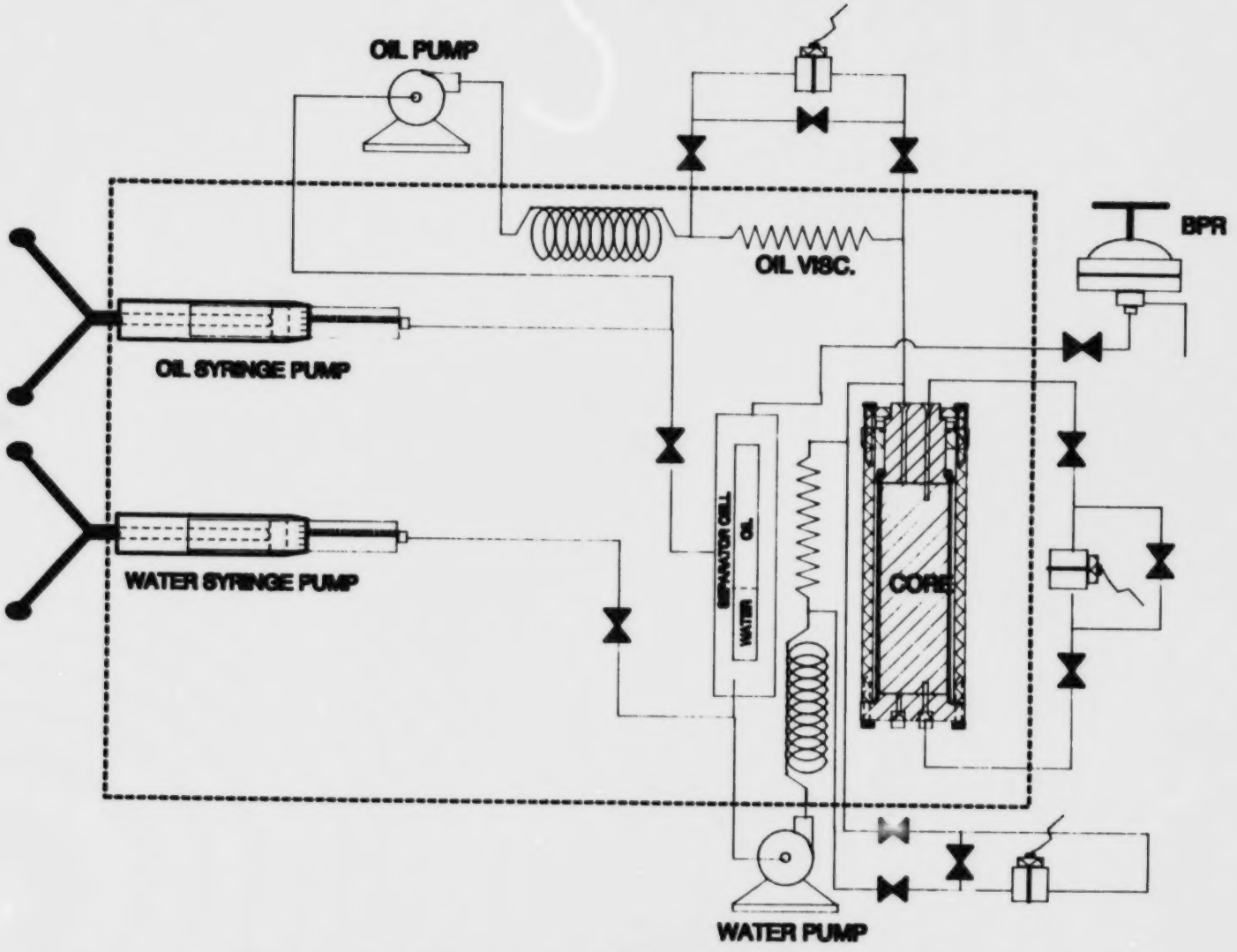

Figure 3. Schematic Diagram of the Equipment for Steady-State Measurements

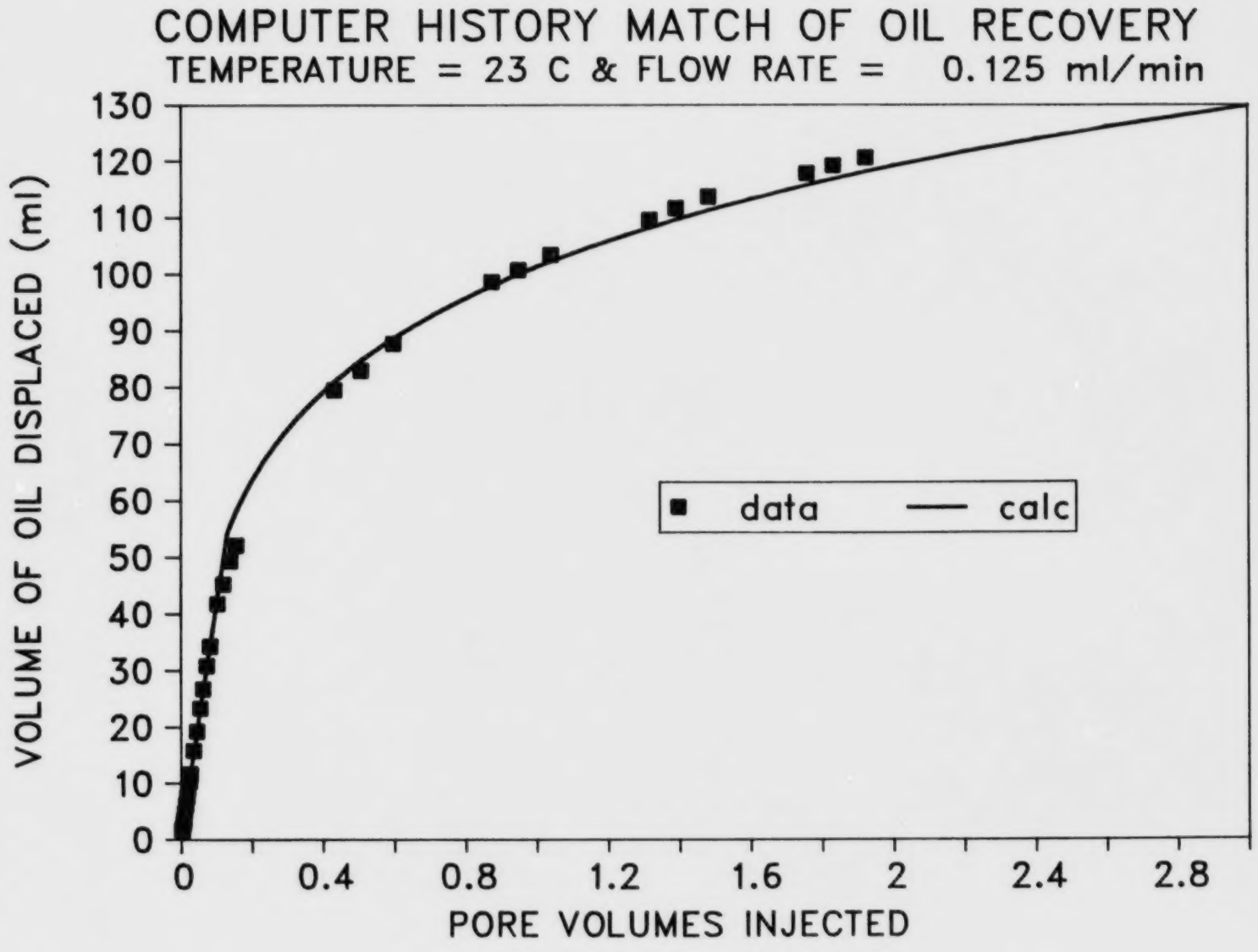
COMPUTER HISTORY MATCH OF OIL RECOVERY
TEMPERATURE = 23 C & FLOW RATE = 0.125 ml/min
VOLUME OF OIL DISPLACED (ml)
130
120
110
100
90
80
70
60
50
40
30
20
10
0
0
0.4
0.8
1.2
1.6
2
2.4
2.8
PORE VOLUMES INJECTED
data
calc

FIGURE 4

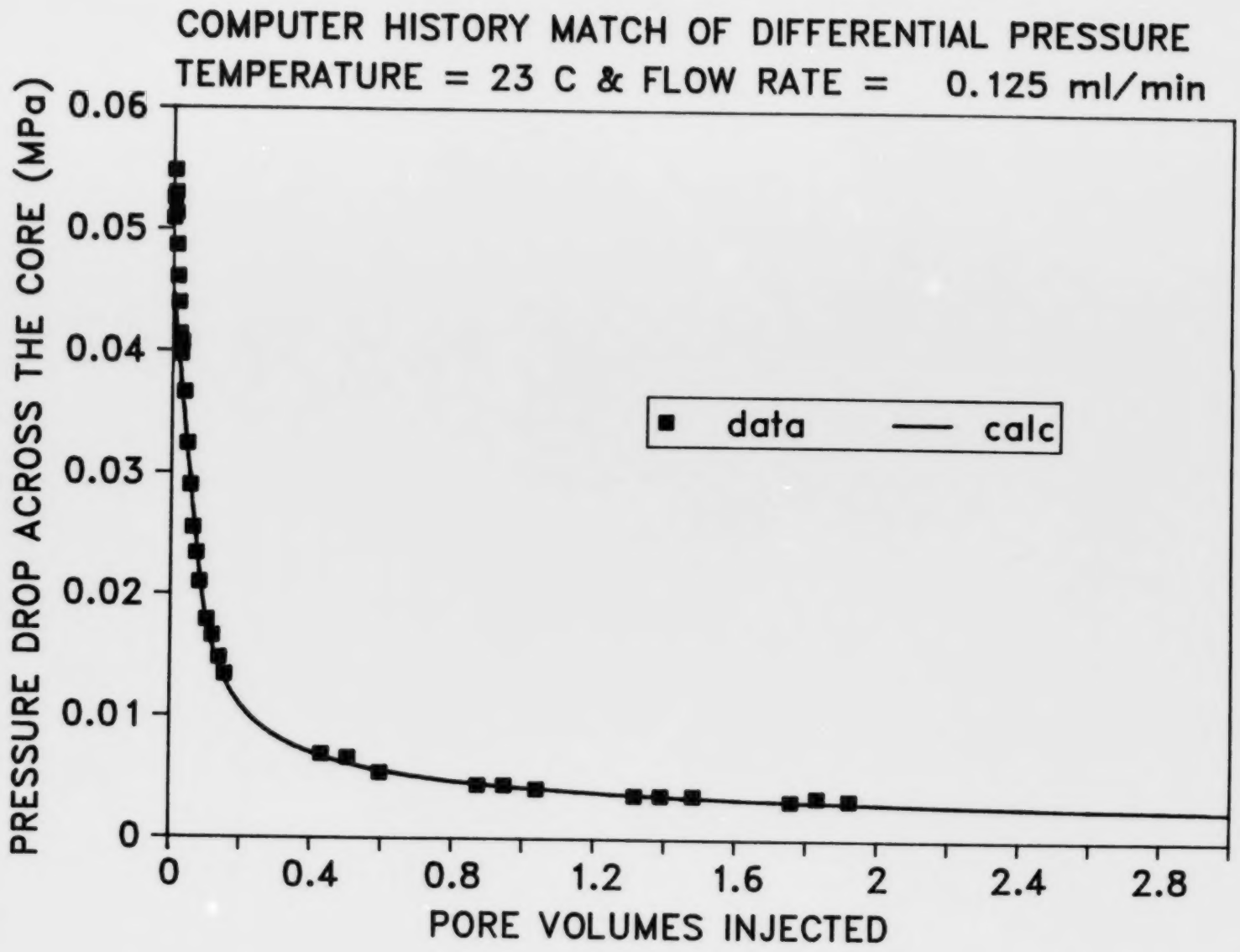
COMPUTER HISTORY MATCH OF DIFFERENTIAL PRESSURE
TEMPERATURE = 23 C & FLOW RATE = 0.125 ml/min
PRESSURE DROP ACROSS THE CORE (MPa)
0.06
0.05
0.04
0.03
0.02
0.01
0
data
calc
0
0.4
0.8
1.2
1.6
2
2.4
2.8
PORE VOLUMES INJECTED

FIGURE 5

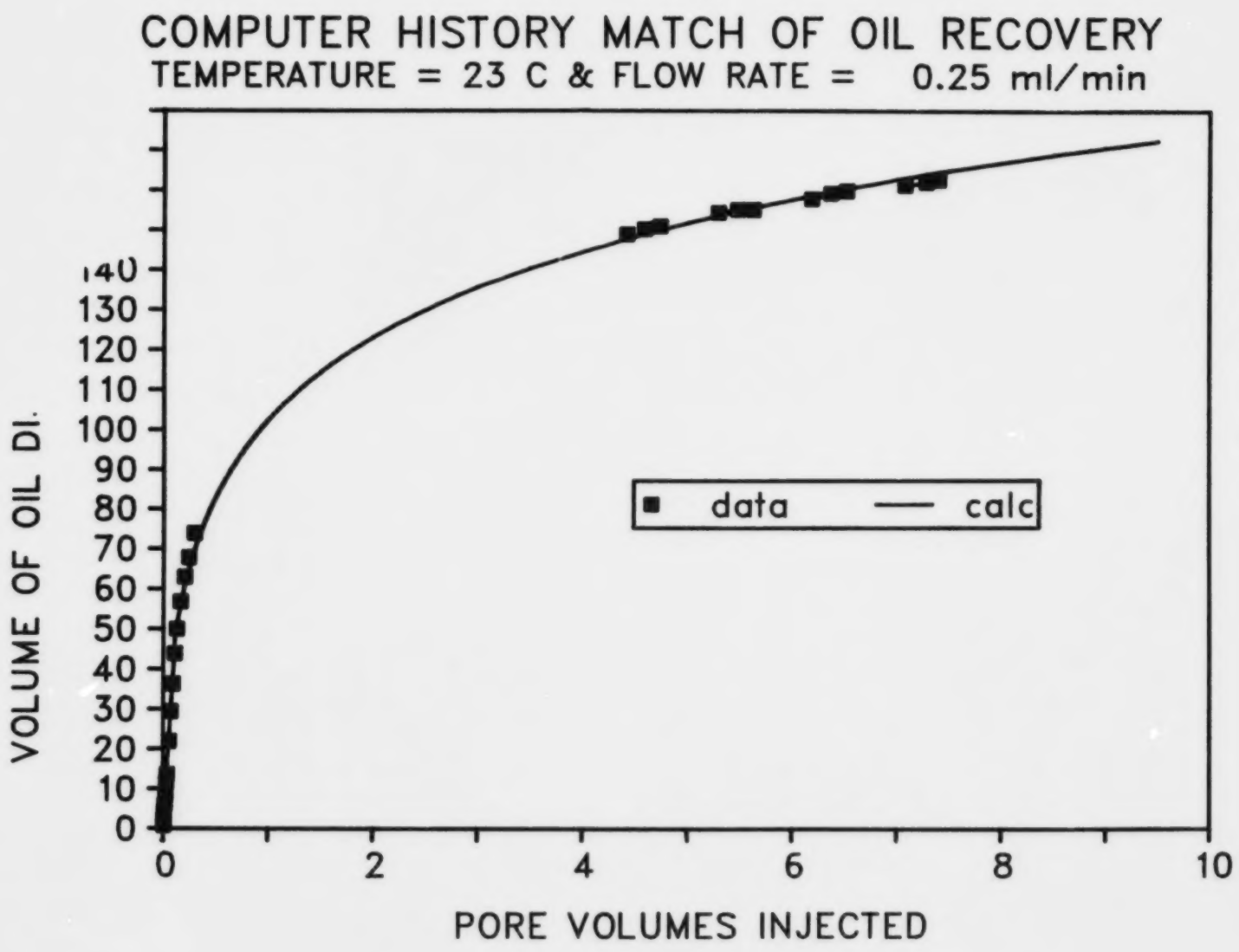
COMPUTER HISTORY MATCH OF OIL RECOVERY
TEMPERATURE = 23 C & FLOW RATE = 0.25 ml/min
VOLUME OF OIL DI.
140
130
120
110
100
90
80
70
60
50
40
30
20
10
0
data
calc
0
2
4
6
8
10
PORE VOLUMES INJECTED

FIGURE 6

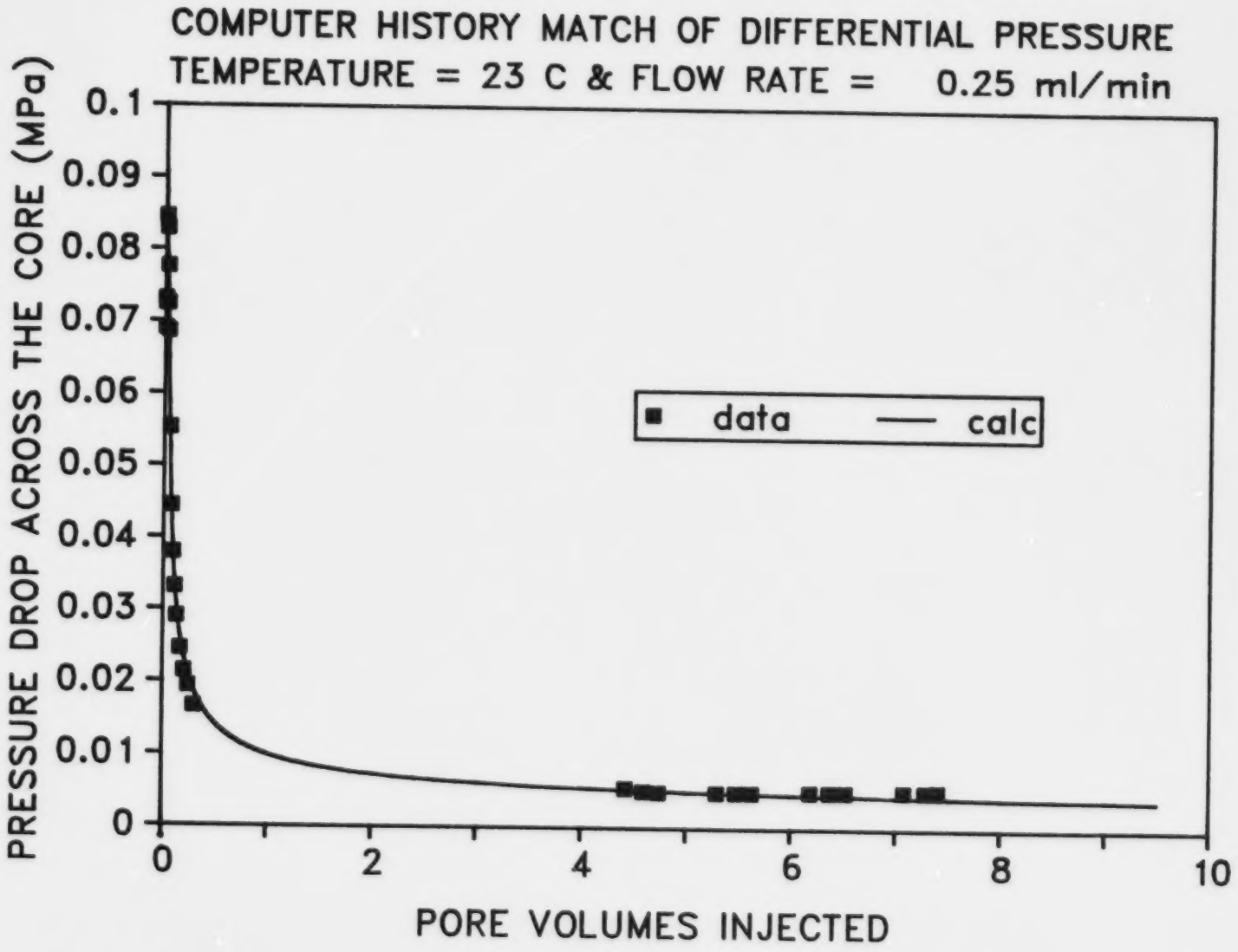
COMPUTER HISTORY MATCH OF DIFFERENTIAL PRESSURE
TEMPERATURE = 23 C & FLOW RATE = 0.25 ml/min
PRESSURE DROP ACROSS THE CORE (MPa)
0.1
0.09
0.08
0.07
0.06
0.05
0.04
0.03
0.02
0.01
0
data
calc
0
2
4
6
8
10
PORE VOLUMES INJECTED

FIGURE 7

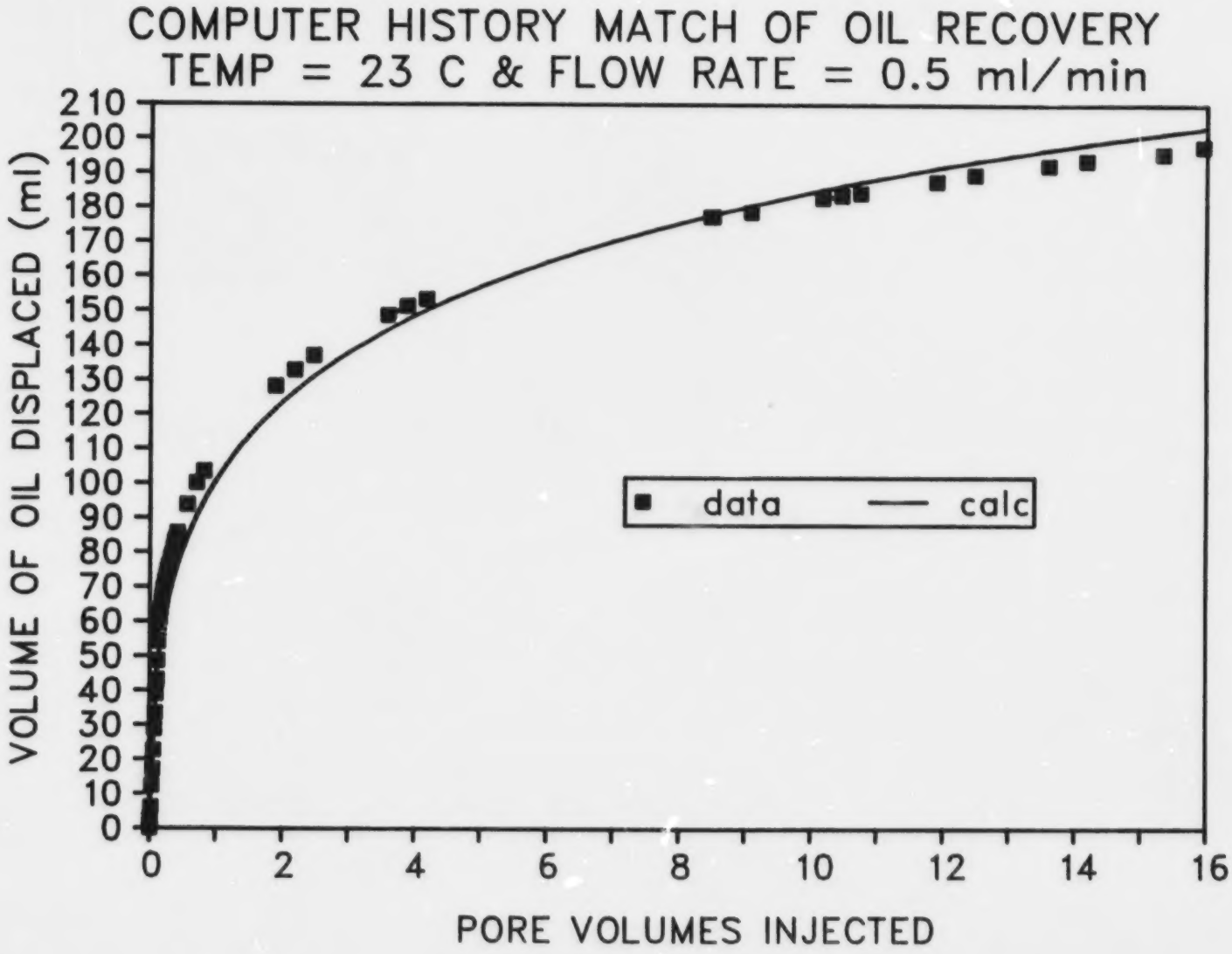
COMPUTER HISTORY MATCH OF OIL RECOVERY
TEMP = 23 C & FLOW RATE = 0.5 ml/min
VOLUME OF OIL DISPLACED (ml)
0
10
20
30
40
50
60
70
80
90
100
110
120
130
140
150
160
170
180
190
200
210
0
2
4
6
8
10
12
14
16
PORE VOLUMES INJECTED
data
calc

FIGURE 8

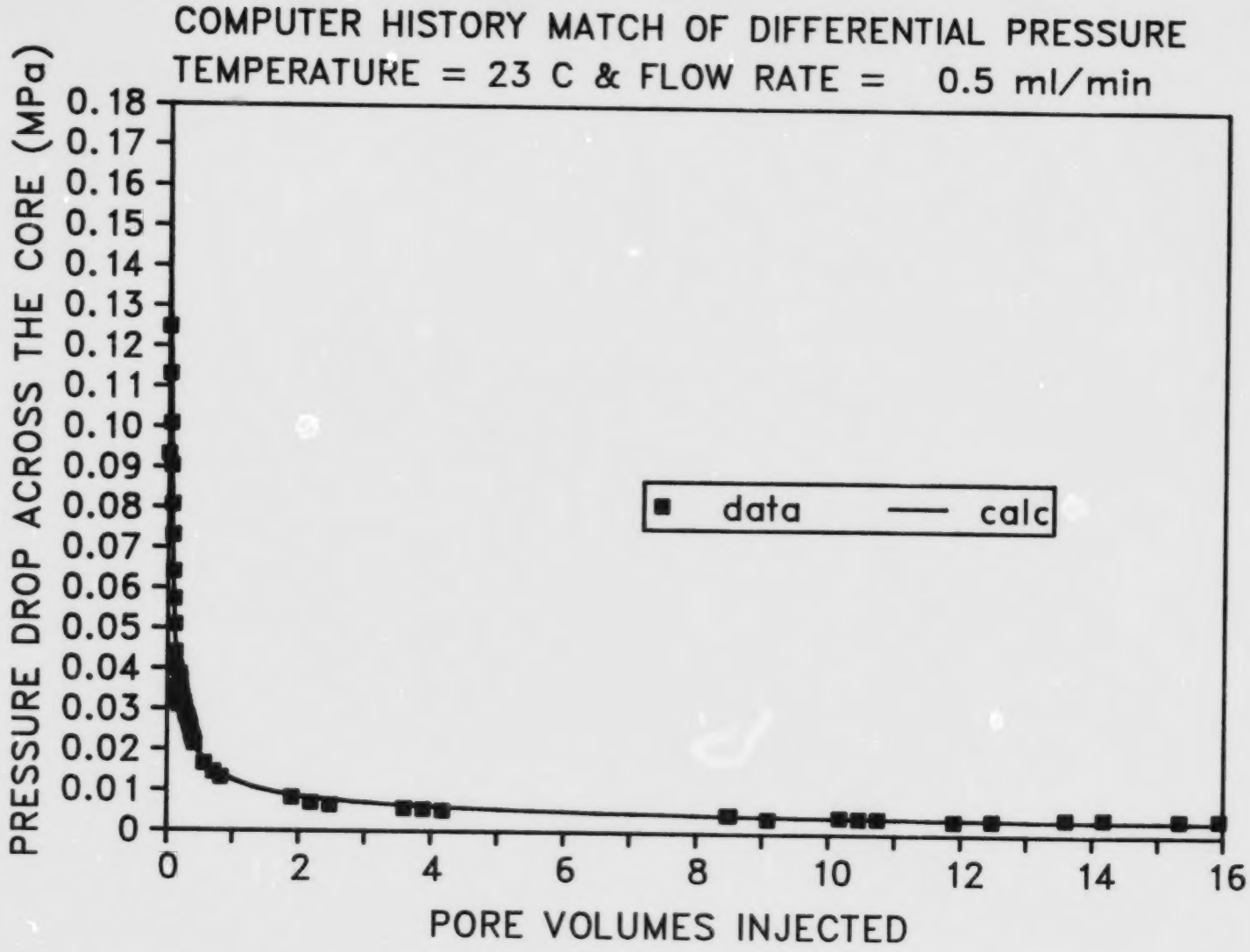
COMPUTER HISTORY MATCH OF DIFFERENTIAL PRESSURE
TEMPERATURE = 23 C & FLOW RATE = 0.5 ml/min
PRESSURE DROP ACROSS THE CORE (MPa)
0.18
0.17
0.16
0.15
0.14
0.13
0.12
0.11
0.10
0.09
0.08
0.07
0.06
0.05
0.04
0.03
0.02
0.01
0
data
calc
0
2
4
6
8
10
12
14
16
PORE VOLUMES INJECTED

FIGURE 9

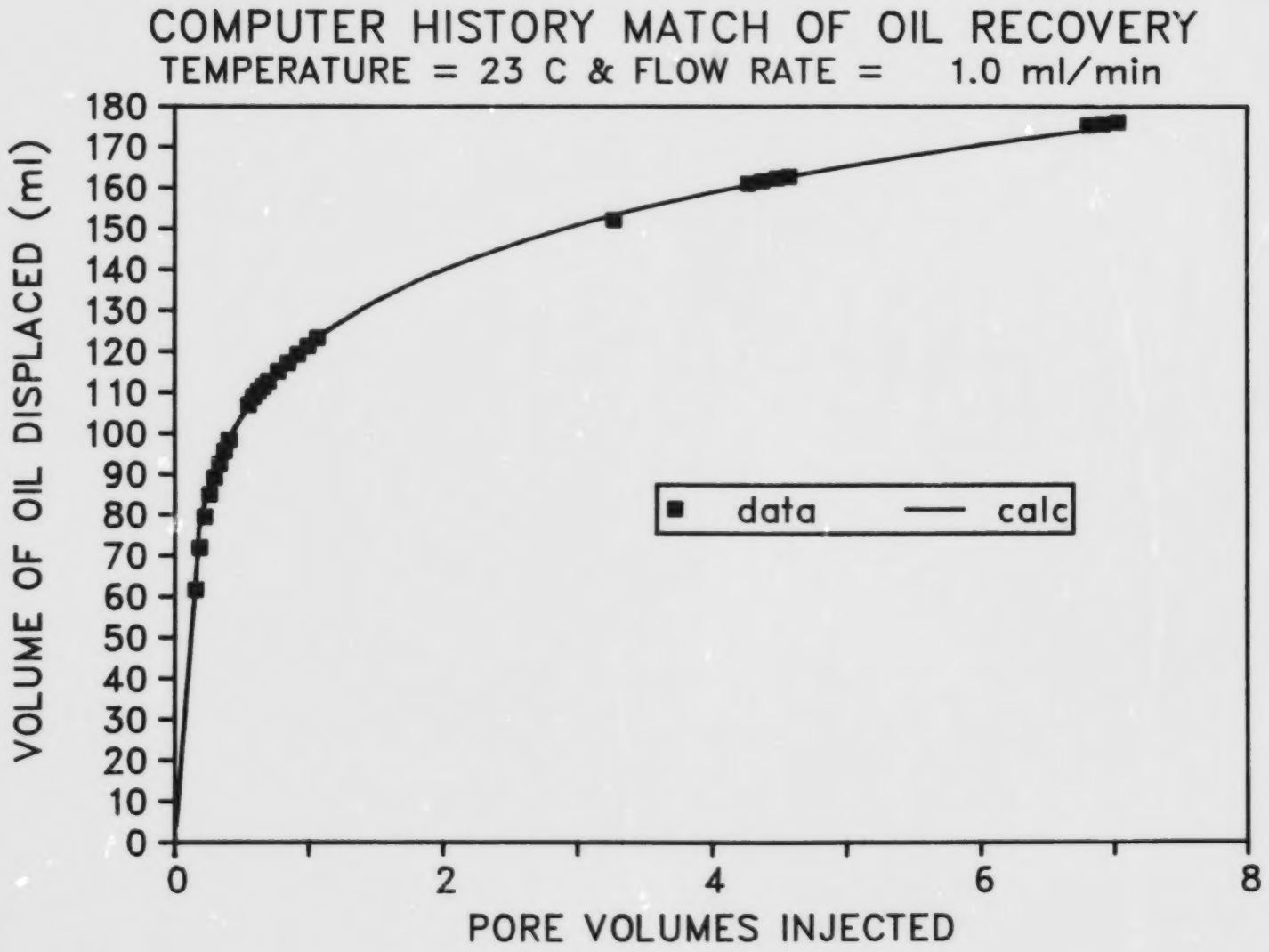
COMPUTER HISTORY MATCH OF OIL RECOVERY
TEMPERATURE = 23 C & FLOW RATE = 1.0 ml/min
VOLUME OF OIL DISPLACED (ml)
180
170
160
150
140
130
120
110
100
90
80
70
60
50
40
30
20
10
0
0
2
4
6
8
PORE VOLUMES INJECTED
data
calc

FIGURE 10

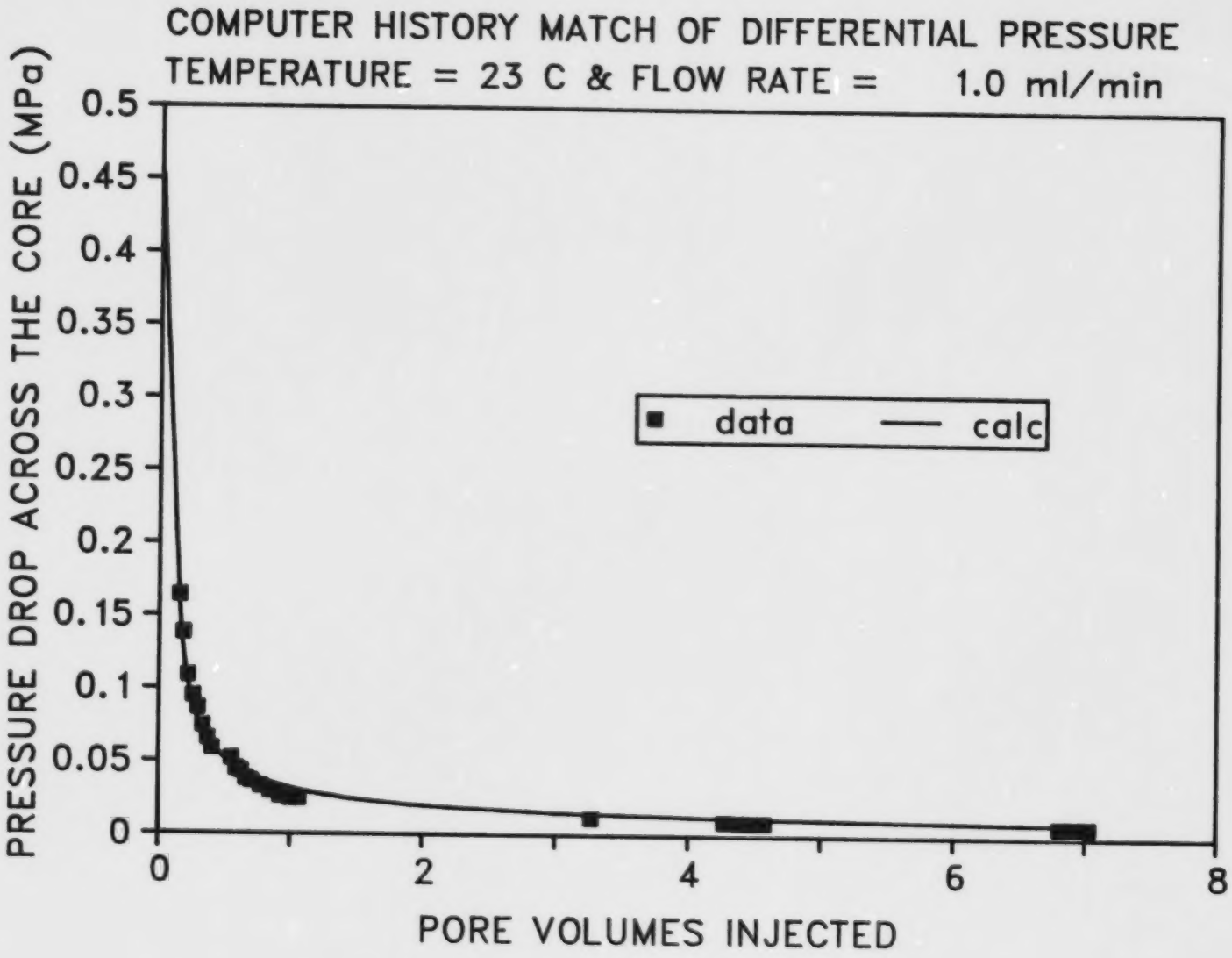
COMPUTER HISTORY MATCH OF DIFFERENTIAL PRESSURE
TEMPERATURE = 23 C & FLOW RATE = 1.0 ml/min
PRESSURE DROP ACROSS THE CORE (MPa)
0.5
0.45
0.4
0.35
0.3
0.25
0.2
0.15
0.1
0.05
0
data
calc
0
2
4
6
8
PORE VOLUMES INJECTED

FIGURE 11

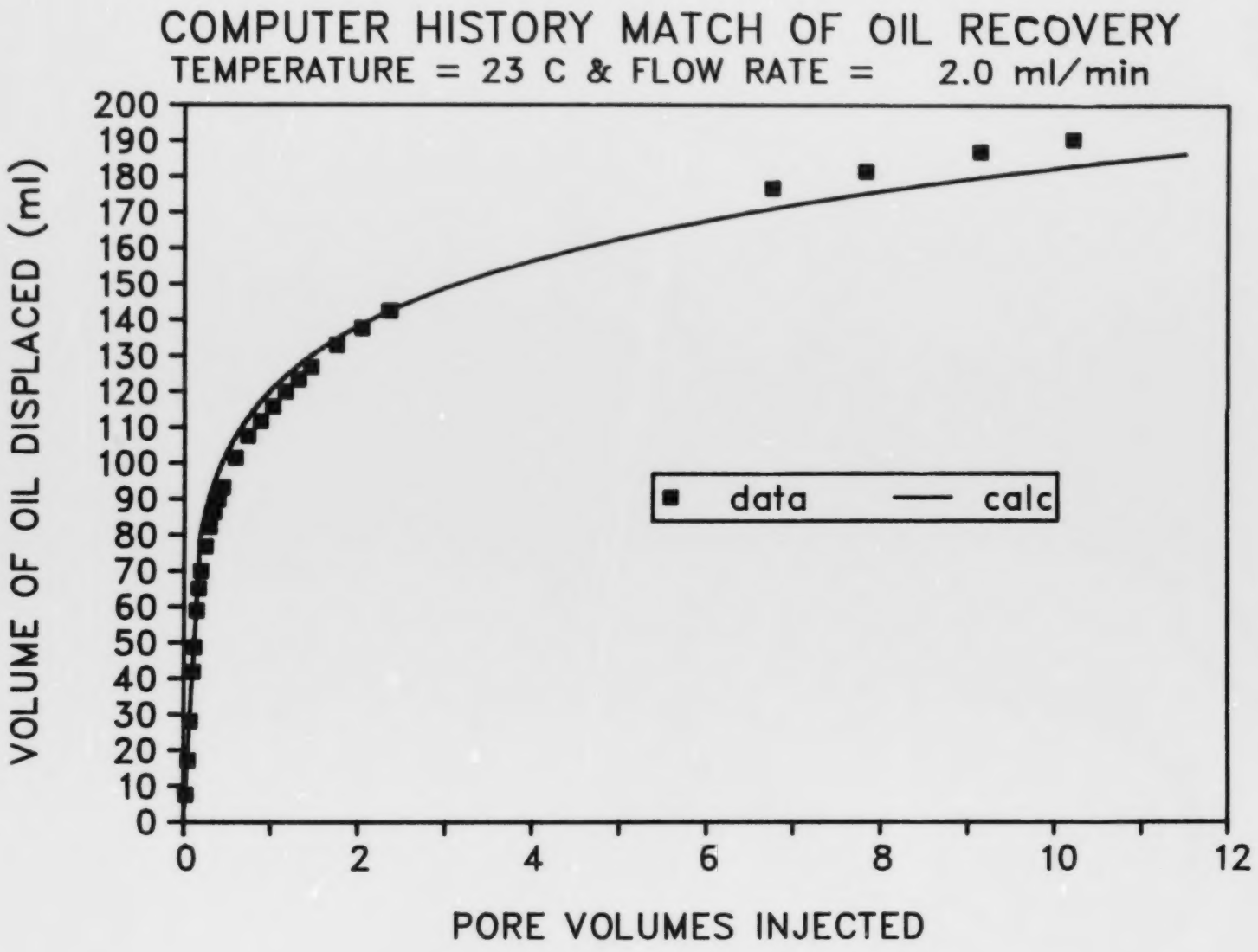
COMPUTER HISTORY MATCH OF OIL RECOVERY
TEMPERATURE = 23 C & FLOW RATE = 2.0 ml/min
VOLUME OF OIL DISPLACED (ml)
200
190
180
170
160
150
140
130
120
110
100
90
80
70
60
50
40
30
20
10
0
0
2
4
6
8
10
12
PORE VOLUMES INJECTED
data
calc

FIGURE 12

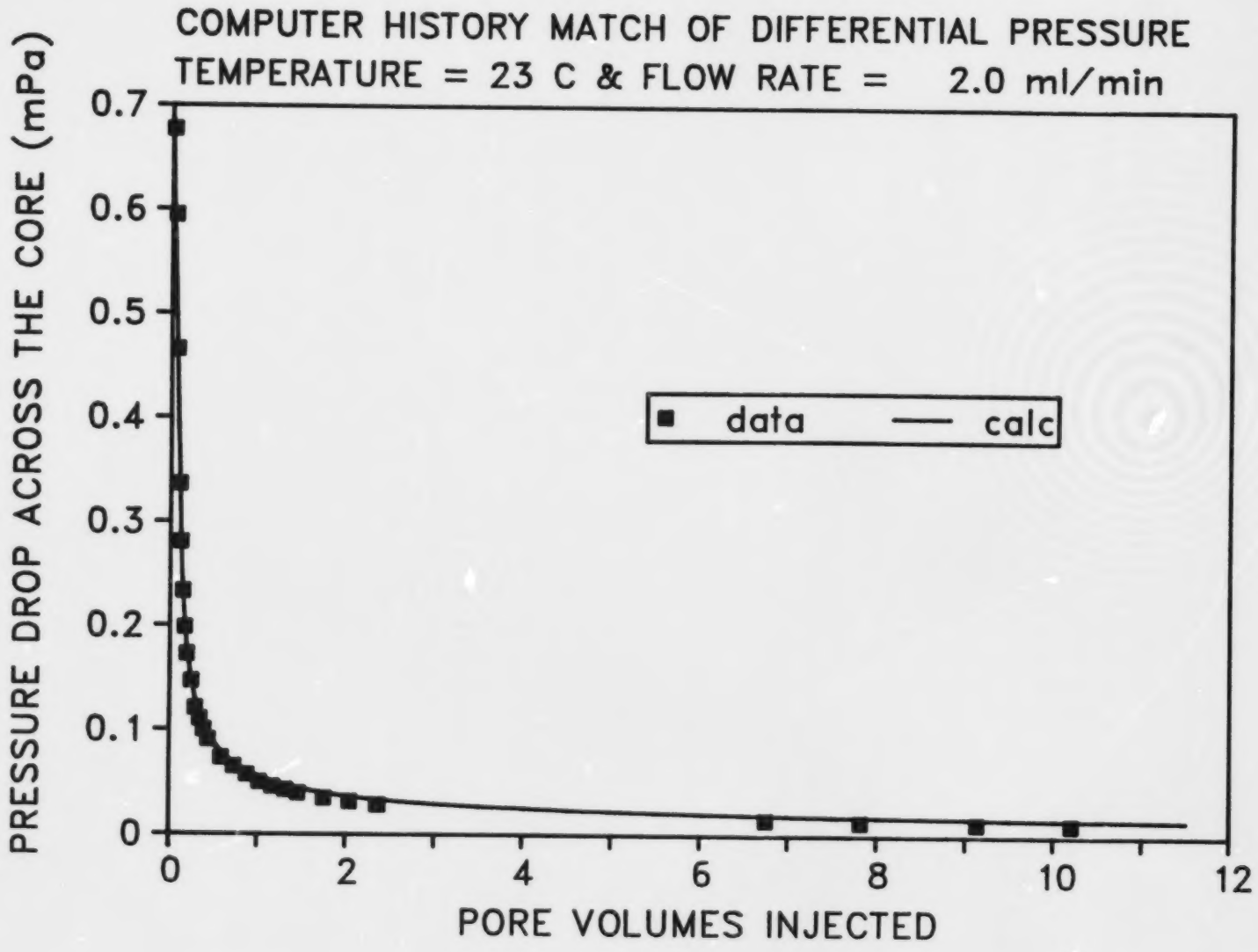
COMPUTER HISTORY MATCH OF DIFFERENTIAL PRESSURE
TEMPERATURE = 23 C & FLOW RATE = 2.0 ml/min
PRESSURE DROP ACROSS THE CORE (mPa)
0.7
0.6
0.5
0.4
0.3
0.2
0.1
0
data
calc
0
2
4
6
8
10
12
PORE VOLUMES INJECTED

FIGURE 13

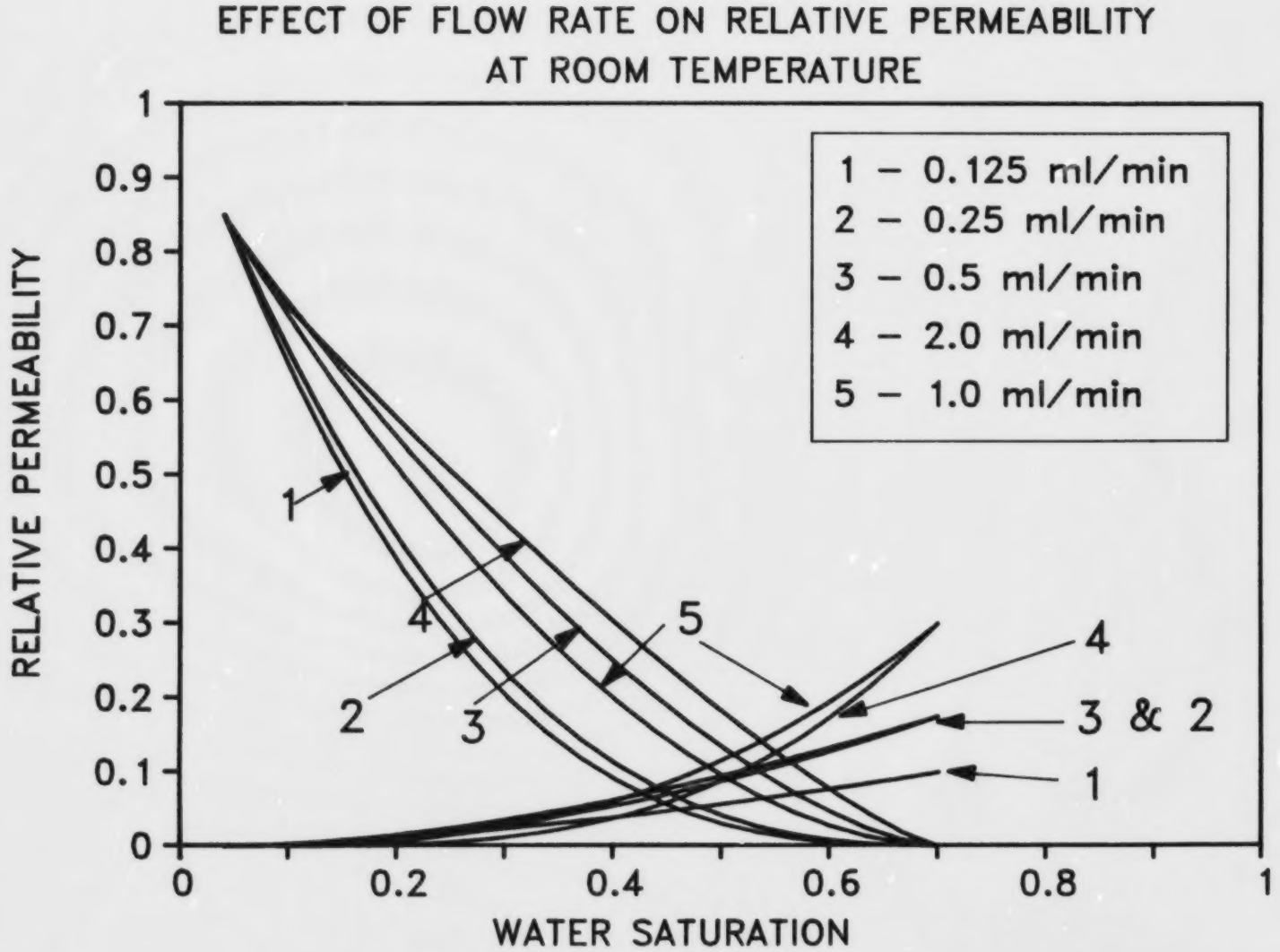
EFFECT OF FLOW RATE ON RELATIVE PERMEABILITY
AT ROOM TEMPERATURE
1 – 0.125 ml/min
2 – 0.25 ml/min
3 – 0.5 ml/min
4 – 2.0 ml/min
5 – 1.0 ml/min
RELATIVE PERMEABILITY
WATER SATURATION
0
0.1
0.2
0.3
0.4
0.5
0.6
0.7
0.8
0.9
1
0.2
0.4
0.6
0.8
1
1
2
3
4
5
3 & 2

FIGURE 14

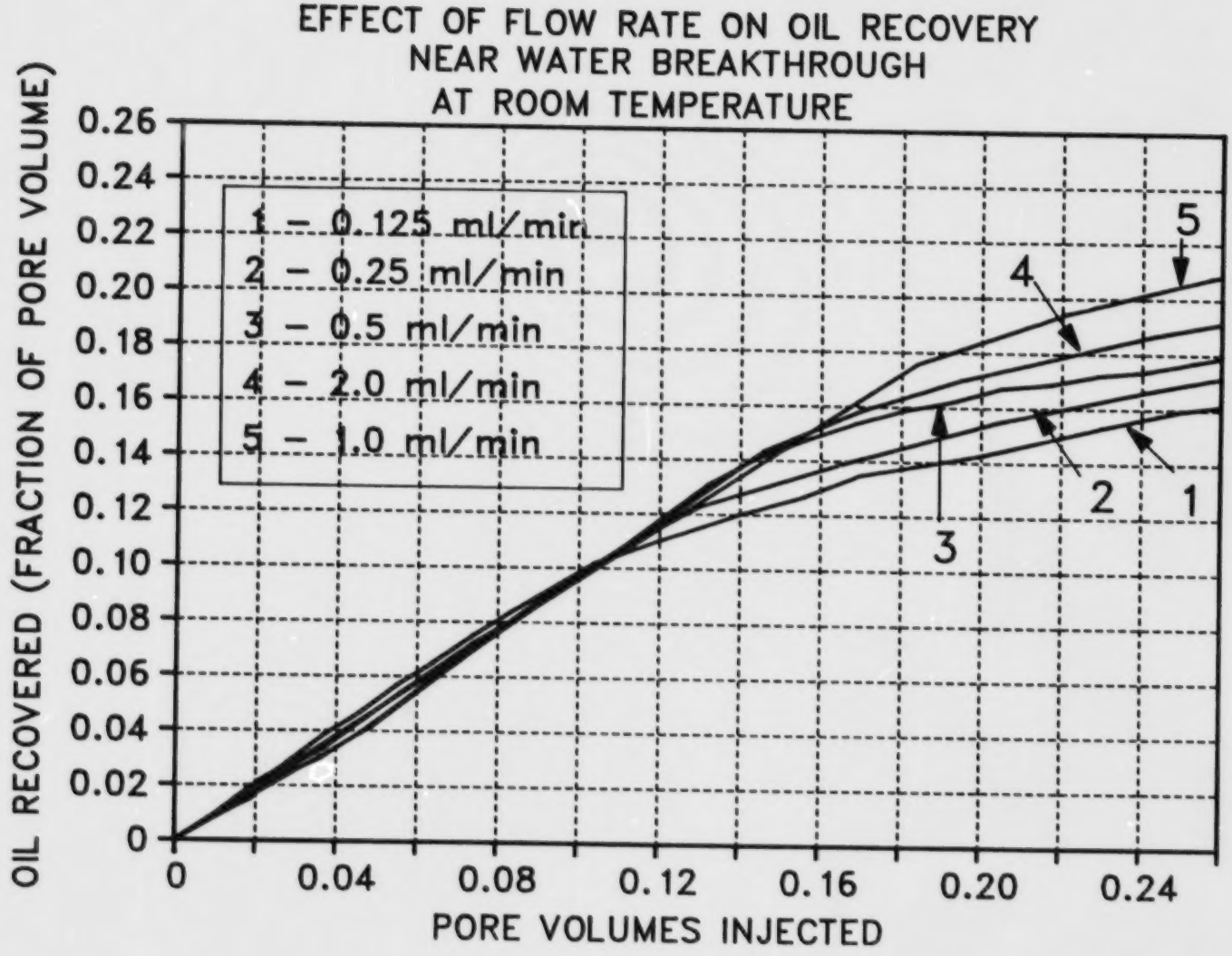
EFFECT OF FLOW RATE ON OIL RECOVERY
NEAR WATER BREAKTHROUGH
AT ROOM TEMPERATURE
OIL RECOVERED (FRACTION OF PORE VOLUME)
0.26
0.24
0.22
0.20
0.18
0.16
0.14
0.12
0.10
0.08
0.06
0.04
0.02
0
1 - 0.125 ml/min
2 - 0.25 ml/min
3 - 0.5 ml/min
4 - 2.0 ml/min
5 - 1.0 ml/min
5
4
2
1
3
0
0.04
0.08
0.12
0.16
0.20
0.24
PORE VOLUMES INJECTED

Figure 15

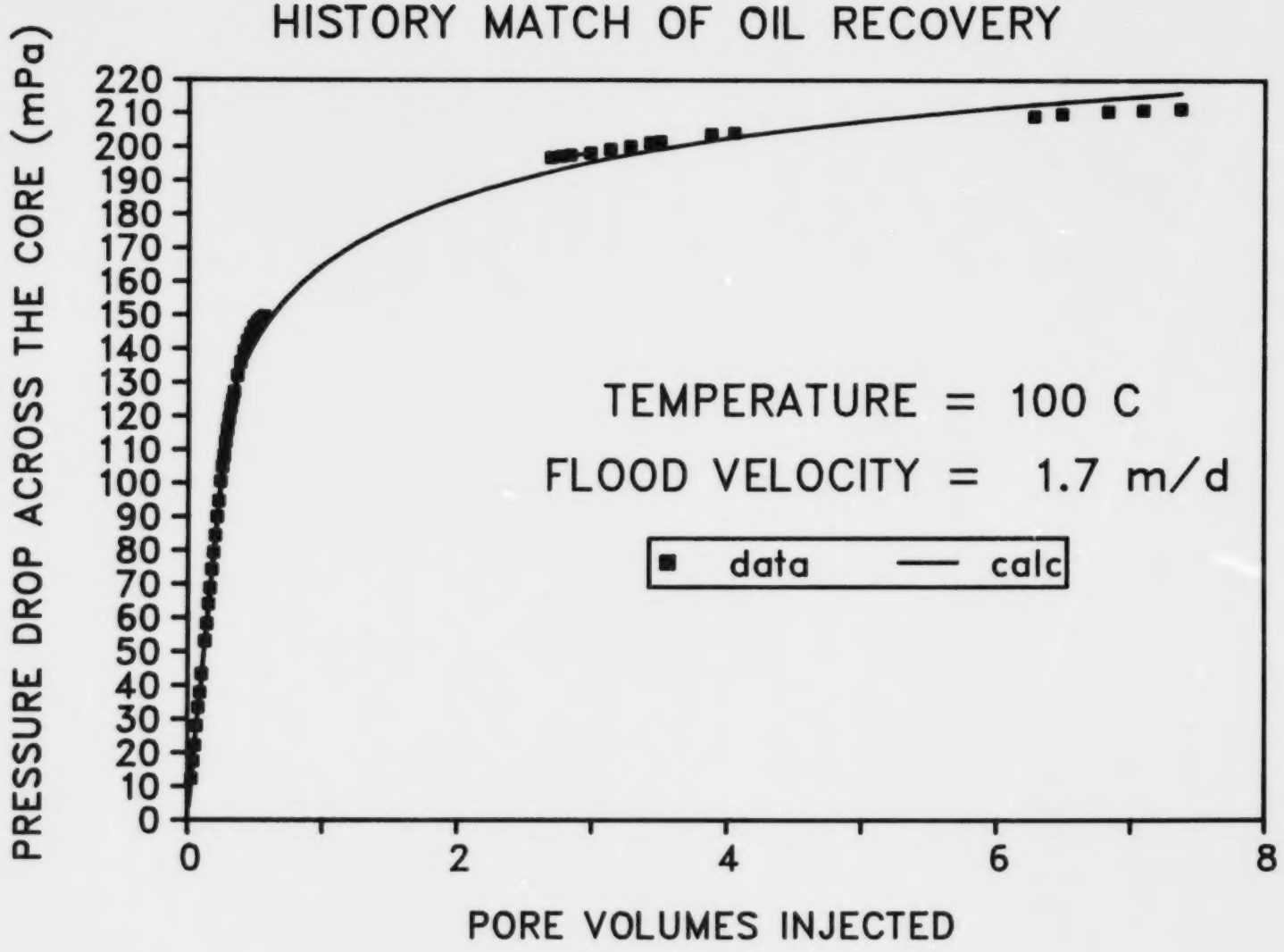
HISTORY MATCH OF OIL RECOVERY
PRESSURE DROP ACROSS THE CORE (mPa)
220
210
200
190
180
170
160
150
140
130
120
110
100
90
80
70
60
50
40
30
20
10
0
0
2
4
6
8
PORE VOLUMES INJECTED
TEMPERATURE = 100 C
FLOOD VELOCITY = 1.7 m/d
data
calc

Figure 16

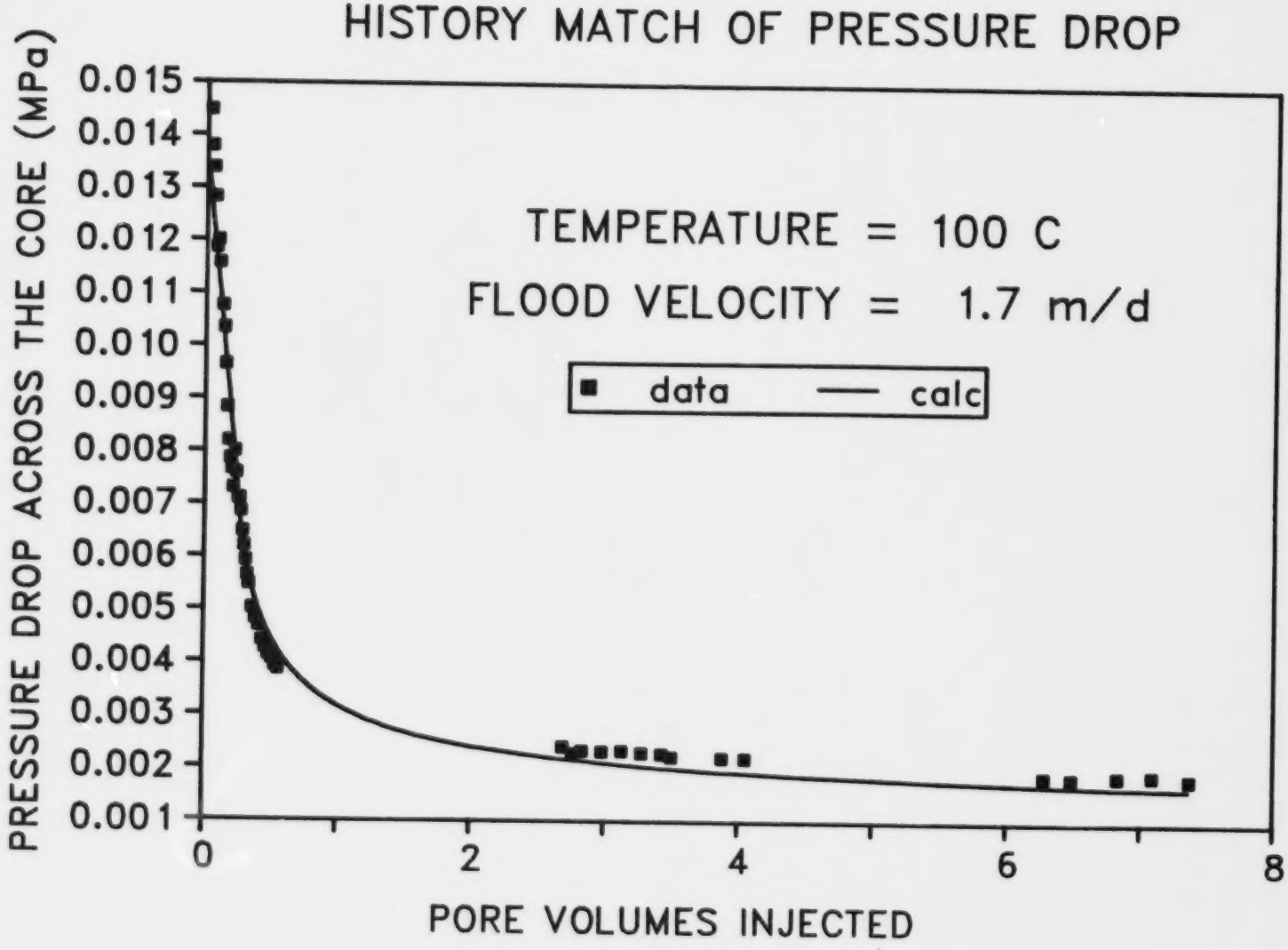
HISTORY MATCH OF PRESSURE DROP
TEMPERATURE = 100 C
FLOOD VELOCITY = 1.7 m/d
data
calc
PRESSURE DROP ACROSS THE CORE (MPa)
0.015
0.014
0.013
0.012
0.011
0.010
0.009
0.008
0.007
0.006
0.005
0.004
0.003
0.002
0.001
0
2
4
6
8
PORE VOLUMES INJECTED

Figure 17

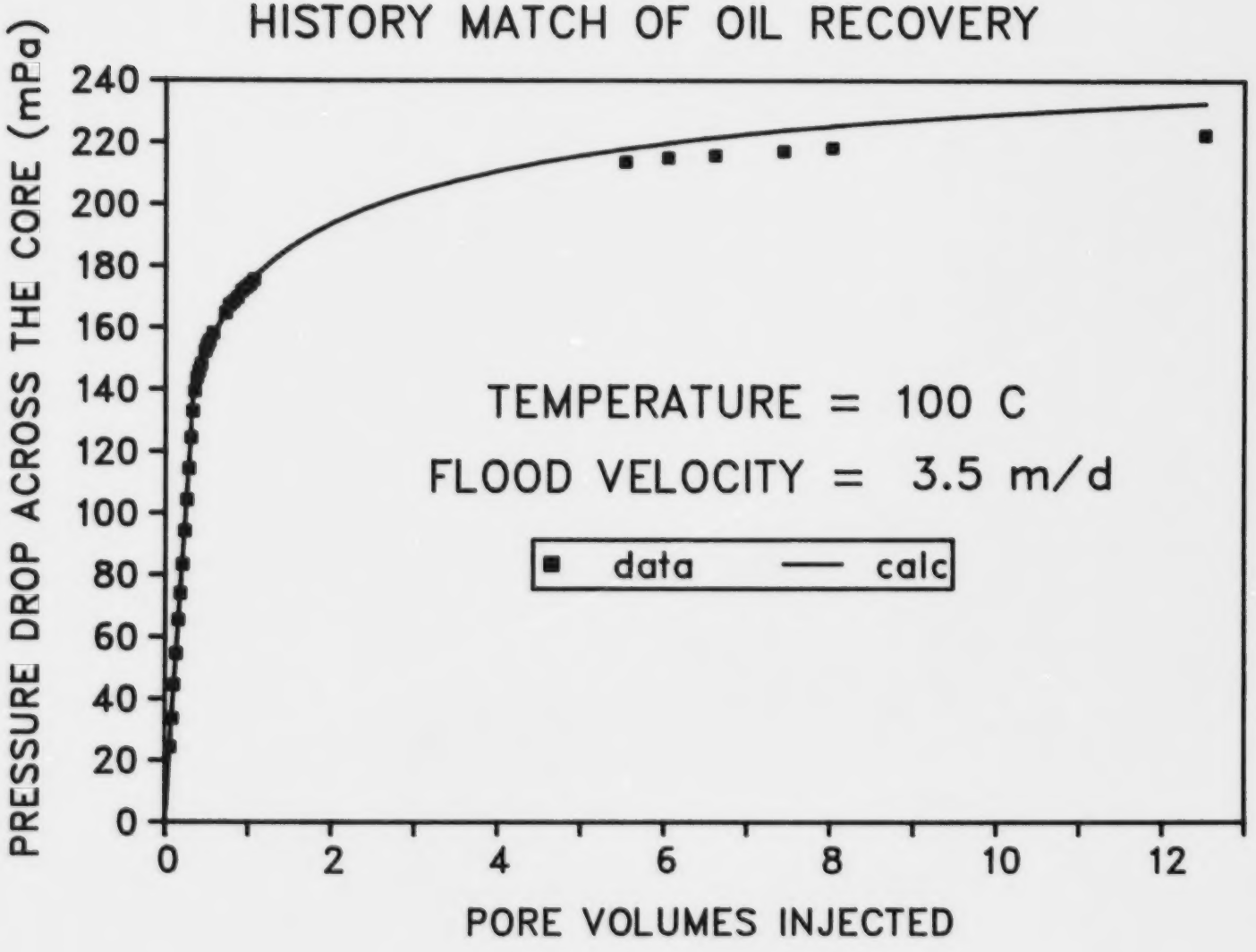
HISTORY MATCH OF OIL RECOVERY
PRESSURE DROP ACROSS THE CORE (mPa)
240
220
200
180
160
140
120
100
80
60
40
20
0
0
2
4
6
8
10
12
PORE VOLUMES INJECTED
TEMPERATURE = 100 C
FLOOD VELOCITY = 3.5 m/d
data
calc

Figure 18

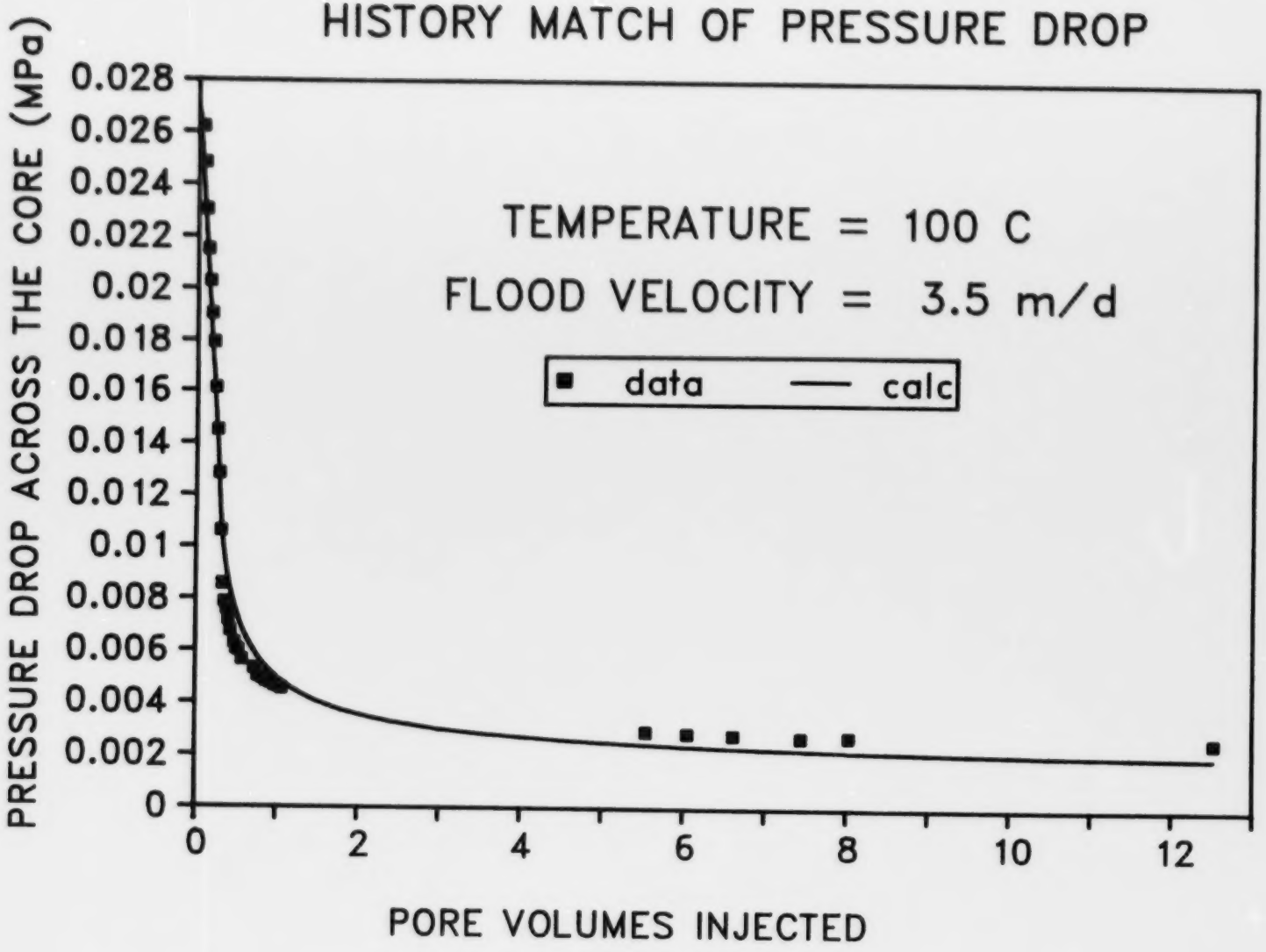
HISTORY MATCH OF PRESSURE DROP
TEMPERATURE = 100 C
FLOOD VELOCITY = 3.5 m/d
data
calc
PRESSURE DROP ACROSS THE CORE (MPa)
0.028
0.026
0.024
0.022
0.02
0.018
0.016
0.014
0.012
0.01
0.008
0.006
0.004
0.002
0
0
2
4
6
8
10
12
PORE VOLUMES INJECTED

Figure 19

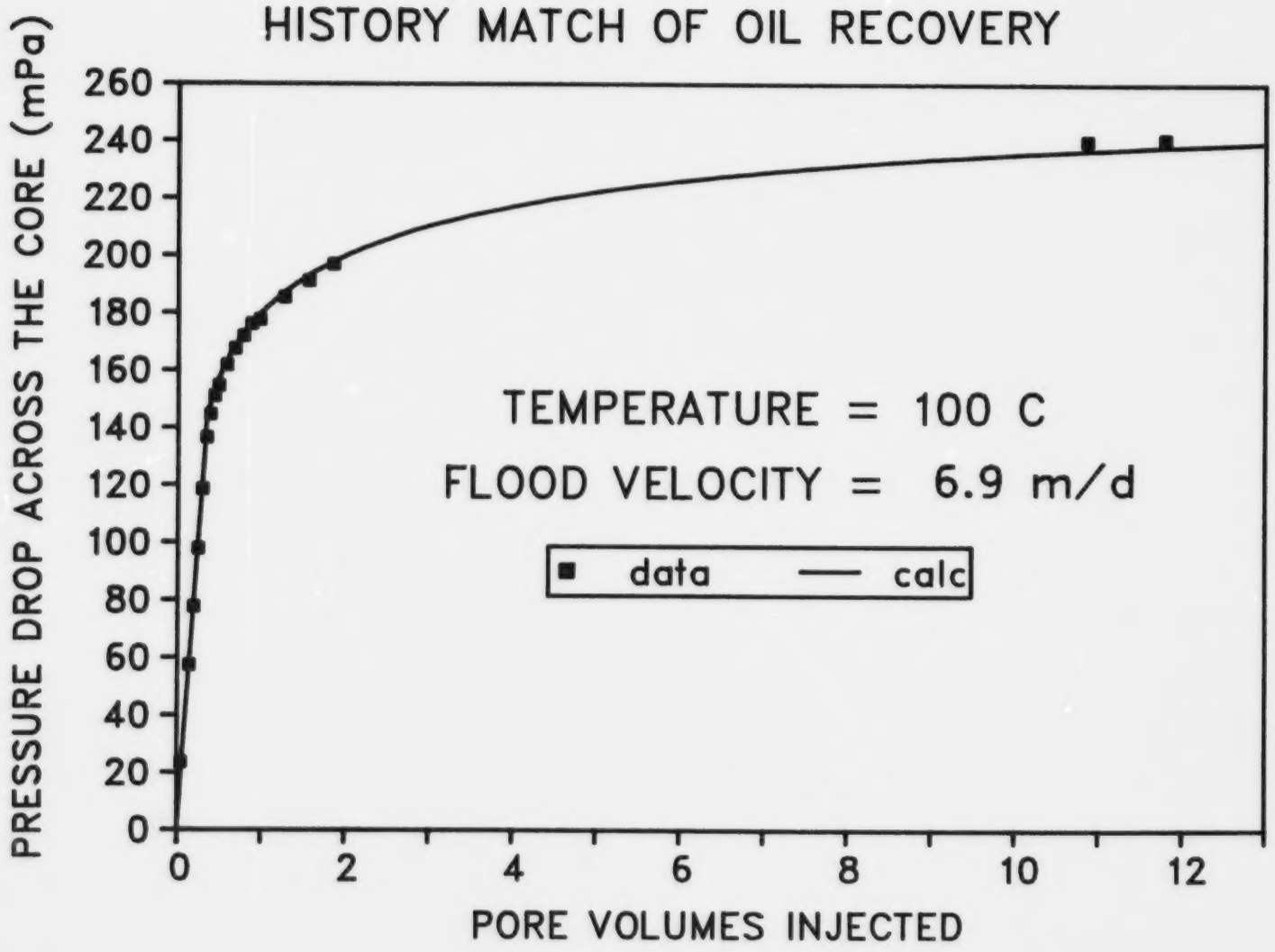
HISTORY MATCH OF OIL RECOVERY
PRESSURE DROP ACROSS THE CORE (mPa)
260
240
220
200
180
160
140
120
100
80
60
40
20
0
0
2
4
6
8
10
12
PORE VOLUMES INJECTED
TEMPERATURE = 100 C
FLOOD VELOCITY = 6.9 m/d
data
calc

Figure 20

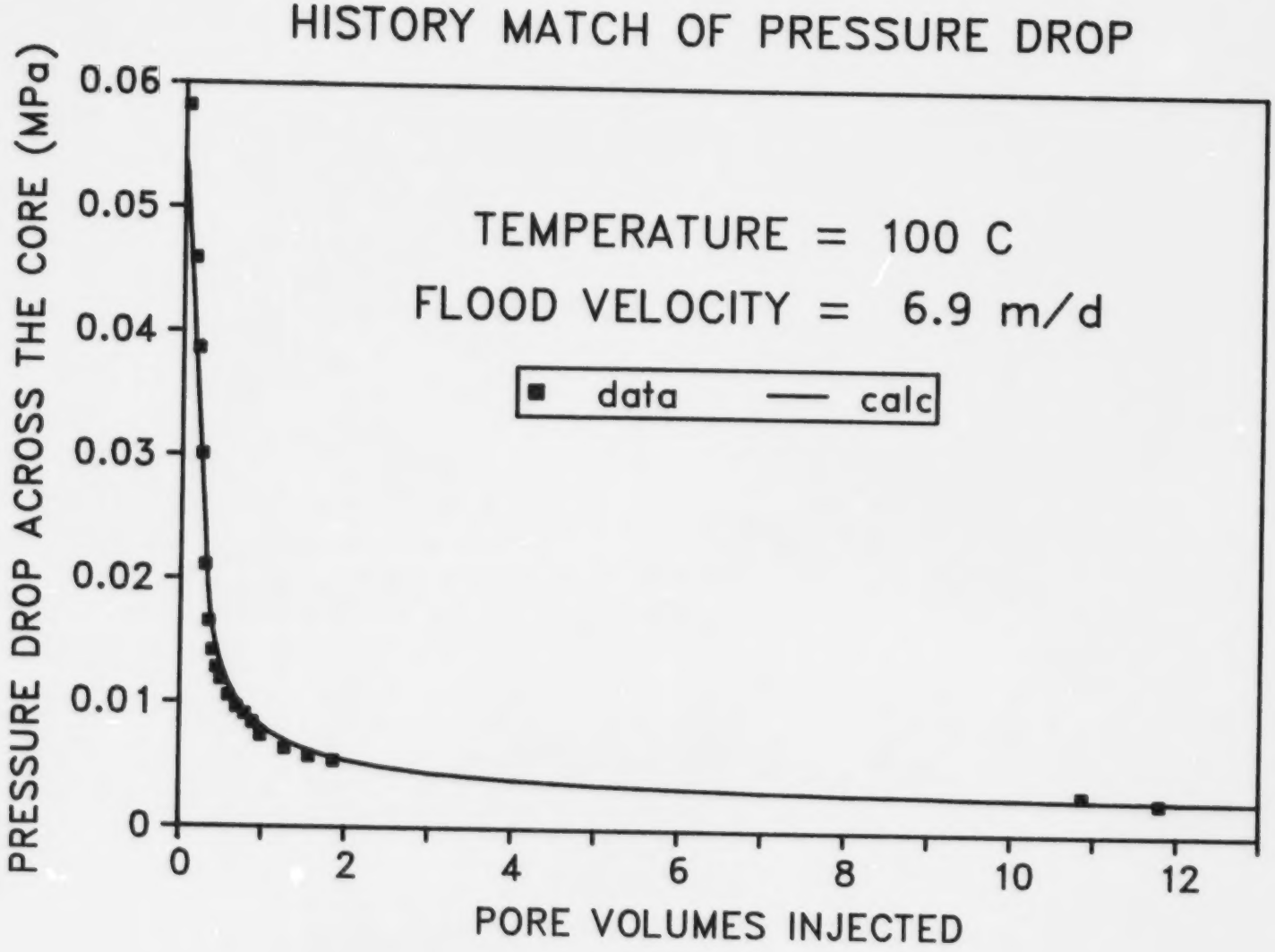
HISTORY MATCH OF PRESSURE DROP
TEMPERATURE = 100 C
FLOOD VELOCITY = 6.9 m/d
data
calc
PRESSURE DROP ACROSS THE CORE (MPa)
0.06
0.05
0.04
0.03
0.02
0.01
0
0
2
4
6
8
10
12
PORE VOLUMES INJECTED

Figure 21

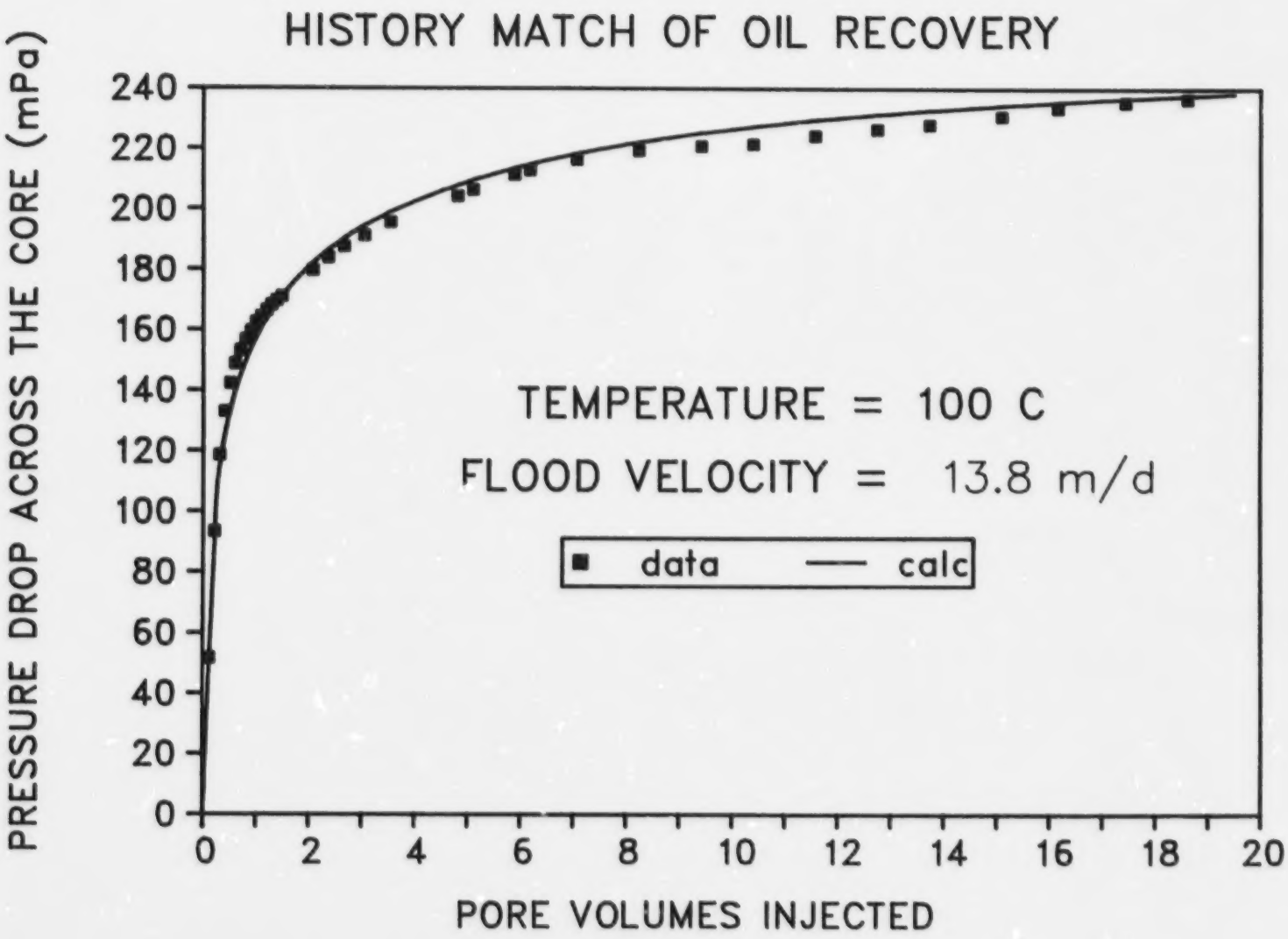
HISTORY MATCH OF OIL RECOVERY
PRESSURE DROP ACROSS THE CORE (mPa)
240
220
200
180
160
140
120
100
80
60
40
20
0
0
2
4
6
8
10
12
14
16
18
20
PORE VOLUMES INJECTED
TEMPERATURE = 100 C
FLOOD VELOCITY = 13.8 m/d
data
calc

Figure 22

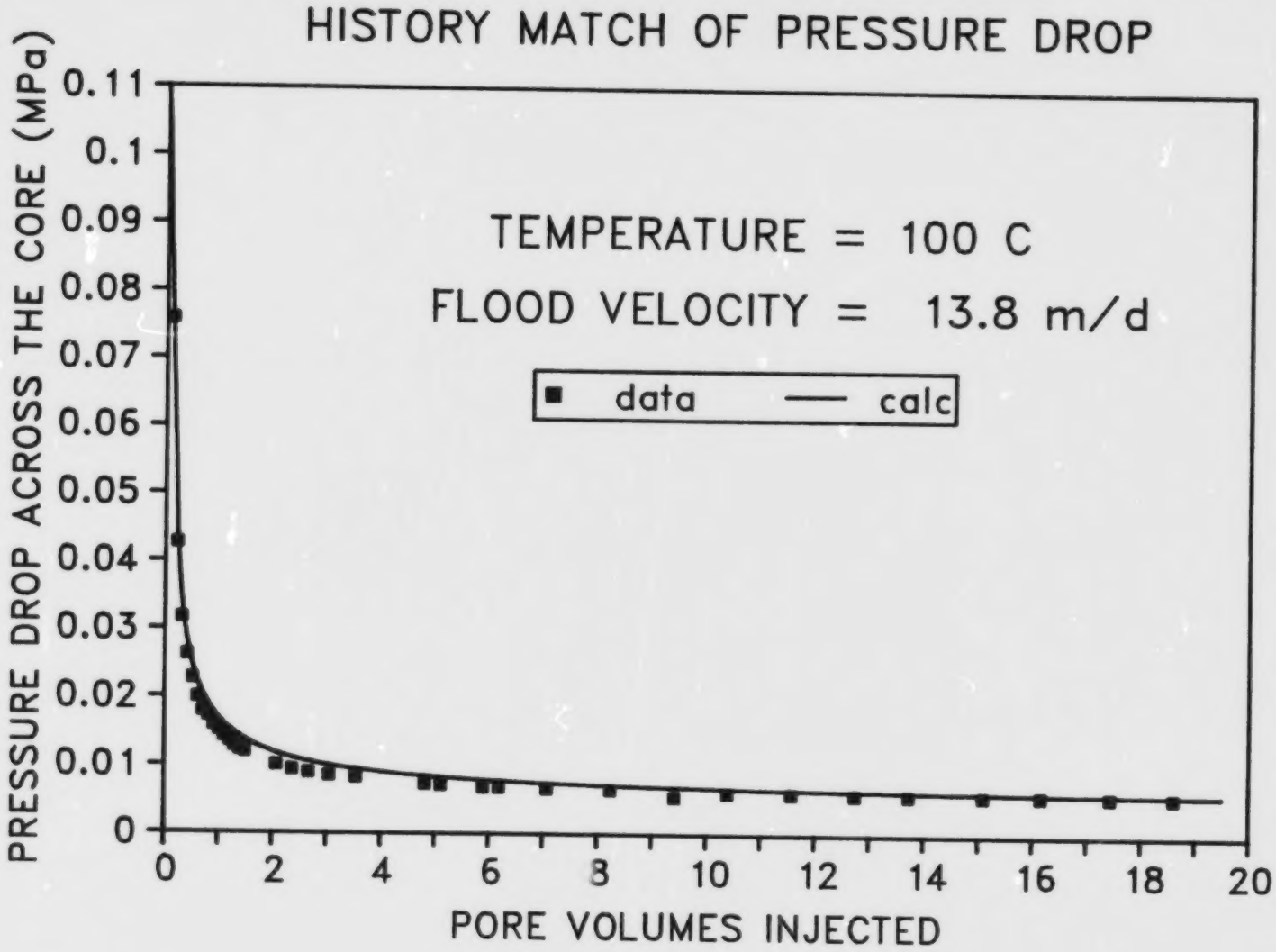
HISTORY MATCH OF PRESSURE DROP
TEMPERATURE = 100 C
FLOOD VELOCITY = 13.8 m/d
data
calc
PRESSURE DROP ACROSS THE CORE (MPa)
0.11
0.1
0.09
0.08
0.07
0.06
0.05
0.04
0.03
0.02
0.01
0
0
2
4
6
8
10
12
14
16
18
20
PORE VOLUMES INJECTED

Figure 23

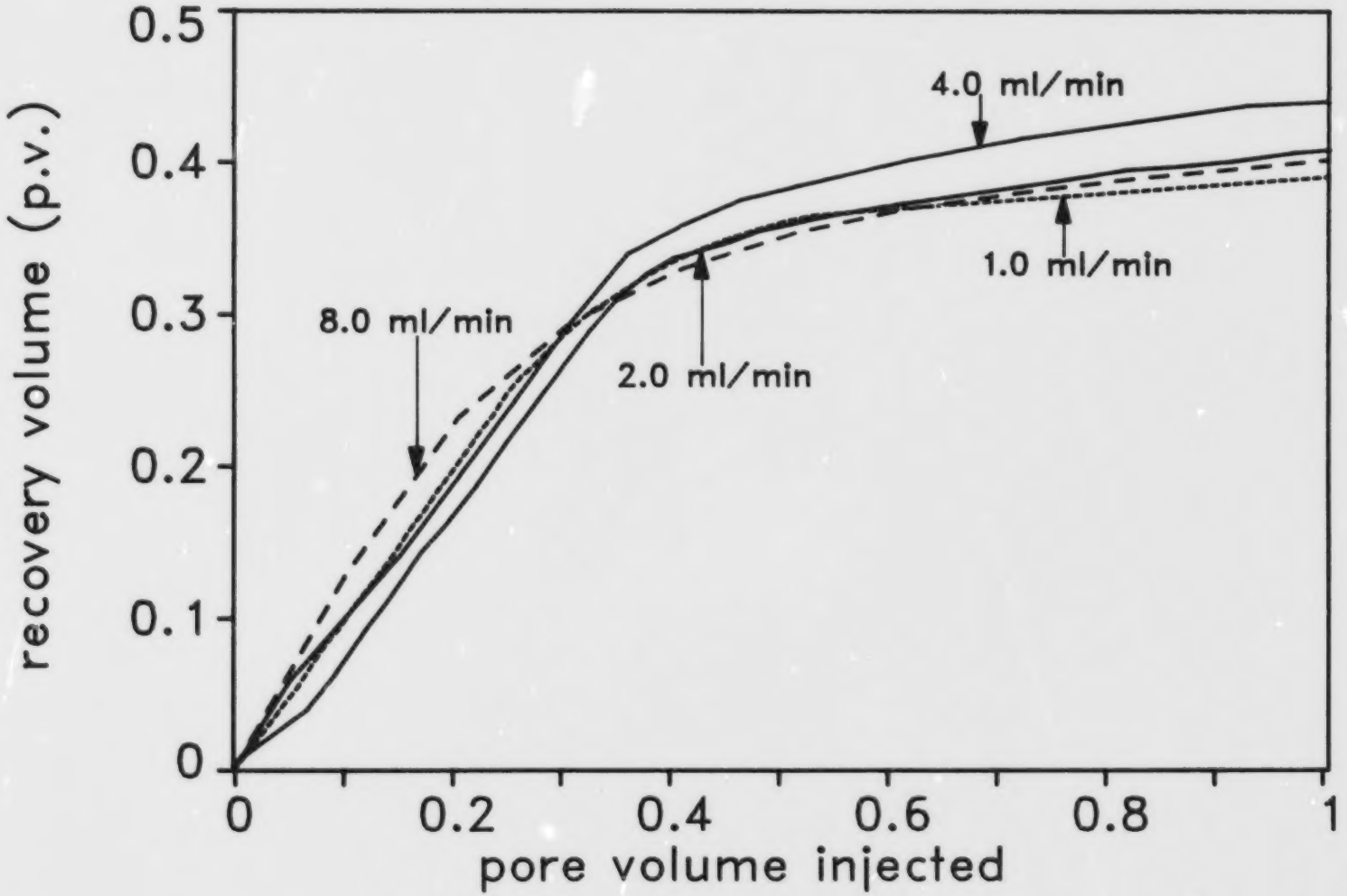
0.5
0.4
0.3
0.2
0.1
0
recovery volume (p.v.)
4.0 ml/min
1.0 ml/min
8.0 ml/min
2.0 ml/min
0
0.2
0.4
0.6
0.8
1
pore volume injected

Figure 24

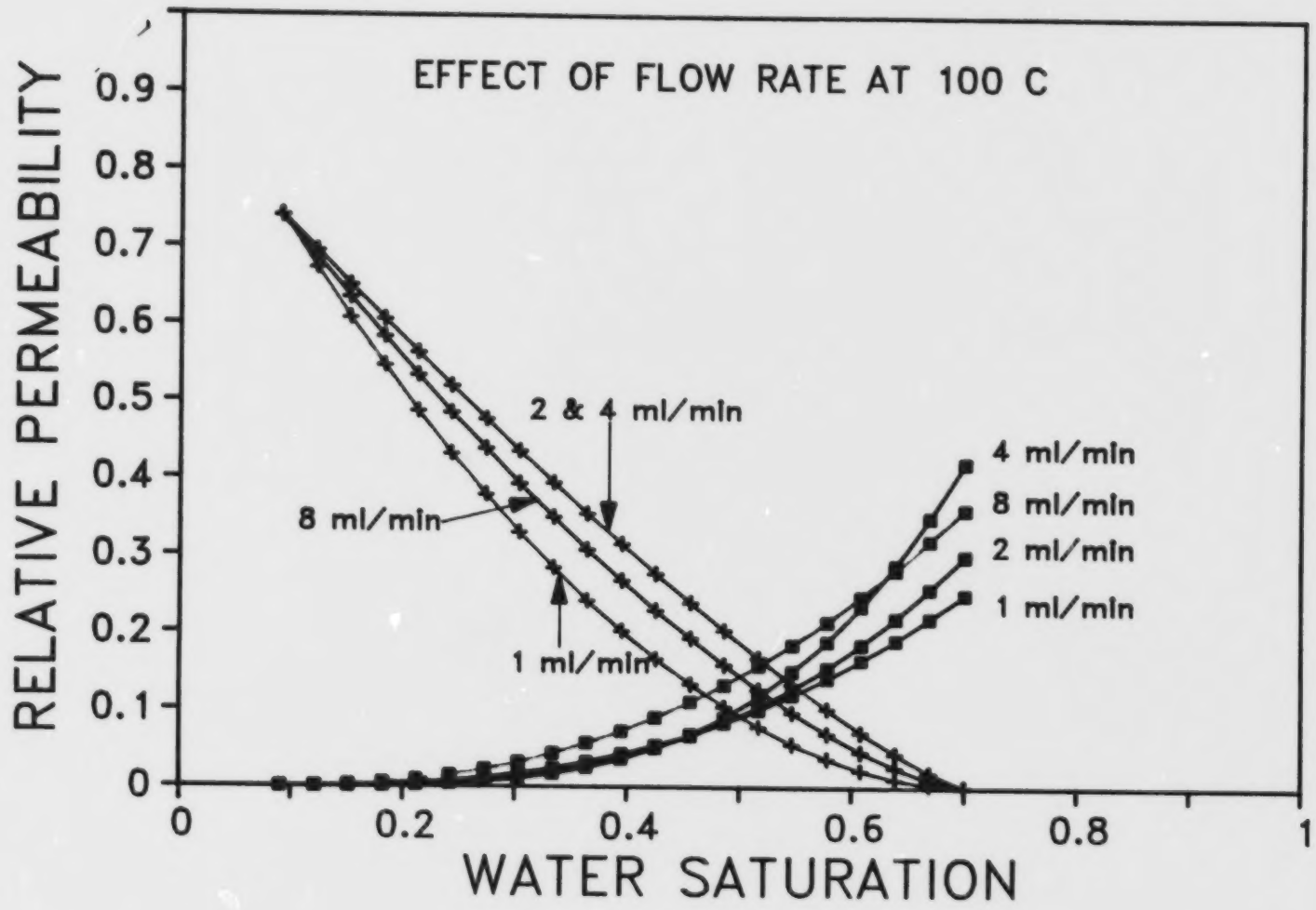
EFFECT OF FLOW RATE AT 100 C
RELATIVE PERMEABILITY
0
0.1
0.2
0.3
0.4
0.5
0.6
0.7
0.8
0.9
0
0.2
0.4
0.6
0.8
1
WATER SATURATION
2 & 4 ml/min
8 ml/min
1 ml/min
4 ml/min
8 ml/min
2 ml/min
1 ml/min

Figure 25

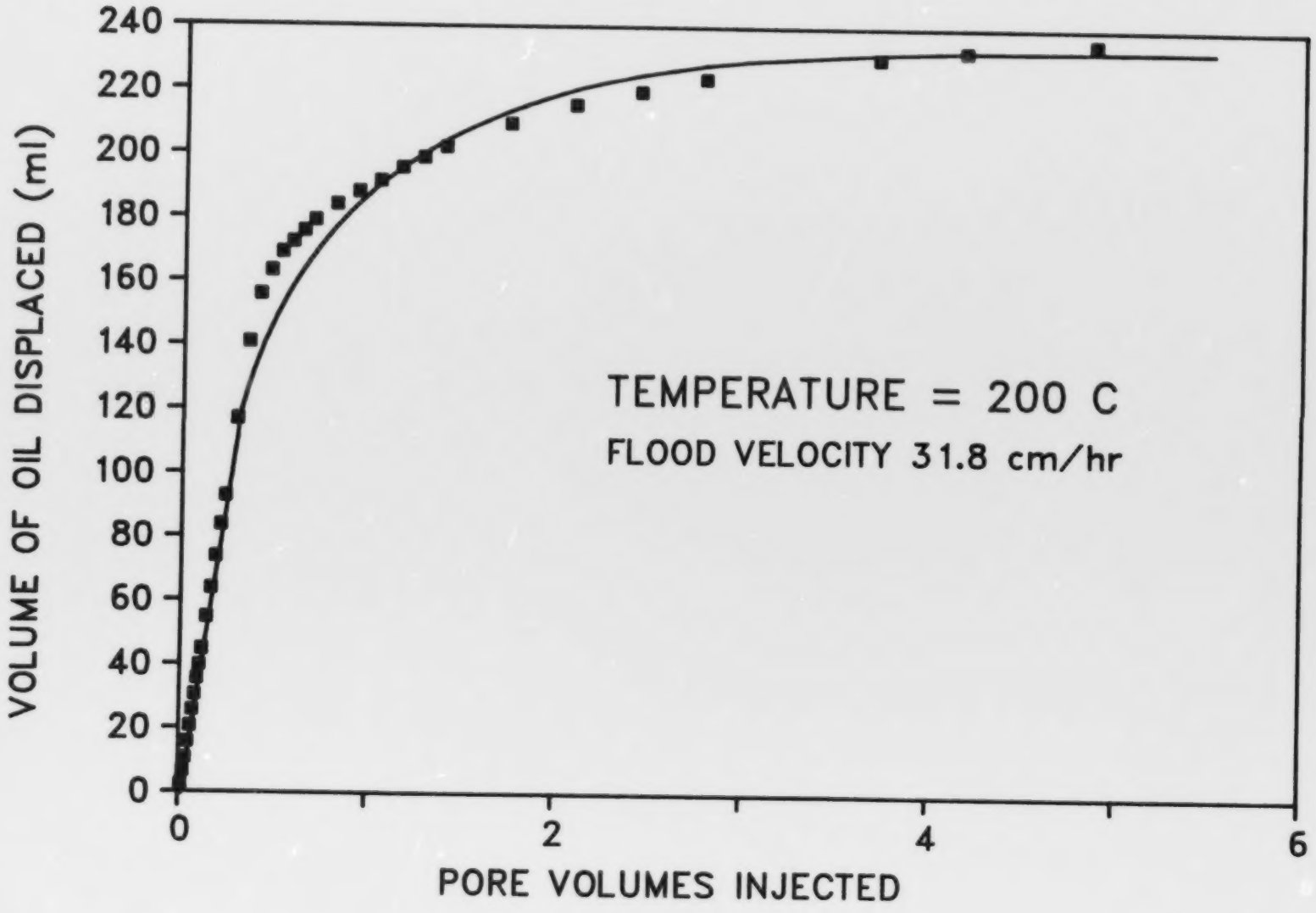
VOLUME OF OIL DISPLACED (ml)
240
220
200
180
160
140
120
100
80
60
40
20
0
0
2
4
6
PORE VOLUMES INJECTED
TEMPERATURE = 200 C
FLOOD VELOCITY 31.8 cm/hr

FIGURE 26

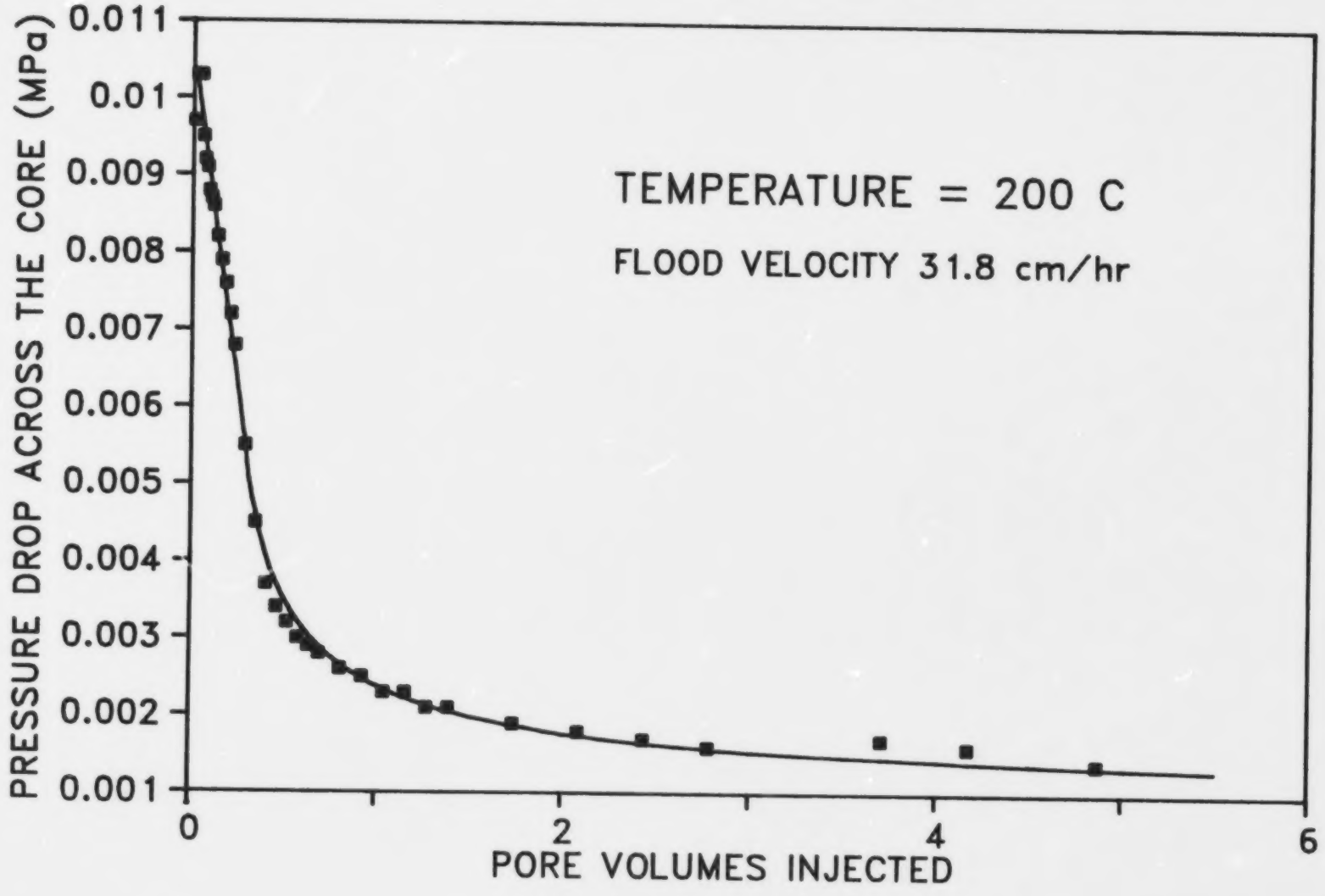
PRESSURE DROP ACROSS THE CORE (MPa)
0.011
0.01
0.009
0.008
0.007
0.006
0.005
0.004
0.003
0.002
0.001
TEMPERATURE = 200 C
FLOOD VELOCITY 31.8 cm/hr
0
2
4
6
PORE VOLUMES INJECTED

FIGURE 27

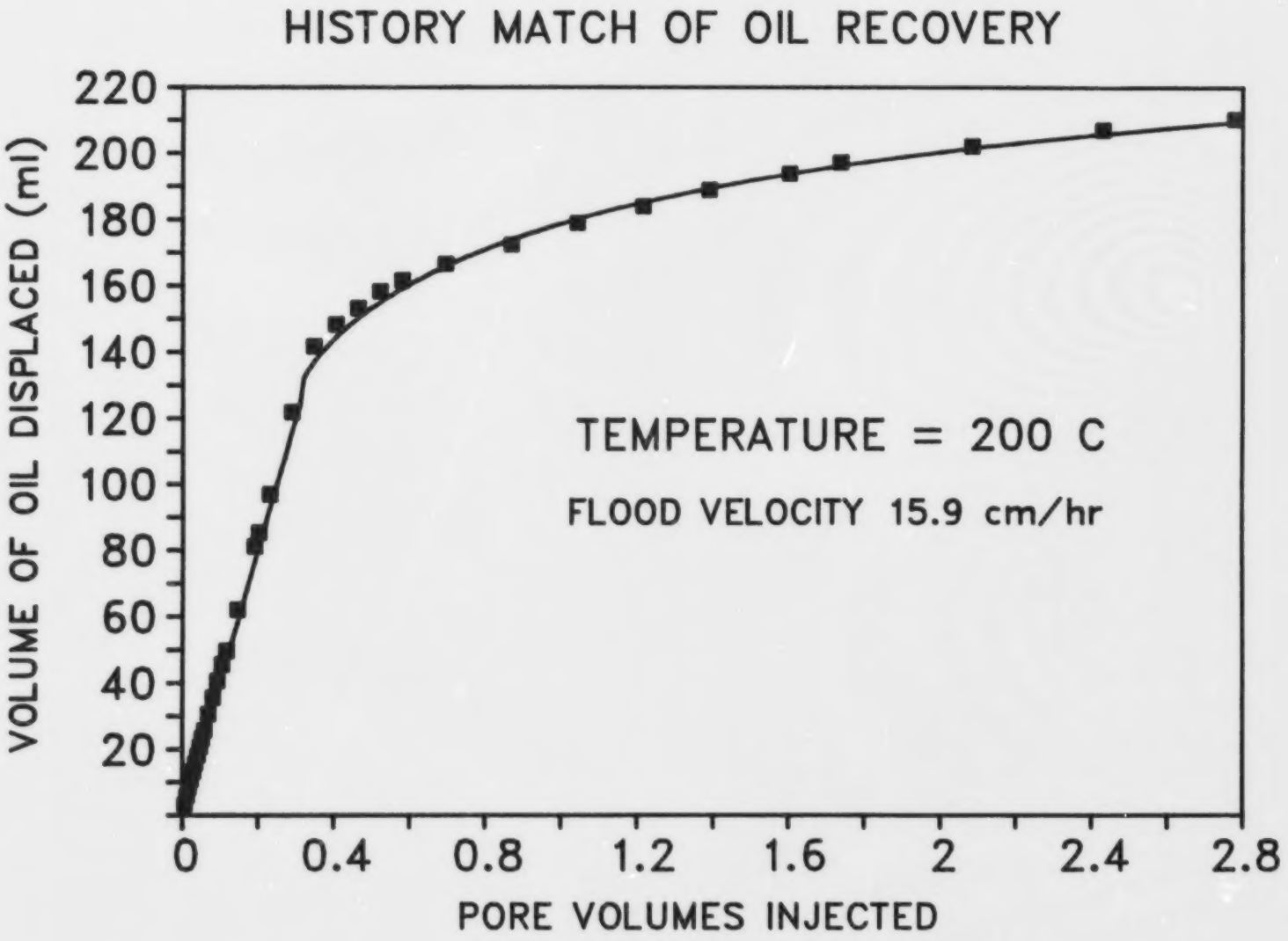
HISTORY MATCH OF OIL RECOVERY
VOLUME OF OIL DISPLACED (ml)
220
200
180
160
140
120
100
80
60
40
20
0
0.4
0.8
1.2
1.6
2
2.4
2.8
PORE VOLUMES INJECTED
TEMPERATURE = 200 C
FLOOD VELOCITY 15.9 cm/hr

FIGURE 28

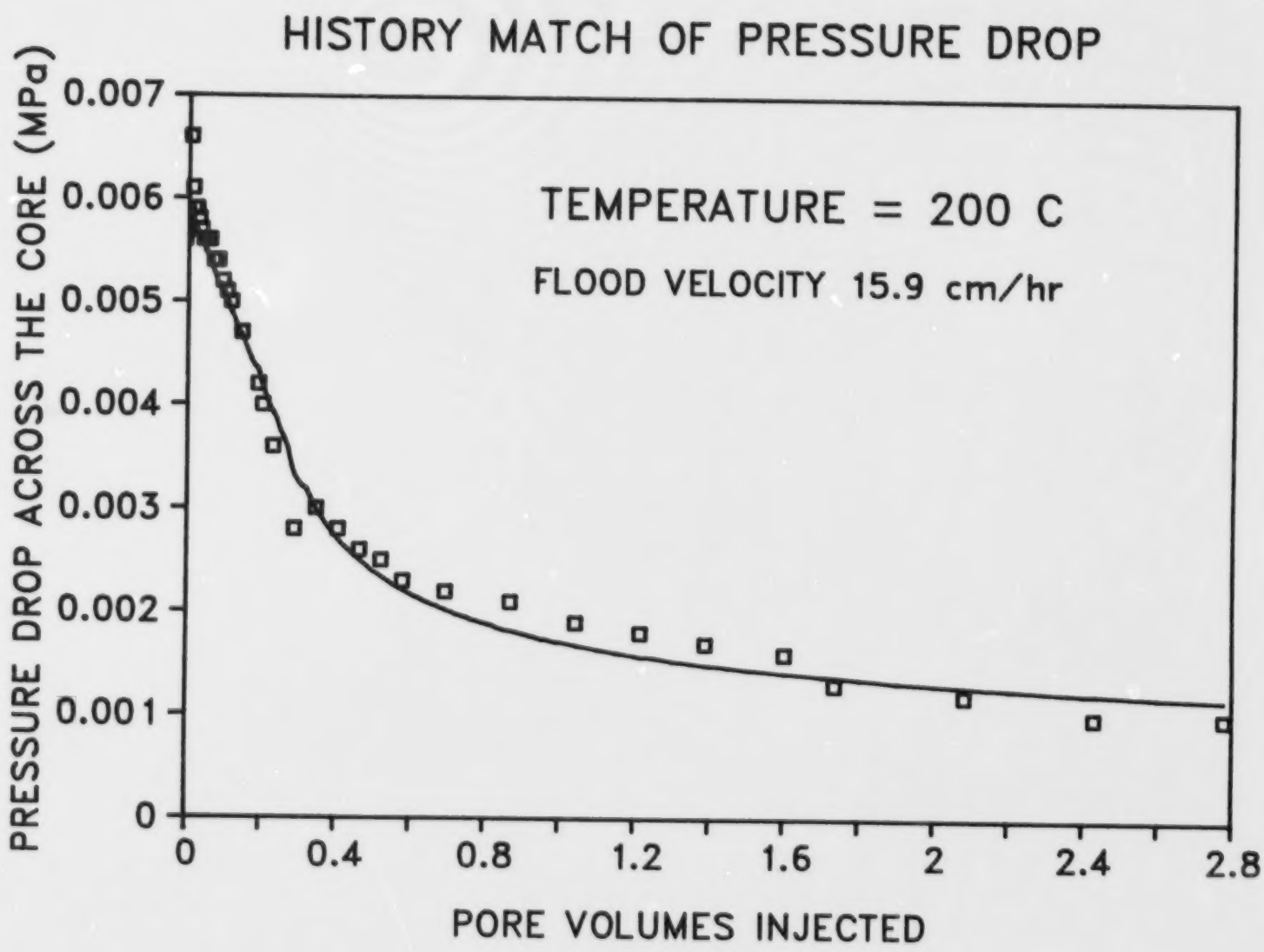
HISTORY MATCH OF PRESSURE DROP
TEMPERATURE = 200 C
FLOOD VELOCITY 15.9 cm/hr
PRESSURE DROP ACROSS THE CORE (MPa)
0.007
0.006
0.005
0.004
0.003
0.002
0.001
0
0
0.4
0.8
1.2
1.6
2
2.4
2.8
PORE VOLUMES INJECTED

FIGURE 29

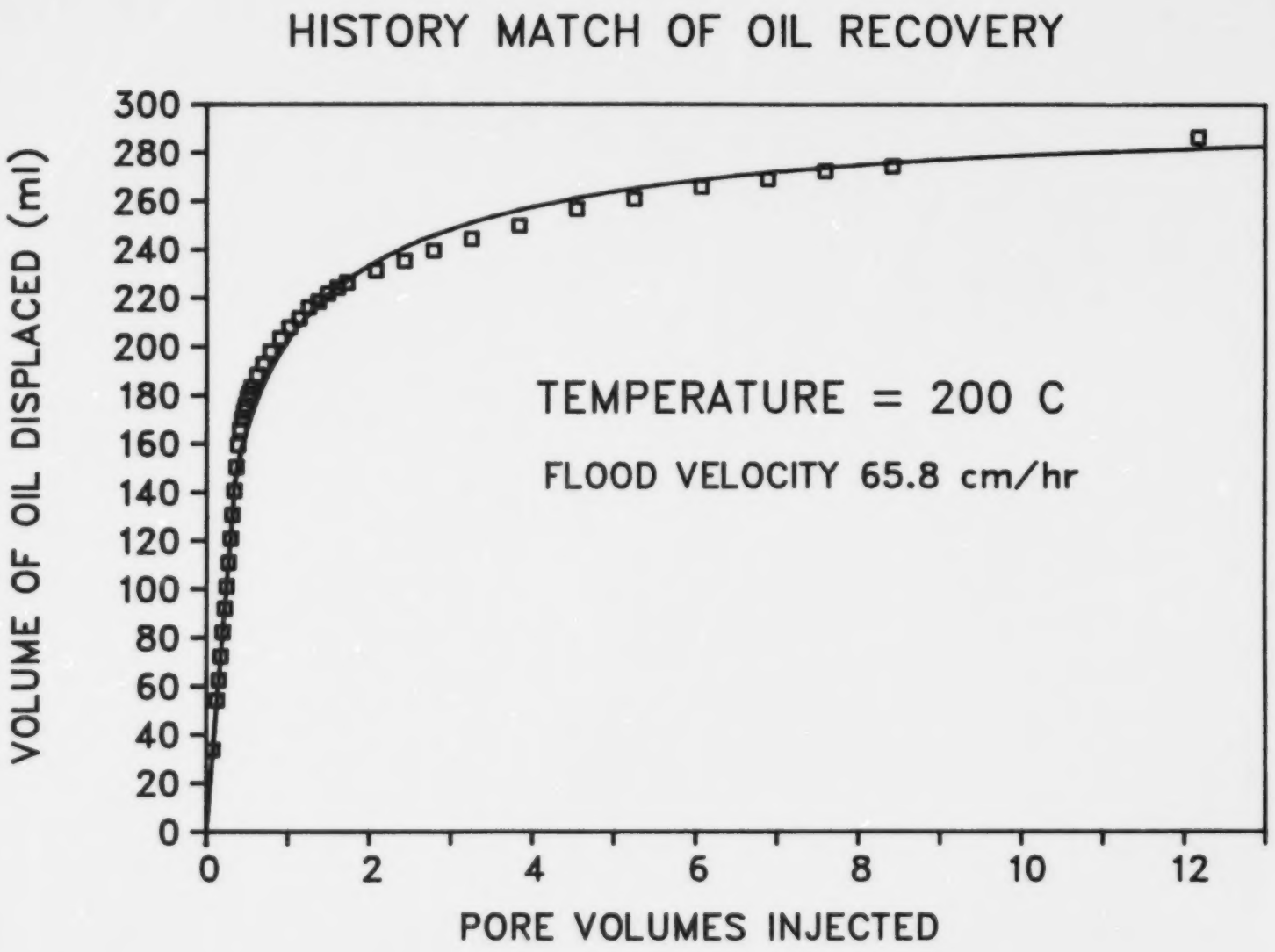
HISTORY MATCH OF OIL RECOVERY
VOLUME OF OIL DISPLACED (ml)
300
280
260
240
220
200
180
160
140
120
100
80
60
40
20
0
0
2
4
6
8
10
12
PORE VOLUMES INJECTED
TEMPERATURE = 200 C
FLOOD VELOCITY 65.8 cm/hr

FIGURE 30

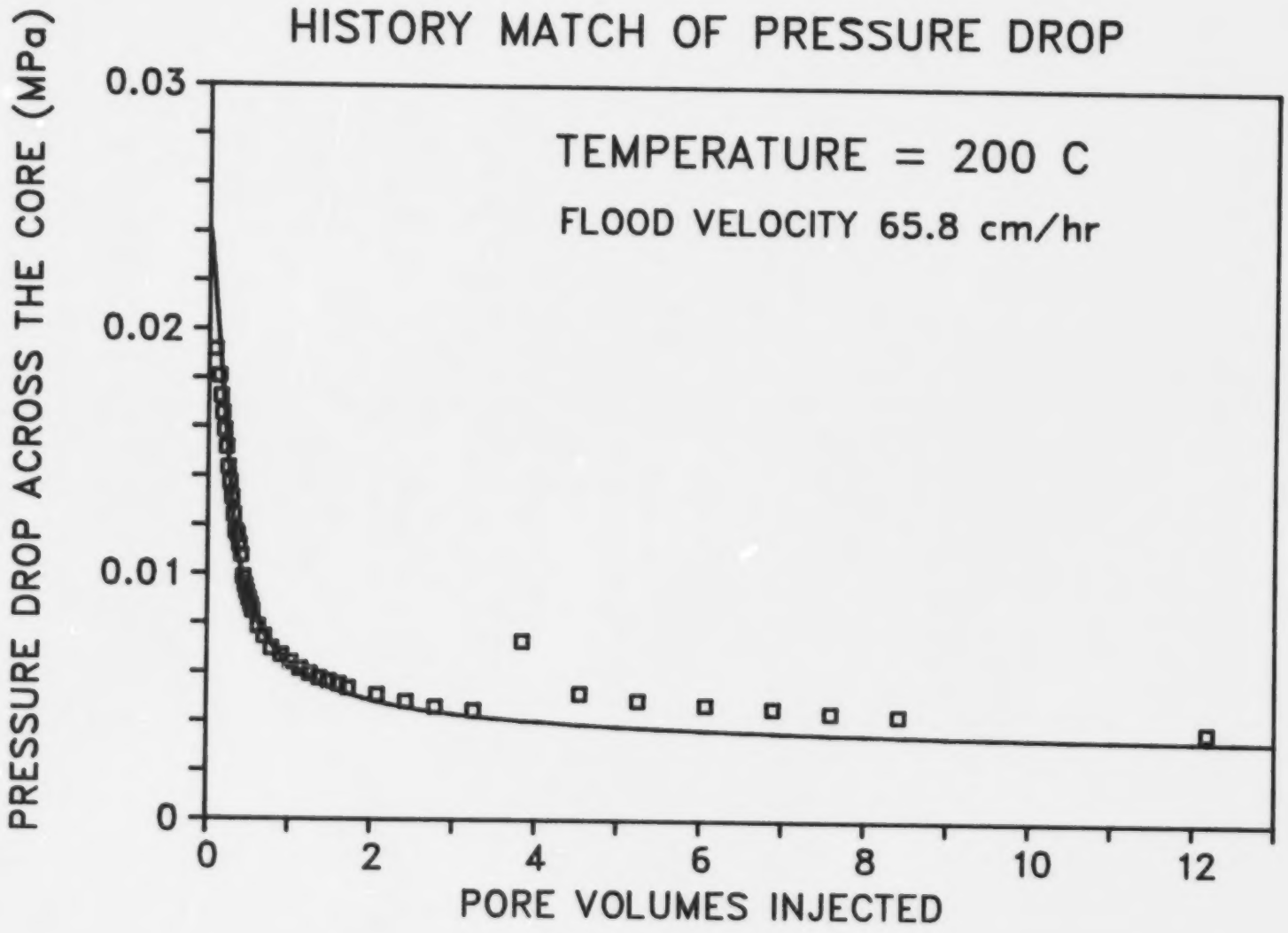
HISTORY MATCH OF PRESSURE DROP
TEMPERATURE = 200 C
FLOOD VELOCITY 65.8 cm/hr
PRESSURE DROP ACROSS THE CORE (MPa)
0.03
0.02
0.01
0
0
2
4
6
8
10
12
PORE VOLUMES INJECTED

FIGURE 31

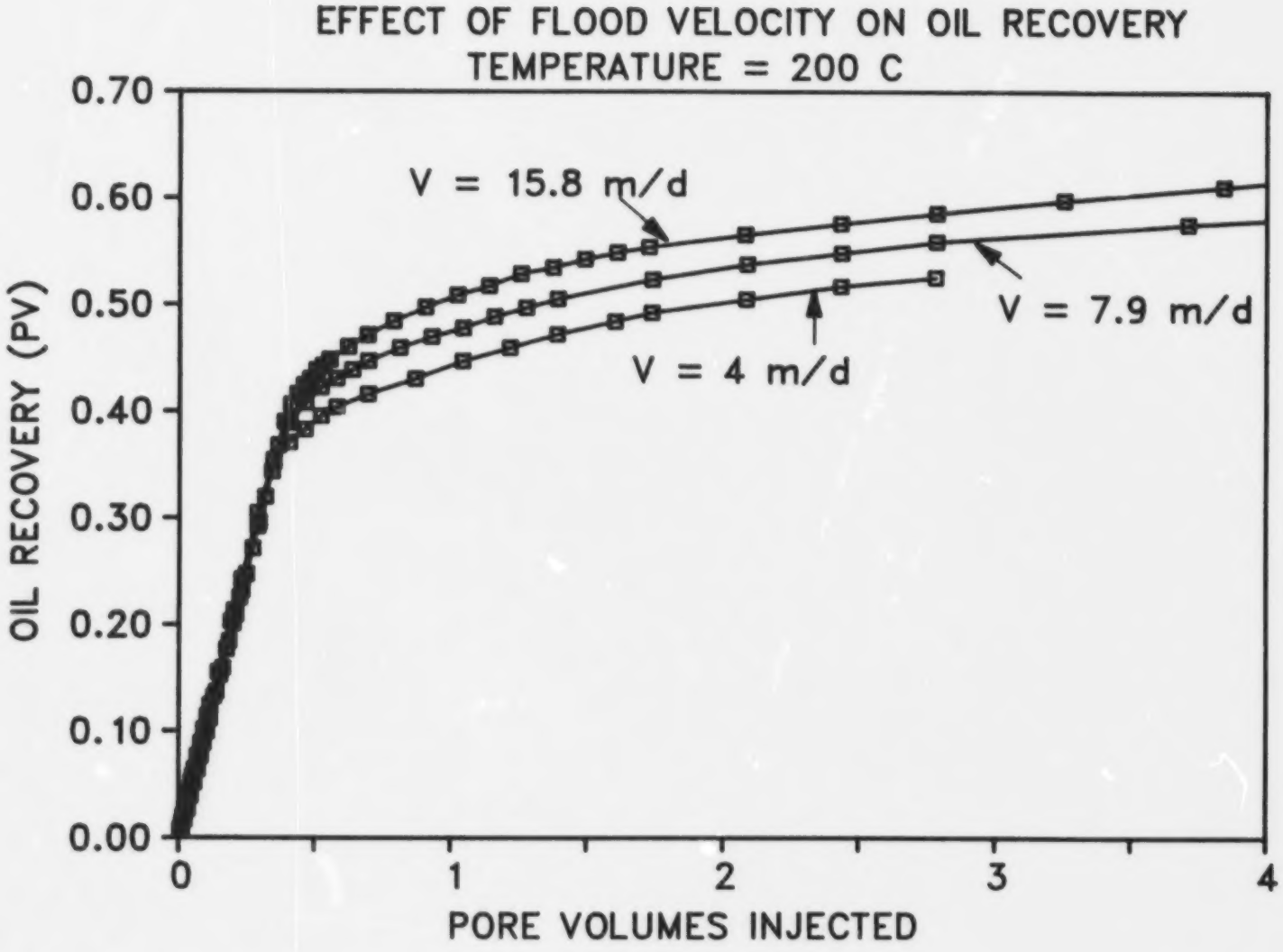
EFFECT OF FLOOD VELOCITY ON OIL RECOVERY
TEMPERATURE = 200 C
OIL RECOVERY (PV)
0.70
0.60
0.50
0.40
0.30
0.20
0.10
0.00
V = 15.8 m/d
V = 7.9 m/d
V = 4 m/d
0
1
2
3
4
PORE VOLUMES INJECTED

FIGURE 32

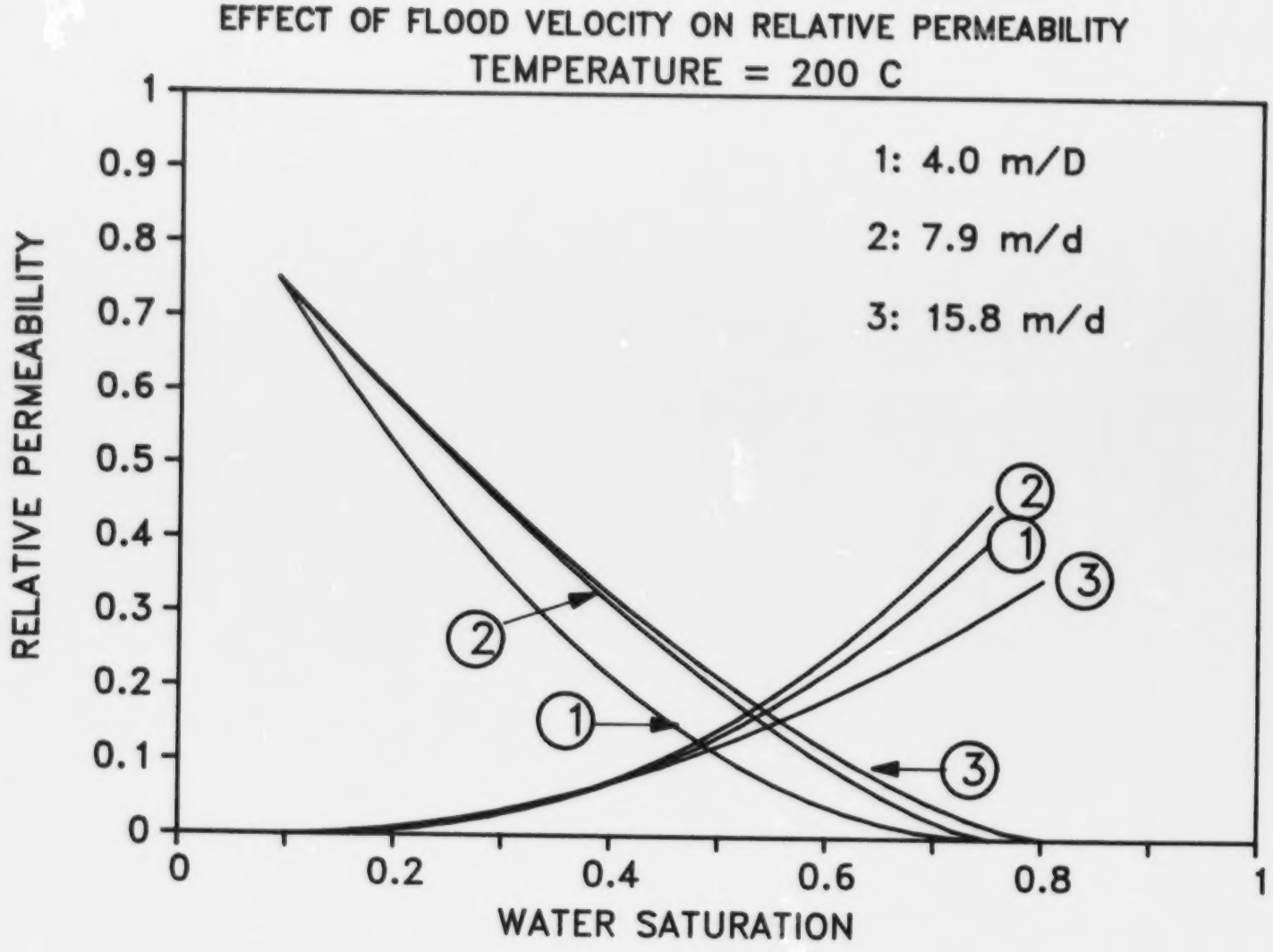
EFFECT OF FLOOD VELOCITY ON RELATIVE PERMEABILITY
TEMPERATURE = 200 C
1: 4.0 m/D
2: 7.9 m/d
3: 15.8 m/d
RELATIVE PERMEABILITY
WATER SATURATION
0
0.1
0.2
0.3
0.4
0.5
0.6
0.7
0.8
0.9
1
0
0.2
0.4
0.6
0.8
1
1
2
3

FIGURE 33

COMPARISON OF STEADY STATE AND DISPLACEMENT TESTS
AT ROOM TEMPERATURE

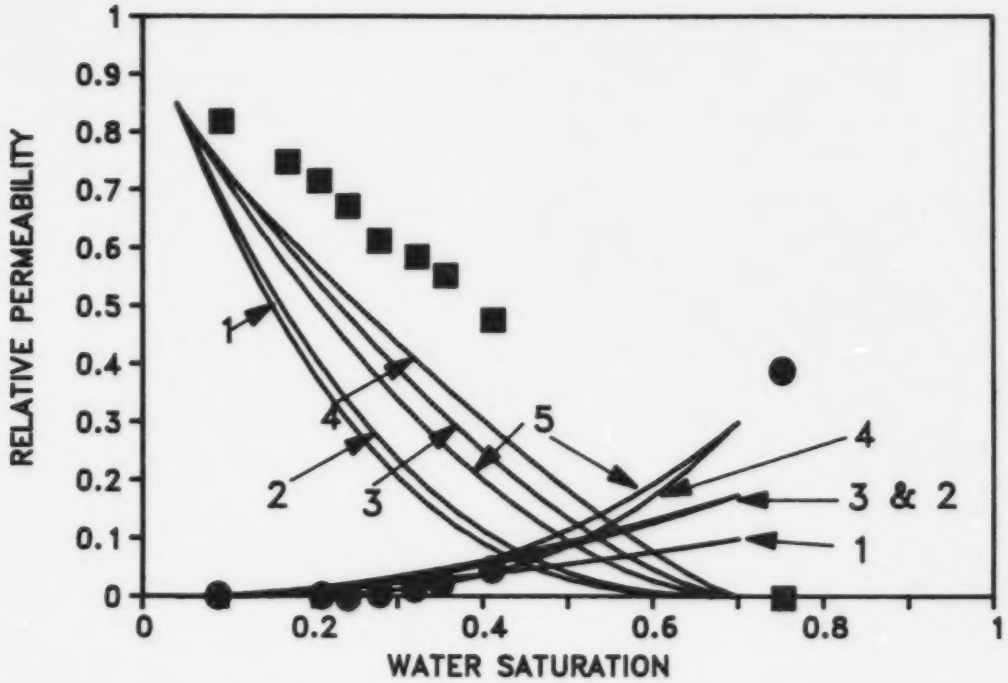

■ STEADY STATE OIL REL. PERM.

● STEADY STATE WATER REL PERM.

—— UN-STEADY STATE TESTS

1 – 0.125 ml/min

2 – 0.25 ml/min

3 – 0.5 ml/min

4 – 2.0 ml/min

5 – 1.0 ml/min

FIGURE 34

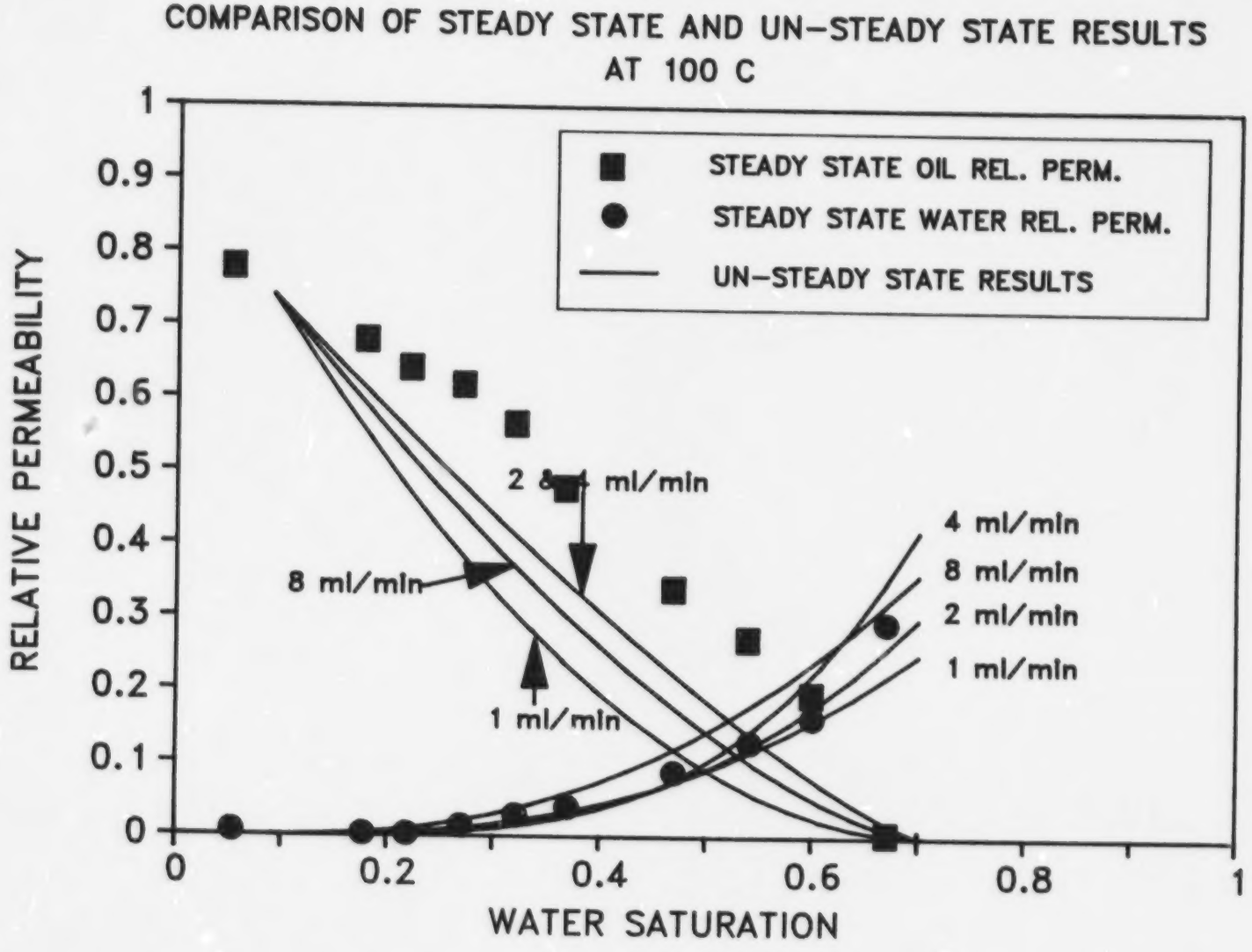
COMPARISON OF STEADY STATE AND UN-STEADY STATE RESULTS
AT 100 C
STEADY STATE OIL REL. PERM.
STEADY STATE WATER REL. PERM.
UN-STEADY STATE RESULTS
RELATIVE PERMEABILITY
WATER SATURATION
1
0.9
0.8
0.7
0.6
0.5
0.4
0.3
0.2
0.1
0
0
0.2
0.4
0.6
0.8
1
2 & 4 ml/min
8 ml/min
1 ml/min
4 ml/min
8 ml/min
2 ml/min
1 ml/min

FIGURE 35

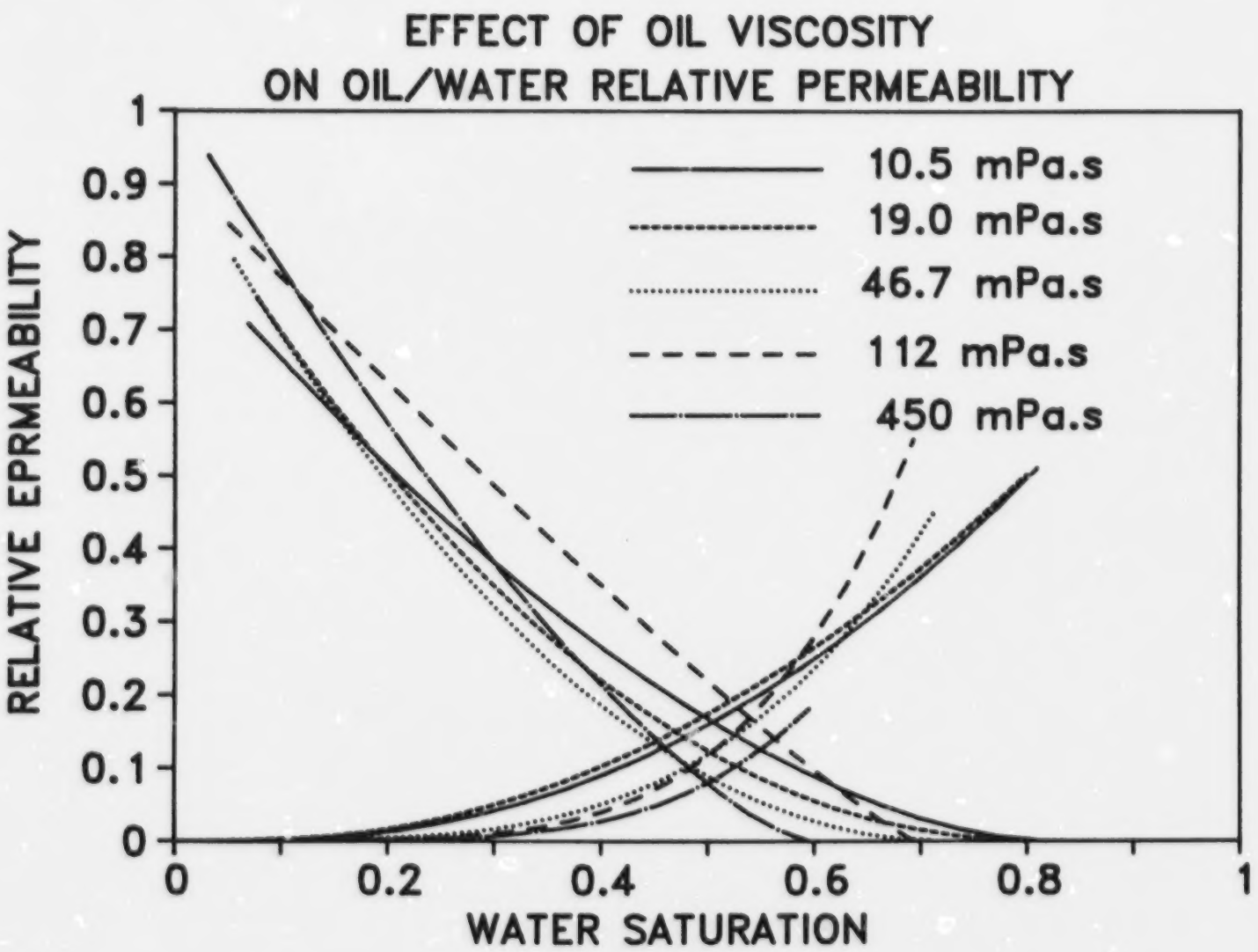
EFFECT OF OIL VISCOSITY
ON OIL/WATER RELATIVE PERMEABILITY
RELATIVE EPRMEABILITY
WATER SATURATION
0
0.1
0.2
0.3
0.4
0.5
0.6
0.7
0.8
0.9
1
0
0.2
0.4
0.6
0.8
1
10.5 mPa.s
19.0 mPa.s
46.7 mPa.s
112 mPa.s
450 mPa.s

FIGURE 36

PART II

THREE-PHASE RELATIVE PERMEABILITIES

1. OBJECTIVES:

The objectives of the measurements reported in this part of the report were:

1. To develop an apparatus capable of measuring three-phase relative permeabilities at elevated temperatures and pressures.
2. To provide a set of good quality experimental data at a high temperature which can be used as a bench mark for testing various models for estimating three-phase relative permeabilities at elevated temperatures.
3. To test the currently available correlations with the new experimental data.
4. To develop an improved correlation for estimating three-phase relative permeabilities.

The system chosen for the measurements of three-phase relative permeabilities was a compromise between the need to maintain the test condition as close to the field conditions in heavy oil recovery as possible and the need to keep the fluids-rock system simple enough to avoid experimental difficulties and complications of fines migration and/or emulsion formation. A high viscosity (500 mPa.s at 20^{o}C) refined mineral oil was used to simulate heavy oil behaviour. The other two fluids were nitrogen gas and de-ionized water. A clean silica sand core under triaxial confining stress (to simulate in situ stress conditions) was used as the porous medium. The steady-state technique was used to measure the three-phase relative permeabilities at elevated temperature (100^{o}C) and pressure (3.5MPa).

2. REVIEW OF THREE-PHASE RELATIVE PERMEABILITY MEASUREMENT TECHNIQUES:

2.1 Steady-State Methods:

The most direct technique for measuring three-phase relative permeability is the steady-state method. It requires establishing steady flow of three fluids through the porous medium and measuring the pressure drop and flow rate for each fluid. The relative permeability for each fluid can then be calculated by applying the following form of Darcy's law to each fluid:

$$\frac{Q_i}{A} = \frac{k_{ri}\, k_{abs}}{\mu_i\, L}\{\Delta P_i\} \qquad (1)$$

where:

Q_i - Flow rate of fluid phase i,

A - Cross sectional area of the porous medium,

k_{abs} - Absolute permeability of the medium,

μ_i - Viscosity of fluid phase i,

L - Length of the porous medium,

ΔP_i - Pressure drop in the fluid i across length L,

k_{ri} - Relative permeability of fluid phase i.

The other variables in equation 1 (A, k_{abs}, μ_i and L) can be measured separately. Since the usual objective of such measurements is to determine the relationship between relative permeability and saturation, it is also necessary to measure the saturation of each fluid under steady-state conditions for each set of flow rates. The flow rates are varied to obtain different saturation conditions and when sufficient data have been collected the saturation versus relative permeability plots can be made.

Measuring the pressure drop is relatively straight forward. Excellent electronic differential pressure transducers are available for such measurements. However, care is needed to ensure that the pressure signal is obtained from the same fluid at both ends of the porous medium. The flow rate measurement also does not present any problem. It is usually set on positive displacement pumps for liquids. Mass flow controllers can be used to maintain constant gas flow rates at desired levels. Simple capillary tubes and differential pressure transducers can be used to monitor the flow rates of the individual fluids. It is the saturation measurement which requires considerable finesse. The methods used to accomplish this vary from simple material balance to elaborate in-situ measurement techniques. These include resistivity measurements, gamma ray, X-ray and microwave attenuation techniques, nuclear magnetic resonance, neutron scattering and use of radiation emitting fluids. Weighing the core and extraction of the fluids from the core have also been used. Even with the most sophisticated in-situ technique, considerable uncertainty remains in the saturation measurements.

The other major problem in the steady-state method is due to the capillary effects at the outflow end of the core. At the outflow boundary of the core, the nature of the flow changes abruptly from flow in porous medium to bulk flow in tubing. This change is accompanied by an abrupt change in the curvature of fluid-fluid interfaces. These interfaces are highly curved inside the porous medium due to the small dimensions of flow channels in the porous medium but become relatively flat immediately after coming out of the core. Therefore, the pressure in two adjacent fluids can be quite different within the porous medium but is nearly equal on the outside boundary. For the fluid having a higher pressure within the porous medium, i.e. the non-wetting

fluid this presents no problem since its pressure would be the same on both sides of the outflow boundary. The fluid which has lower pressure within the porous medium, i.e. the wetting fluid faces an increase in pressure in going from the porous medium side of the boundary to the other side. Therefore it can not flow out until its pressure at the inside boundary becomes equal to that of the non-wetting fluid. This can only happen when its saturation becomes equal to that which corresponds to the zero capillary pressure on the capillary pressure versus saturation diagram. Therefore, the wetting phase saturation must buildup near the inside boundary of the porous medium. This buildup of wetting phase saturation can cause serious error in relative permeability measurement if core average saturations and pressure drops are used for relative permeability calculations. Several ways of minimizing or overcoming this problem have been reported in the literature. Some of the more useful among these are:

2.1.1 Capillary Pressure (Hassler) Method:

This method was developed by Hassler (1944) for two-phase relative permeability measurements but can be adopted to three-phase measurements also. It is based on the idea that the end effects will not arise if the fluids do not have to come out of the porous medium simultaneously from same location. To ensure this condition, semi-permeable membranes are provided at each end to produce different fluids from different outlets. Pressure is measured separately in different fluids and the pressure difference between phases at the outflow end can be adjusted by controlling the back pressure for each fluid separately. Therefore, the capillary pressure can be kept same at inlet and outlet ends which ensures uniform saturation along the core. Using this

technique for three-phase measurements will require three different semi-permeable membranes each permeable to one fluid only. If only two membranes, one permeable to water and the other permeable to oil and gas, are used the end effects would be reduced but not completely eliminated. The method is quite cumbersome and is currently not very popular. Finding suitable membranes for three-phase measurements and maintaining their semi-permeable character over extended periods can be difficult.

2.1.2 Dynamic (Penn-State) Method:

This method was initially developed by Morse et. al.(1947) for two-phase relative permeability measurements. They placed three pieces of similar core material in series in a core holder, with the idea that the front piece will serve as the inlet section and the last piece will absorb the capillary end effects. Measurements of saturation and pressure drop were made on the central piece which was the core to be tested. It should work reasonably well in a three-phase system also, provided a perfect capillary contact can be ensured between the adjoining cores. This method of minimizing end effects makes the saturation measurement more difficult. Unless in-situ techniques are used, the saturation measurements require removing the test core from the holder for each measurement. Moreover, a recent report indicates that the capillary contact may not be perfect even when materials like tissue paper are placed between the adjoining cores (Olsen et.al;1986).

2.1.3. Use of High Flow Rates:

Perhaps the simplest technique for minimizing the end effects is to use

high flow rates. As the flow rate is increased the region over which wetting phase saturation accumulates shrinks in size and at high flow rates may be confined to a narrow section near the outflow face of the core (Geffen et.al.;1951). If the pressure drop and saturations are measured away from the core, the end effects' problem can be solved. The advantage of this method over the Penn-State method is that there is no uncertainty about the capillary contact. However, in some cores the use of high flow rates may cause fines migration problems.

2.1.4. Use of Long Cores:

The problem of end effects can also be solved by using a long core and obtaining measurements away from ends. If unconsolidated sand is being used it is possible to attach a long but narrow extension (in a small diameter tube) to the main core without interrupting the continuity of the sand. In this situation the end effects will probably remain confined to this tube and the measurements can be obtained in the main body of the core.

2.2. Unsteady-State Methods:

For two-phase relative permeability measurements, the unsteady-state technique has become the industry standard (Saraf and McCaffery; 1981). Its main advantage is the speed of measurements. In view of the considerably larger effort required for three-phase measurements, a fast unsteady-state technique would be even more advantageous for three-phase relative permeability measurements. Sarem (1966) reported three-phase measurements calculated from displacement experiments involving gas injection into a core containing mobile saturations of water and oil. In order to calculate

relative permeabilities, he assumed that the relative permeability to each phase depends only on its own saturation. This is generally not acceptable. Corey et. al. (1956) used a semi-permeable membrane to prevent water from flowing out of the core during gas injection into a core containing mobile water and oil. In this case the flood is similar to two-phase oil-gas displacement and the calculation schemes developed for two-phase systems can be used. However, maintaining the water stationery changes the character of the flow and may introduce undesirable artifacts.

A three-phase displacement experiment involving displacement of one fluid with simultaneous injection of the other two fluids can also be used. Unfortunately, there is no well accepted calculation scheme to infer the relative permeabilities from unsteady-state experiments. Computer simulation of the experiments can be used in theory, but it has also not been successful in practice. Most simulation programs incorporate a preconceived model of three-phase relative permeability, and the results obtained by history matching would always produce results consistent with the model used.

2.3. Centrifuge Method:

A centrifuge method has also been proposed for three-phase relative permeability measurements (van Spronsen; 1982). In some respects it is similar to the unsteady state experiments except that the fluids are mobilized by centrifugal forces. Relative permeabilities are calculated from the observed desaturations rates at different rotational speeds. As in the displacement technique the analysis of the fluid production data to calculate relative permeabilities is based on several simplifying assumptions. The centrifugal force is assumed to be constant along the length of the core and

the capillary pressure is neglected in the analysis. The assumption of negligible capillary pressure may not be valid in such experiments. Furthermore, the displacement mechanisms involved in a centrifugal experiments are not same as in a normal displacement. Therefore the results obtained by this method may not be totally reliable. However, the technique is relatively fast and easy to automate. An experimental study is needed for documenting the similarities and differences in results obtained by this method and the steady-state method. However, this technique can not be used with unconsolidated sand if tests under overburden pressures are required.

3. EXPERIMENTAL EQUIPMENT AND PROCEDURE

A schematic diagram of the experimental equipment is shown in Figure 1. The parts within the dotted enclosure were contained in a convection oven equipped with a temperature controller capable of maintaining constant temperature within $\pm 0.5^{o}C$. The equipment was designed for the steady-state method of relative permeability measurements but can be used for displacement tests also. Water and oil were circulated in closed loops. The re-circulation loop for water included the separator cell, a dual piston HPLC pump (Beckman Model 100 A), a heat exchanger coil, a capillary viscometer, and the test core. The water flow started from bottom of the separator cell and passed successively through the circulation pump, the heat exchanger tube, the water viscometer and the core before returning to the separator cell. Similarly the oil started from middle of the separator cell and passed

successively through the oil circulation pump (Beckman Model 100 A), heat exchanger tube, the oil viscometer and the test core before returning to the separator cell. Two syringe pumps, one containing water and the other containing oil, were connected to the separator cell as shown in figure 1. These were used to maintain the required volumes of the liquids in the separator cell by injecting or withdrawing metered quantities of the fluids. Gas flow was in once through mode. The gas was taken from a compressed gas cylinder, flowed through a mass flow controller, a fixed bed humidifier, a mist filter, a gas viscometer, the test core, the separator cell, a second mist filter, a back pressure regulator and a soap film gas flow meter. An electronic differential pressure transducer and a chart recorder were used to monitor and record the differential pressure across the core. The pressure ports were located in the sand 2.5 cm away from the ends to reduce capillary end effects. Pressure drops across the three capillary viscometers were also monitored and recorded continuously. These provided a visual confirmation of the satisfactory performance of the pumps and the gas flow controller.

A triaxially loaded core holder shown schematically in Figure 2 was used for confining the test cores. The cores were wet packed and then confined by application of triaxial stress.

At start of each run the core was solvent cleaned, dried with hot nitrogen, evacuated and then filled with metered volume of water to determine its pore volume. The water re-circulation loop was filled with water but the syringe pump for water and the separator cell were kept almost empty. The oil syringe pump was filled with oil and most of the separator cell also contained oil (except for a small volume of water at the bottom and a gas cap at the top). The system was then pressurized by injecting the gas. The absolute

permeability of the core was measured by flowing water through the core. This also allowed the water to contact and become saturated with the gas. The oil was equilibrated with the gas by circulating it through the gas cap in the separator cell without going through the core. The levels of water and oil in the separator cell and the volumes contained in the syringe pumps were recorded after both fluids became saturated with the gas.

The next step was an oil flood to drive the core to its irreducible water saturation. The volume of water produced was monitored by reading the water level in separator cell and withdrawing water into the water syringe pump when needed. The oil flow was continued till water production ceased and the pressure drop across the core became constant.

Simultaneous flow of water, gas and oil was then started with low flow rates of water and gas and relatively high oil flow rate. After reaching a steady-state condition (as indicated by constant pressure drop and constant fluid levels in the separator cell for at least 12 hours) the pressure drop across the core and the liquid levels in the cell were recorded. Usually 24 hours were enough for each set of flow rates except at the flood out (zero oil flow) where three to five days were needed. The fractional flows of water and gas were increased and oil flow rate was decreased in each successive flow rate settings. If the pressure drop across the core became too low, flow rates of all three fluids were doubled. Eight to ten different flow rate settings were used to reach the zero oil flow condition. After reaching the residual oil condition the core was isolated and depressurized. The liquids produced with the gas were collected in a cold trap. The core was then extracted by flowing hot toluene through it. The liquids produced from the core were collected and distilled to determine water and oil saturations

existing in the core at end of the test. The core was then ready for the next run. Thus the end point saturations in the core were determined independently by two methods (by reading the fluid levels and by extraction). If the two measurements of oil and water saturations agreed within ±2% PV the test was considered successful. Otherwise, the data was considered unreliable.

Relative permeability to each phase was calculated by applying equation 1 to flow of each fluid. Even though the pressure gradient was measured away from the core ends, the saturations were the core average. This introduces an additional error in the saturation measurement, however, since the core length was more than 45 cm and high flow rates were used this error is likely to be small. The maximum error in saturation measurements was estimated to be about ±2.5%. The average error would be considerably less.

4. RESULTS:

The relevant petrophysical properties of the core and fluids used in this study are listed in Table 1. All measurements were carried out at 100°C. Before starting three-phase measurements the two-phase oil/water and oil/gas relative permeabilities were measured by the steady-state technique. The two-phase oil/water relative permeabilities are shown in Figure 3. The smooth lines shown in the figure were numerically fitted to the experimental data using the following equations.

$$k_{ro} = k^{o}_{ro} \frac{(1-S)^{\epsilon_o} + 0.01(1-S)}{1.01} \qquad (2a)$$

and

$$k_{rw} = k^{o}_{rw} \frac{S^{\epsilon w} + 0.01S}{1.01} \qquad (2b)$$

where $S = (S_w - S_{wi})/(S_{wm} - S_{wi})$, S_{wi} and S_{wm} being the irreducible and maximum water saturations and k_{ro} and k_{rw} are the end point relative permeabilities to oil and water. Figure 4 shows the results of two-phase oil/gas measurements which were carried out at the irreducible water saturation. The smooth curves were obtained by fitting equations similar to those listed above for the oil/water case.

A total of ten three-phase runs were carried out, each providing eight to ten steady-state measurements. The change in saturations during several representative runs is shown in figure 5. Water, oil and gas relative permeabilities corresponding to each steady-state saturation condition were calculated by applying the Darcy's law. Since the pressure drop was measured 2.5 cm away from the ends the capillary end effects were assumed to be negligible. The pressure drop measured in water phase was applied to all phases.

4.1 Water Relative Permeability:

Figure 6 shows a plot of water relative permeabilities as a function of water saturation including the two phase oil/water data. Although, there was considerable scatter in the data, no consistent trends were found with the saturations of other phases. Therefore, it was concluded that for this system, the high temperature water relative permeability was a function of water saturation alone. This conclusion is reflected in the straight line isoperms for water shown in Figure 7. To show the degree of scatter involved,

experimental values of the water relative permeability around a selected isoperm are included in the figure.

4.2 Gas Relative Permeability:

A plot of gas relative permeability against gas saturation is shown in Figure 8. The gas relative permeability also did not show any trend with saturations of the other two phases. Therefore it was concluded that the gas relative permeability is also a function of its own saturation only. Gas isoperms are shown in Figure 9 along with some experimental values to show the degree of scatter involved.

4.3 Oil Relative permeabilities:

Figure 10 shows a plot of the oil relative permeabilities as a function of oil saturation. The oil/water and oil gas data are included in the plot. It was observed that the three-phase point were generally between the two limiting cases represented by the two-phase data. Also in general the oil relative permeabilities from runs involving low gas saturations were closer to the oil/water two-phase measurements and similarly the runs involving low water saturations showed results closer to the oil/gas measurements. Smoothed contours of oil relative permeability are shown in Figure 11. The oil isoperms show significant curvature. The line representing 1% relative permeability shows that when both water and gas are used to displace the oil a significantly lower residual oil saturation results.

5. CORRELATIONS FOR ESTIMATING THREE-PHASE RELATIVE PERMEABILITIES:

The correlations used most frequently in reservoir simulation studies in the absence of three-phase data are the two models of Stone designated as Method I and II. These methods use two sets of two-phase data to predict the three-phase relative permeabilities. This approach seems reasonable because three-phase oil-water-gas system is bounded by oil-water, oil-gas and water-gas flow on the three sides. Stone's Method I suggests the use of two sets of oil-water and oil-gas data to obtain the three-phase relative premeabilities. Hysteresis effects are taken into consideration by using the appropriate two-phase data. For systems with water as the wetting phase, oil as the intermediate wetting phase and gas as the non-wetting phase, Stone suggested that three phase gas and water relative permeabilities were dependent only on their own saturations and are equal to the two-phase values,

$$k_{rg} = f(S_g) \tag{3a}$$

$$k_{rw} = f(S_w) \tag{3b}$$

while the relative permeability to oil depends on the saturations of all three phases. For the oil phase, the relative permeability under three-phase flow conditions is obtained from:

$$k_{ro} = S_o^* \beta_w \beta_g \tag{4}$$

where:

$$\beta_w = \frac{k_{row}}{(1-S_o^*)} \tag{5a}$$

$$\beta_g = \frac{k_{rog}}{(1-S_g^*)} \tag{5b}$$

$$S_o^* = \frac{S_o - S_{om}}{(1 - S_{wc} - S_{om})} \tag{6}$$

$$S_w^* = \frac{S_w - S_{wc}}{(1 - S_{wc} - S_{om})} \tag{7}$$

$$S_g^* = \frac{S_g}{(1 - S_{wc} - S_{om})} \tag{8}$$

β_g and β_w are factors to allow for oil blockage by gas and water respectively. Equations (5a) and (5b) involve two-phase data only. One of the advantages of Stone's Method I is the parameter S_{om}, the minimum residual oil saturation, which can be adjusted to match the three-phase data. Stone suggested the use of S_{om} between $0.25S_{wc}$ to $0.5S_{wc}$ based on experimental data. S_{om} should be less that or equal to the lesser of S_{orw}, the residual oil saturation in oil-water flow and S_{org}, the residual oil saturation in oil-gas flow. Fayers and Matthews suggested the use of;

$$S_{om} = \alpha\, S_{orw} + (1 - \alpha)\, S_{org} \tag{9}$$

where:

$$\alpha = \frac{(1 - S_{wc} - S_{org} - S_g)}{(1 - S_{wc} - S_{org})} \tag{10}$$

In the absence of any experimental data equation (9) should be used to obtain S_{om}.

Stone later suggested the following (method II) equation for obtaining the three-phase relative permeability to oil

$$k_{ro} = (k_{row} + k_{rw})\ (k_{rog} + k_{rg}) - (k_{rw} + k_{rg}) \qquad (11)$$

where k_{row} and k_{rw} are the two-phase relative permeability to oil and water from two-phase oil-water data and k_{rog} and k_{rg} are the relative permeabilities to oil and gas from two-phase oil-gas data. Stone's Method I and II have only been partially successful as demonstrated by Dietrich and Bondor (1976), Saraf et al. (1982), van Spronsen (1982), Fayers and Matthews (1984) and Oak et al (1988). One of the problems associated with the Stone's models is the implicit assumption that k_{row} and k_{rog} are equal to unity at connate water saturation (oil-water) and zero gas saturation (oil-gas).This is not true in general and consequently the three-phase relative permeability predicted by Stone's model do not match the two-phase data at the oil-water and oil-gas boundaries. A few modifications have been made to the Stone's models by Dietrich and Bondor (1976), Aziz and Settari (1979), Fayers and Matthews (1984), Fayers (1987), Aleman et al. (1984). These modifications have only been partially successful. In a recent paper Baker reported that simple interpolation models (both linear and saturation weighted) provide as good or better match of experimental data than any of the previous models including those of Stone's.

5.1 MODIFICATIONS OF STONE METHOD I

One of the limitations of Stone's method arises from the fact that if k_{row} and k_{rog} are not equal to unity at connate water saturation (oil-water) and zero gas saturation (oil-gas), then a match in relative permeabilities cannot be made at the two-phase boundaries. Aziz and Settari modified Stone's method I by assuming that the gas-oil data are measured in the presence of irreducible water. For this case, k^o_{row}, the relative permeability of oil at connate water saturation in an oil-water system is equal to k^o_{rog}, the relative permeability to oil at zero gas saturation in an oil gas system. They modified the Stone's method I as follows:

$$k_{ro} = k^o_{row}\, S_o\, \beta_w\, \beta_g \tag{12}$$

$$\beta_w = \frac{k_{row}}{k^o_{row}\,(1-S^*_w)} \tag{13}$$

$$\beta_g = \frac{k_{rog}}{k^o_{rog}\,(1-S^*_g)} \tag{5}$$

The effect of this modification is to normalize the relative permeability. The problems with Aziz and Settari's method are (a) some measurements of two-phase oil gas relative permeability data are not necessarily conducted at connate water saturation and (b) k^o_{row} is in general

not equal to k^o_{rog} due to experimental error. To overcome these problem it is necessary to modify the Stone's model by incorporating another normalizing factor. The following expression for kro was found to work well for this purpose:

$$k_{ro} = S^*_o \frac{(k_{row})}{k^o_{row}\,(1 - S^*_w)} \frac{(k_{rog})}{k^o_{rog}\,(1 - S^*_g)} \frac{(k^o_{rog}\,S^*_g + k^o_{row}\,S^*_w)}{(1 - S^*_o)} \qquad (15)$$

where k^o_{row} and k^o_{rog} are the relative permeabilities to oil at connate water saturation (oil-water) and zero gas saturation (oil-gas) respectively. At connate water saturation during oil-water flow, equation (15) reduces to

$$k_{ro} = k_{rog} \qquad (16)$$

and at zero gas saturation during oil-gas flow equation (15) reduces to

$$k_{ro} = k_{row} \qquad (17)$$

Equations (16) and (17) are the required equations for a two-phase match of relative permeabilities at the oil-gas and oil-water boundaries. The term

$$\frac{(k^o_{rog}\,S^*_g + k^o_{row}\,S^*_w)}{(1 - S^*_o)}$$

is a normalization factor which forces a match at the two-phase ends.

6. COMPARISON WITH EXPERIMENTAL DATA:

6.1 New Experimental Data:

The results of Stone's method I and II are shown in Figures 12 and 13 along with the new experimental data for comparison. These figures show that the predicted oil isoperms are consistently lower than the experimental values with the method I results slightly superior to the method II results. Figures 12 and 13 also show that the oil relative permeabilities are not matched at the oil-water and oil-gas (at S_{wc}) boundaries. This is due to the fact that k^o_{row} and k^o_{rog} are not equal to unity at S_{wc} (oil-water) and $S_g = 0$ (oil-gas) respectively. This is an inherent disadvantage of the Stone's two models.

The calculated results using the modified Stone's method I (equation 15) are plotted in Figure 14. There is considerable improvement over the Stone's original models. The modified version not only provides a good match of k_{ro} at the oil-water and oil-gas ends, but also appears to improve the fit of the curvature of experimental isoperms.

4.2 Corey et al. (1956) Data.

In this study three-phase relative permeability measurements were made on Berea Sandstone. Capillary end effects were reduced by using capillary barriers or semi-permeable membranes at both ends. This does not necessarily eliminate end effects. To avoid hysteresis the cores were used only twice, once with fixed brine saturation and once without any brine. Their data show scatter and lack consistency. The results of their work are shown in Figure 15-17 for oil, water and gas relative permeabilities. The oil isoperms are concave to the oil vertex. Water isoperms were not measured but were

calculated by assuming (a) that water relative permeability was dependent only on S_w and (b) water relative permeability in a water wet system is the same as the oil relative permeability in an oil-wet system. The gas relative permeability was found to be a function of gas saturation alone.

Three-phase oil relative permeability was calculated using equation (15) for the system of Corey et al. and are plotted in Figure 15. Two phase k_{row} and k_{rog} data were obtained by digitizing the figures in Corey's and Stone's papers. S_{wi}, S_{or} and S_{og} values for Corey et al. data are given in Table 2. The minimum residual oil saturation was taken to be 0.10 to give a better fit of the lower isoperms. This however spoils the fit for the higher isoperms. The gas and water isoperms were calculated from the two-phase data and are also plotted in Figure 16-17.

6.3 Data of Donaldson and Dean (1966)

Donaldson and Dean reported three-phase relative permeabilities of Berea sandstone and Arbuckle limestone. Tests were made under the conditions in which oil and water were displaced by the gas and the flow rates of all three phases were measured simul_aneously. They used an unsteady state method in which end effects were reduced by using high flow rates. However, hysteresis was ignored.

Their results for the Berea sandstone are shown in Figure 18-20. The oil isoperms are concave to the oil saturation vertex on the ternary diagram and k_{rw} are concave to the water saturation vertex. The gas isoperms are convex at low gas saturations and concave towards the gas vertex at higher gas saturations (Figure 20). The interpretation of unsteady-state data of Donaldson and Dean involve inherent difficulties making them rather

inconclusive. The calculated results using the modified Stone approach are also plotted in Figure 18. The values of S_{wc}, S_{or} and S_{og} are presented in Table 2. Some of these values were extrapolated from the data of Donaldson and Dean and the experimental data were replotted by digitizing. The value of S_{om} can be modified to match the data either at low k_{ro} or at high k_{ro} . With a value of S_{om} equal to 0.15 the calculated k_{ro} are more concave (to the oil apex) at low k_{ro} and less concave than the experimental data at higher k_{ro}. At the highest k_{ro} reported, the match is very good.

6.4 Data of Saraf and Fatt (1967)

Saraf and Fatt reported three-phase relative permeability for a Boise sandstone using nuclear magnetic resonance (NMR) technique to determine liquid saturations. End effects were minimized by placing the pressure differential taps 2.5 cm from the ends of the core while saturations were measured 5 cm away from the ends. Hysteresis effects were also minimized by using a new core for each run. This however introduced a greater scatter in the data because no two cores were identical. They found k_{rw} to be a function of S_w and k_{rg} to be a function of S_g only. Oil isoperms were found to depend on the saturation of all phases and were convex to the oil vertex. They explained this nature of the oil isoperms based on the network theory of Fatt. However they suggest that at high gas saturations, experimental errors were high. The most convex isoperm was at low oil saturations where the scatter in the data was probably very high.

Their oil isoperms are shown in Figure 21 along with the calculated results using equation 15. S_{om} was taken to be equal to S_{or} (0.17). Except for the 1% isoperm, the fit is very good. As stated earlier the 1% isoperm of

Saraf and Fatt involved considerable scatter. The water and gas isoperms are plotted in Figure 22 and 23 and are straight lines as they are functions of S_w and S_g respectively.

6.5 Data of Dalton et al. (1970):

The data of Dalton et al. (1970) have been reported in the paper of Stone. Their data are for unconsolidated miocene sand pack. Not much was explained for this data set by Stone. Only oil relative permeabilities were reported by Stone which are shown in Figure 24. The fit with the calculated values is not very good and not much can be said in the absence of detailed description of the data.

6.5 Data of Saraf et al. (1982):

Saraf et al. measured three-phase relative permeabilities to oil, water and gas by steady state and non-steady state methods in fired Berea sandstone. The relative permeabilities were measured from the fractional flow displacement data using an extended Welge's method. They found the water relative permeability to be a function of S_w and independent of saturation histories. K_{rg} were found to be dependent on the total liquid saturation or in other words, on the gas saturation alone. They were however sensitive to the saturation history of the gas phase. Oil relative permeabilities were found to be dependent on all three phase saturations and are concave to the oil vertex. They also compared their data with predictions made by Stone's method I and II and found them to be inadequate.

Values of S_{wc}, S_{or} and S_{og} obtained from experimental data are presented in Table 2. k_{row} and k_{rog} functions were also regressed from the two-phase

data in their report. With a constant value of S = 0.15, the fit of equation (15) with experimental data is very good (Figure 25). Further improvement can be made for low k_{ro} by increasing this value of S_{om}. Three phase k_{rw} and k_{rg} are plotted in Figures 26-27.

6.7 Data of Oak et al. (1988):

Recently Oak et al. (1988) reported two-and three-phase relative permeability of fired Berea sandstone during drainage and imbibition saturation histories. They used the steady state Penn State method and saturations were measured by an X-ray method. Capillary end effects were minimized. They found the relative permeabilities to depend on the saturation history significantly. In the drainage case (water decreasing, oil decreasing and gas increasing) the oil and gas relative permeabilities depended on the saturation of the other phases while in the imbibition case (water increasing, oil increasing and gas decreasing) k_{rw} and k_{rg} were found to be dependent on their own phase saturations. They compared their results with the Stone models and found them to be only partially successful.

Their results for oil-water and gas relative permeabilities are shown in Figures 28-30 for the imbibition case. Very few data points were available in the three-phase region for oil relative permeability as shown in Figure 28. The predictions using equation (15) are also plotted in the figure and shows a very good match for the limited number of data points. Water and gas relative permeabilities were found to be dependent on their own saturations and are reproduced in Figures 29 and 30.

7. CONCLUSIONS:

1. An apparatus for measuring three-phase relative permeabilities at elevated temperatures and pressures has been developed.
2. The three-phase relative permeability of Ottawa sand to water at 100°C was found to be a function of water saturation only.
3. The three-phase relative permeability of Ottawa sand to gas at 100°C was found to be a function of gas saturation only.
4. The three-phase relative permeability of Ottawa sand to a viscous mineral oil at 100°C was found to depend on saturations of the other fluids also.
5. Stone's method I and II predictions of oil relative permeabilities were compared with a new set of experimental data and were found to be inadequate.
6. The oil relative permeability correlation as suggested by Stone method I was modified to obtain a better fit of the new experimental data.
7. The modified Stone's method I was tested with data from six other sources and found to provide better fits than the original Stone's method I and II.

7. REFERENCES:

Aleman-Gomez, M., Ramamohan, T.R. and Slattery, J.C., "A Statistical Structural Model for Unsteady State Displacement in Porous Media," SPE # 13265. Paper presented at the 59th Annual Technical Conference and Exhibition in Houston, Texas, Sept. 16-19, 1984.

Aziz, K. and Settari, T., Petroleum Reservoir Simulation, Applied Science Publishers, London, pp 30-38, 1979.

Baker, L.E.,: "Three-Phase Relative Permeability Correlations" SPE/DOE 17369, presented at 1988 EOR Symposium.

Corey, A.T., Rathjens, C.H., Henderson, J.H. and Wyllie, M.R.J.: "Three-Phase Relative Permeability," J.Pet. Tech. (Nov. 1956) 8, 63-65; Trans., AIME (1956) 207, 349-351.

Dalton, R.C., Daumann, V.D. and Kyte, J.R., Unpublished data reported in Stone 1970.

Dietrich, J.K. and Bondor, P.B., "Three Phase Oil Relative Permeability Models," SPE # 6044. Paper presented at the 51st Annual Fall Technical Conference and Exhibition, New Orleans, LA, 1976.

Donaldson, E.C. and Dean, G.W., "Two and Three Phase Relative Permeability Studies," Report 6826, US Bureau of Mines, Washington DC, 1966.

Fatt, I., "Influence of Dead-End Pores on Relative Permeability of Porous Media," Science, 134, p 1750-, 1961.

Fayers, F.J. and Mathews, J.D., "Evaluation of Normalized Stone's Methods for Three Phase Relative Permeability," SPE J., 4, pp 224-232, 1984.

Fayers, F.J., "Estimation of Stone's Method I and Conditions for Real Characteristics in Three Phase Flow," SPE # 16965, Paper presented at the 62nd Annual Technical Conference and Exhibition of SPE in Dallas, Texas, Sept 27-30, 1987.

Geffen, T.M., Owens, W.W., Parish, D.R., and Morse, R.A.; "Experimental Investigation of Factors Affecting Laboratory Relative Permeability Measurements", Trans AIME (1951)192 99 - 110.

Hassler, G.L., "Methods and Apparatus for Permeability Measurements", U.S. Patent No. 2,345,935 (1944)

Honarpour, M., Koederitz, L. and Hawey, A.M. Relative Permeability of Petroleum Reservoirs, CRC Press, Florida, 1986.

Josendal, V.A., Sandiford, B.B., and Wilson, J.W.; Improved Multiphase Flow Studies Employing Radioactive Tracers", Trans AIME (1952) 195 65 - 76.

Leverett, M.C. and Lewis, W.B.: "Steady Flow of Gas-Oil-Water Mixtures Through Unconsolidated Sands," Trans., AIME (1941) 142, 107-116.

Manjnath, A., and Honarpour, M.M., "An Investigation of Three Phase Relative Permeability," SPE # 12915. Paper presented at the Rocky Mountain Regional Meeting in Casper, WY, May 21-23, 1984.

Morse, R.A., Terwillinger, P.L., and Yuster, S.T.; "Relative Permeability Measurements on Small Core Samples", Oil and Gas J. (Aug. 1947) 109.

Oak, M.J., Baker, L.E. and Thomas, D.C., "Three Phase Relative Permeability of Berea Sandstone," SPE # 17370. Paper presented at the SPE/DOE EOR Symposium in Tulsa, OK, April 17-20, 1988.

Olsen, D.K., Goodlett, G., and Josephson, C.B.; "Effect of Capillary Bridges on Dispersion Coefficient", U.S. Dept. of Energy Report NO.NIPER-186 (DE87001390) 1986.

Parmeswar, R. and Maerefat, N.L., "A Comparison of Methods for the Representation of Three Phase Relative Permeabilities," SPE # 15061. Paper presented at the 56th California Regional Meeting in Oakland, CA, April 2-4, 1986.

Saraf, D.N. and Fatt, I., "Three Phase Relative Permeability Measurements using a NMR Technique for Estimating Fluid Saturations," SPE J., pp 235-242, Sept. 1967.

Saraf, D.N. and McCaffery, F.G.; "Two and Three-Phase Relative Permeabilities: A Review", Report No. 81-8, Petroleum Recovery Institute, Calgary, Alberta, September 1981.

Saraf, D.N., Batycky, J.P., Jackson, C.H. and Fisher, D.G., "An Experimental Investigation of Three Phase Flow of Water-Oil-Gas Mixtures Through Water Wet Sandstone," PRI Report 1982-1, Petroleum Recovery Institute, Calgary, Alberta, 1982.

Sarem, A.M.: "Three-Phase Relative Permeability Measurements by Unsteady-State Method," Soc. Pet. Eng. J. (Sept. 1966) 6, 199-205; Trans., AIME (1966), 237, 199-205.

Snell, R.W.: "Three-Phase Relative Permeability in an Unconsolidated Sand," J.Inst. Pet. (March 1962) 48, 80-88.

Stone, H.I., "Probability Model for Estimating Three Phase Relative Permeabilities," JPT, 2, pp 214-218, 1970.

Stone, H.I., "Estimation of Three Phase Relative Permeabilities and Residual Oil Data," JCPT, 12, pp 53-61, 1973.

van Spronsen, E.: "Three-Phase Relative Permeability Measurements Using the Centrifuge Method," paper SPE/DOE 10688, presented at the 1982 SPE/DOE Third Joint Symposium on Enhanced Oil Recovery, Tulsa, April 4-7.

Table 1: Properties of the Core and fluids Used for Three-phase Relative Permeability Tests.

Type of sand:	140-200 mesh silica sand
Core length:	46.7 cm
Cross-sectional area:	25 cm^2
Pore volume:	409 ml
Absolute permeability:	3.6 Darcy
Confining pressure:	10.3 MPa.
Pore pressure	3.45 MPa.
Type of oil:	Paraffinic mineral oil
Viscosity at 20°C	500 mPa.s
Viscosity at 100°C	12 mPa.s
Density at 100°C	0.828 g/ml

TABLE 2: Two Phase Relative Permeability Data

	S_{or}	S_{wi}	S_{og}	S_{om}
New Data	0.33	0.07	0.43	0.20
Corey et al. (1956)	0.20	0.17	0.35	0.10
Donaldson and Dean (1966)	0.23	0.31	0.54	0.15
Saraf and Fatt (1967)	0.17	0.30	0.60	0.17
Dalton et al. (1970)	0.22	0.16	0.55	0.15
Saraf et al. (1982)	0.39	0.23	0.39	0.25
Oak et al. (1988)	0.30	0.36	0.40	0.10

TABLE 3: Two Phase Oil-Water Relative Permeability Constants

	k^{o}_{row}	A	B
New Data	0.8219	0.4079	1.7776
Corey et al. (1956)	0.9217	3.0299	2.7419
Donaldson and Dean (1966)	0.8573	3.5913	0.1455
Saraf and Fatt (1967)	0.5574	4.1289	0.9003
Dalton et al. (1970)	0.7551	1.2230	0.0000
Saraf et al. (1982)	0.9629	1.5070	0.0000
Oak et al. (1988)	0.9266	1.1968	0.0000

TABLE 4: Two Phase Oil-Gas Relative Permeability Constants

	k^{o}_{rog}	A	B
New Data	0.7823	0.9697	0.0000
Corey et al. (1956)	0.9816	3.2538	0.0000
Donaldson and Dean (1966)	0.7774	2.6694	0.0000
Saraf and Fatt (1967)	0.5937	4.9733	1.1571
Dalton et al. (1970)	0.7372	5.6189	0.3826
Saraf et al. (1982)	0.9647	3.2503	0.0000
Oak et al. (1988)	0.5697	3.1245	0.0000

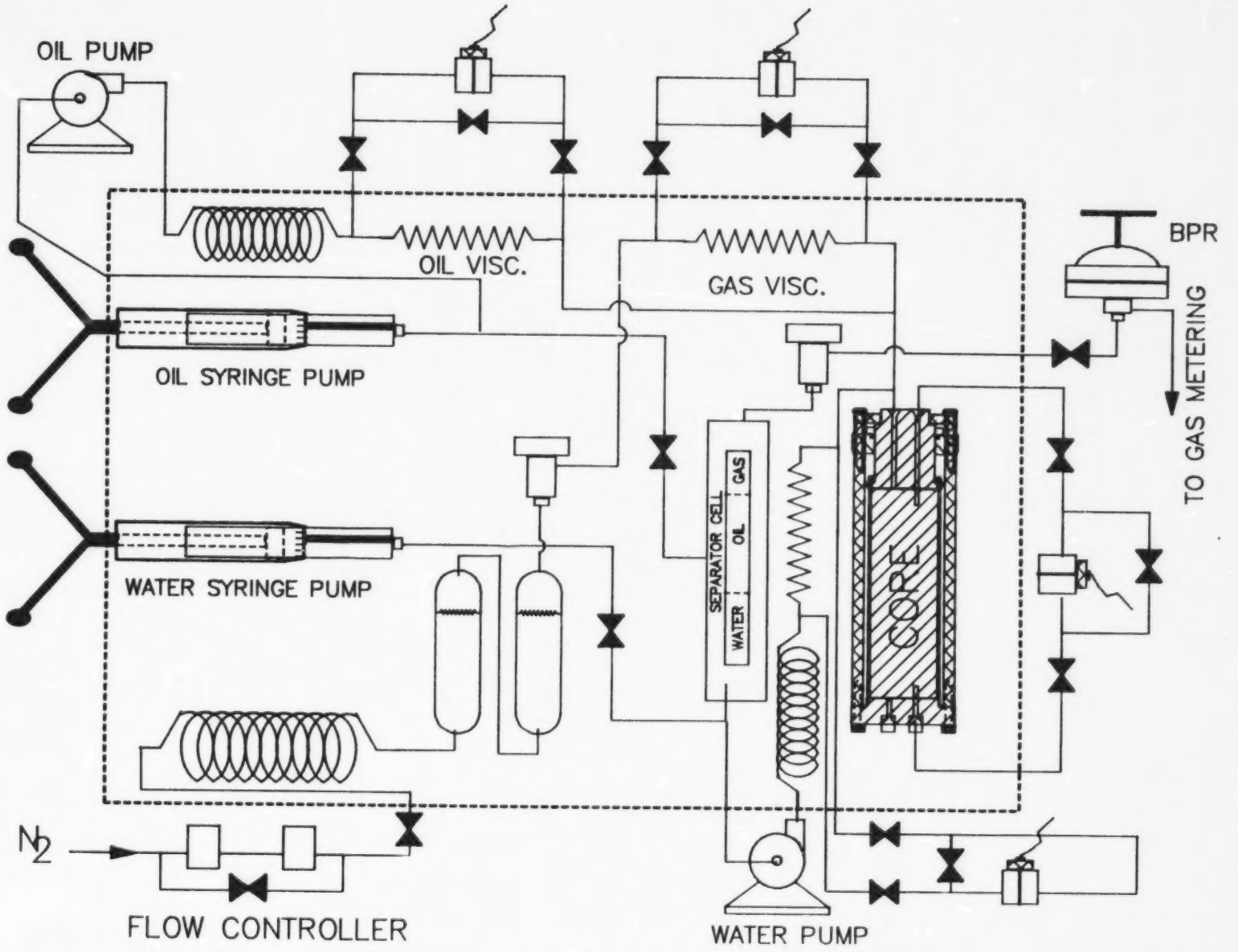

FIGURE 1: SCHEMATIC DIAGRAM OF THREE–PHASE EQUIPMENT

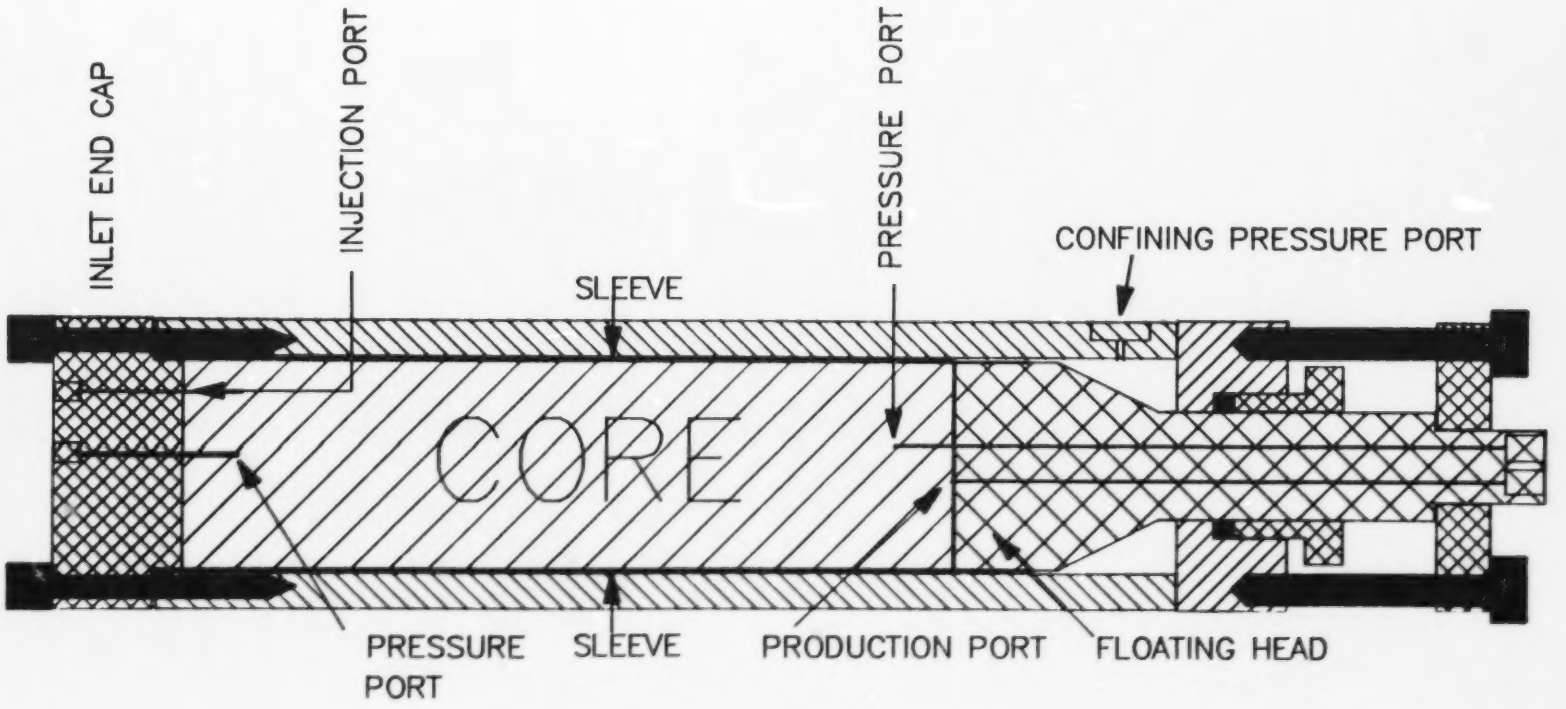

FIGURE 2: SCHEMATIC DIAGRAM OF CORE HOLDER

Two Phase Oil–Water Relative Permeability

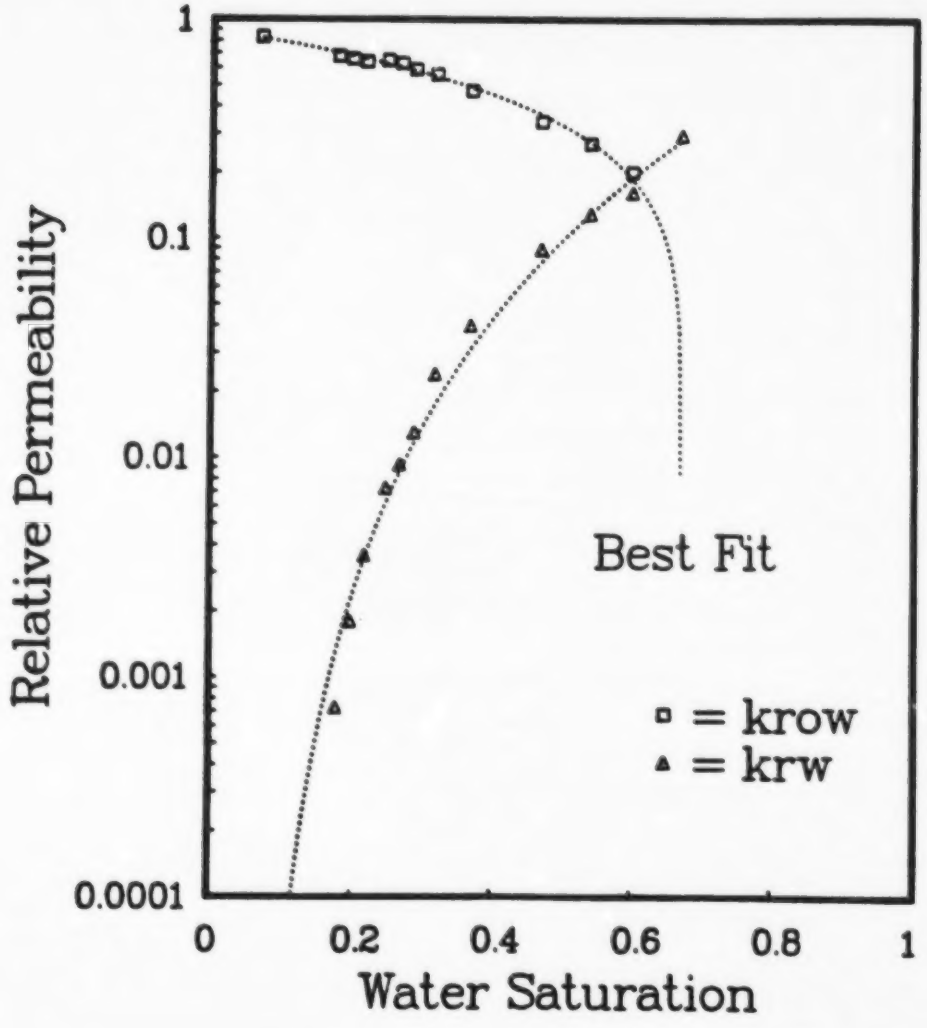

FIGURE 3

Two Phase Oil–Gas Relative Permeability

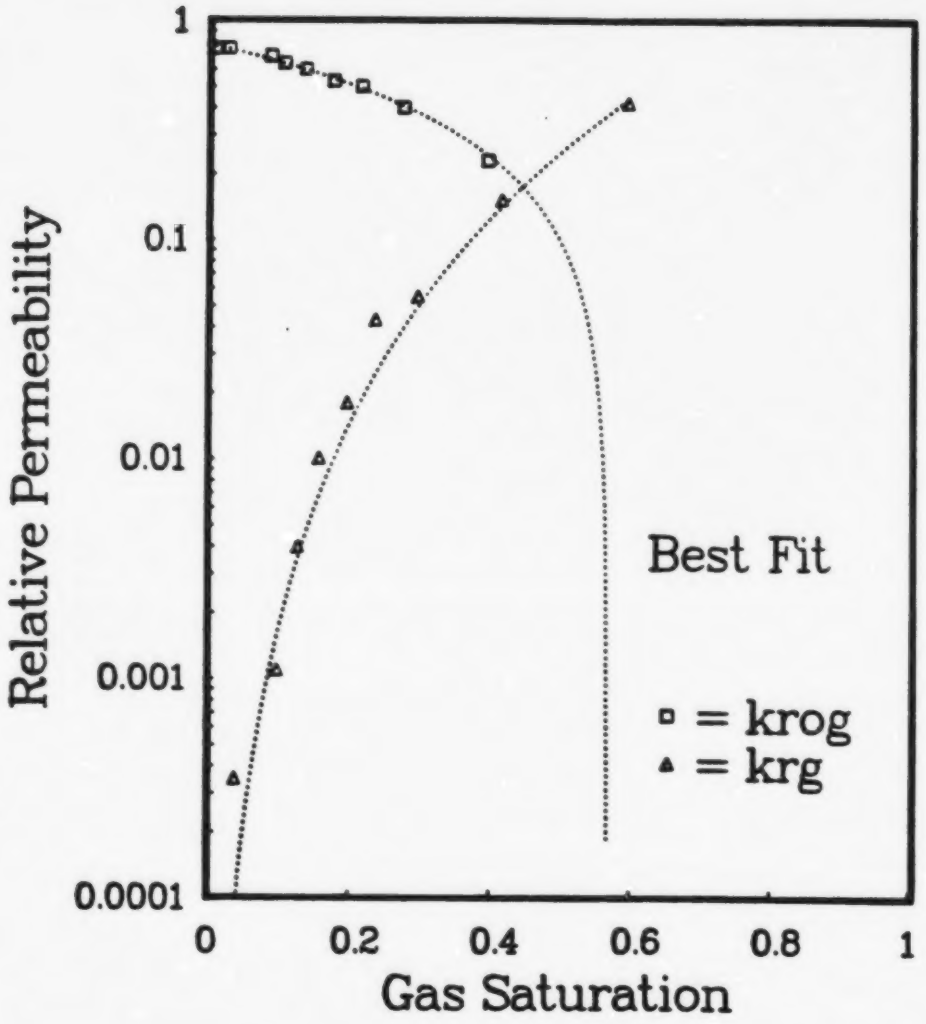

FIGURE 4

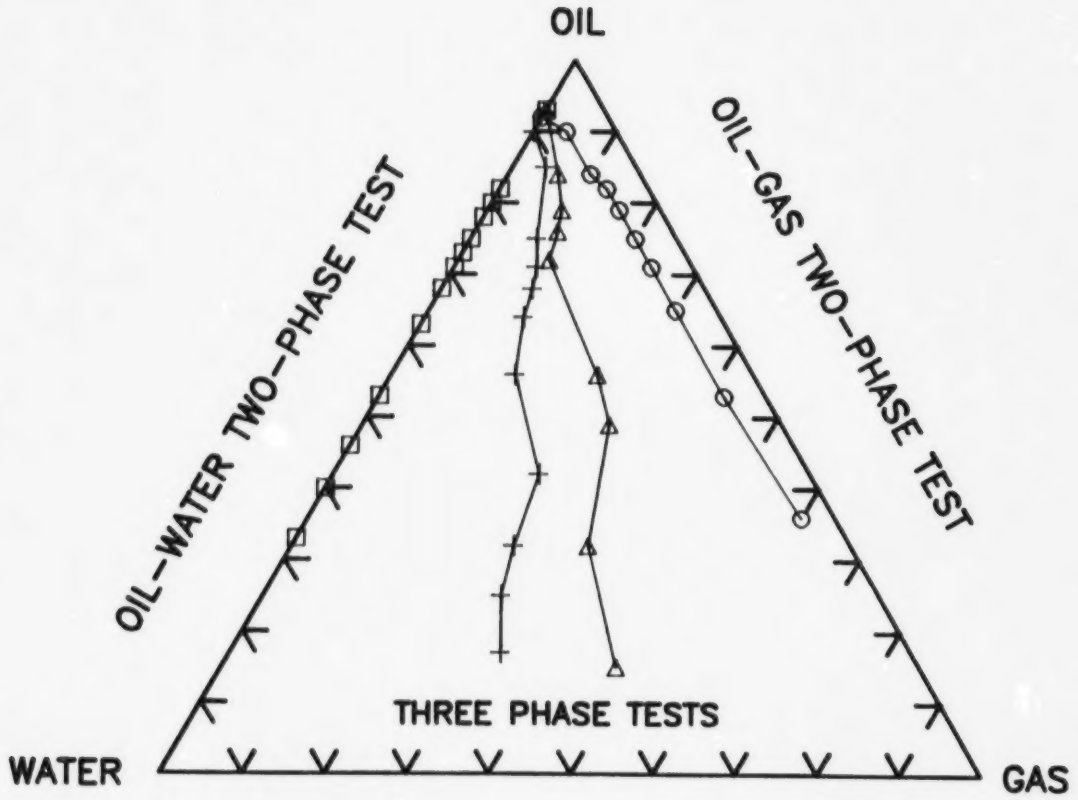

Figure 5: Locus of typical saturation changes during steady-state tests

Three Phase Water Relative Permeability

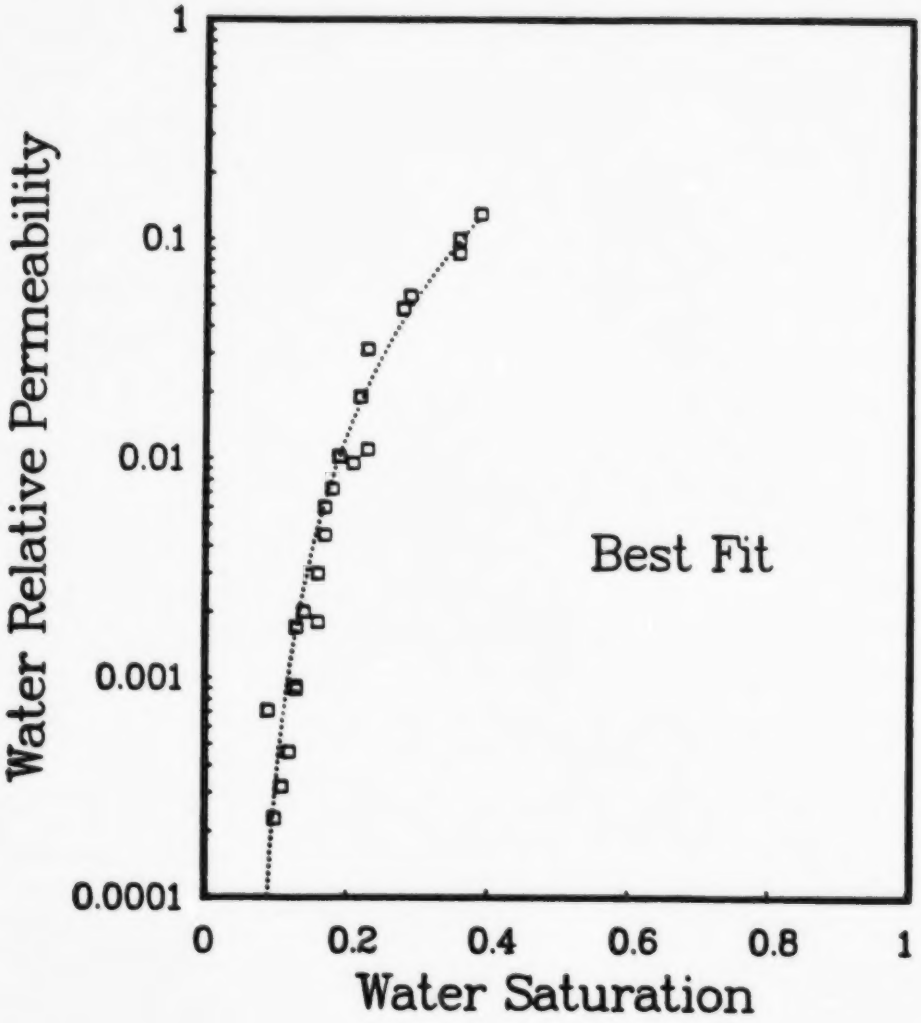

FIGURE 6

Three Phase Water Relative Permeability

New Experimental Data

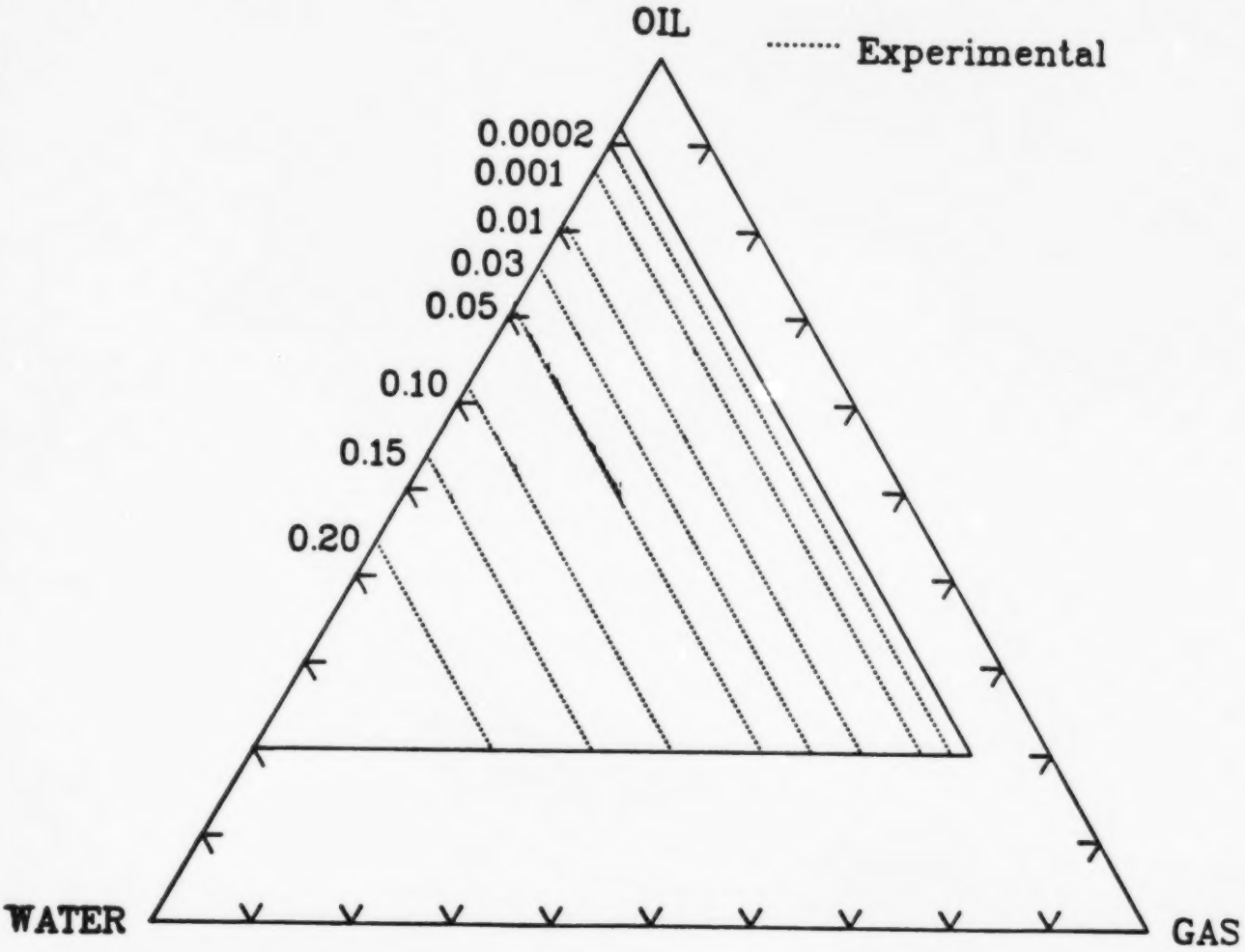

FIGURE 7

Three Phase Gas Relative Permeability

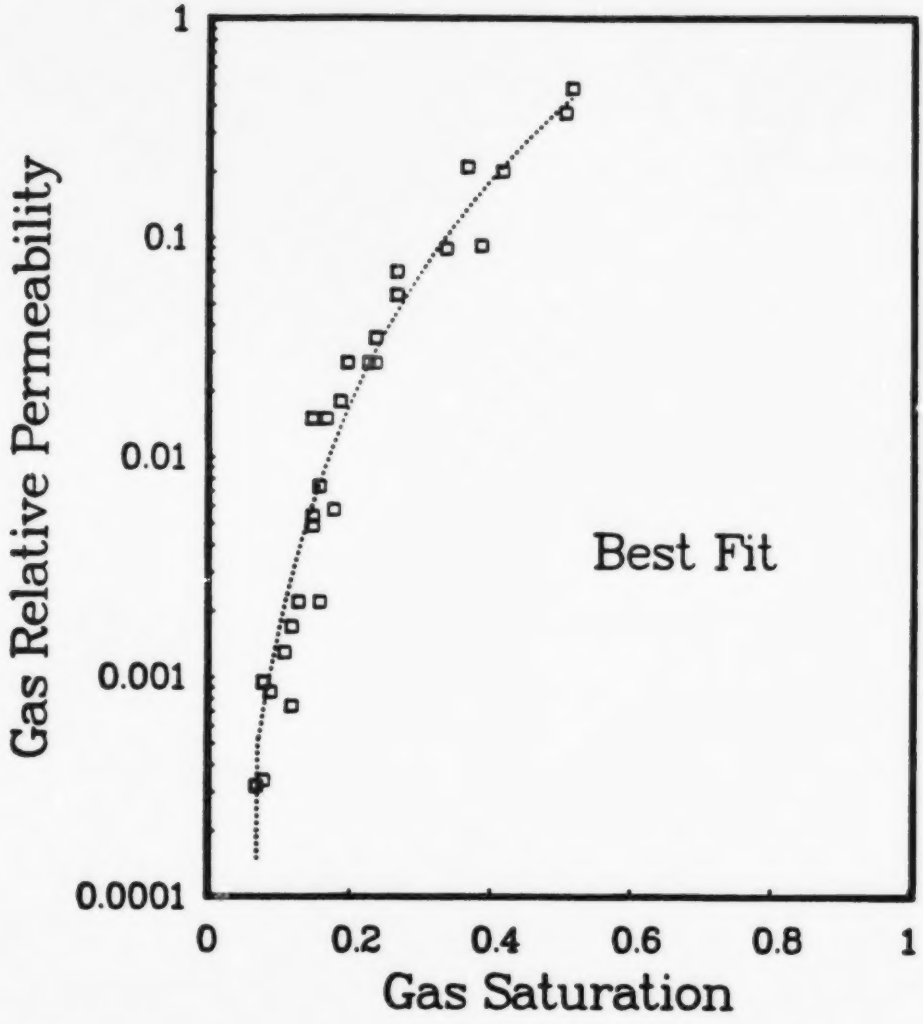

FIGURE 8

Three Phase Gas Relative Permeability

New Experimental Data

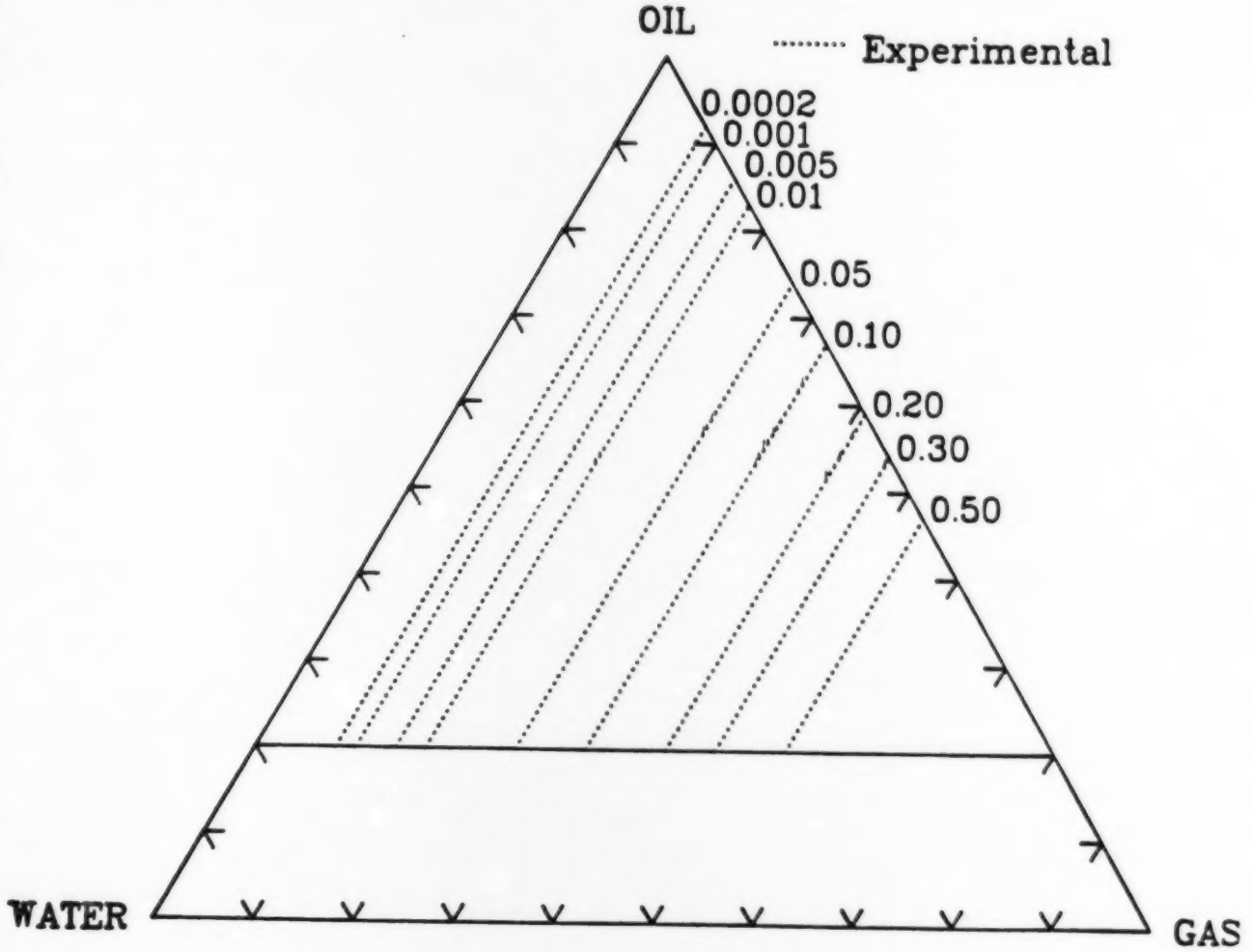

FIGURE 9

Three Phase Oil Relative Permeability

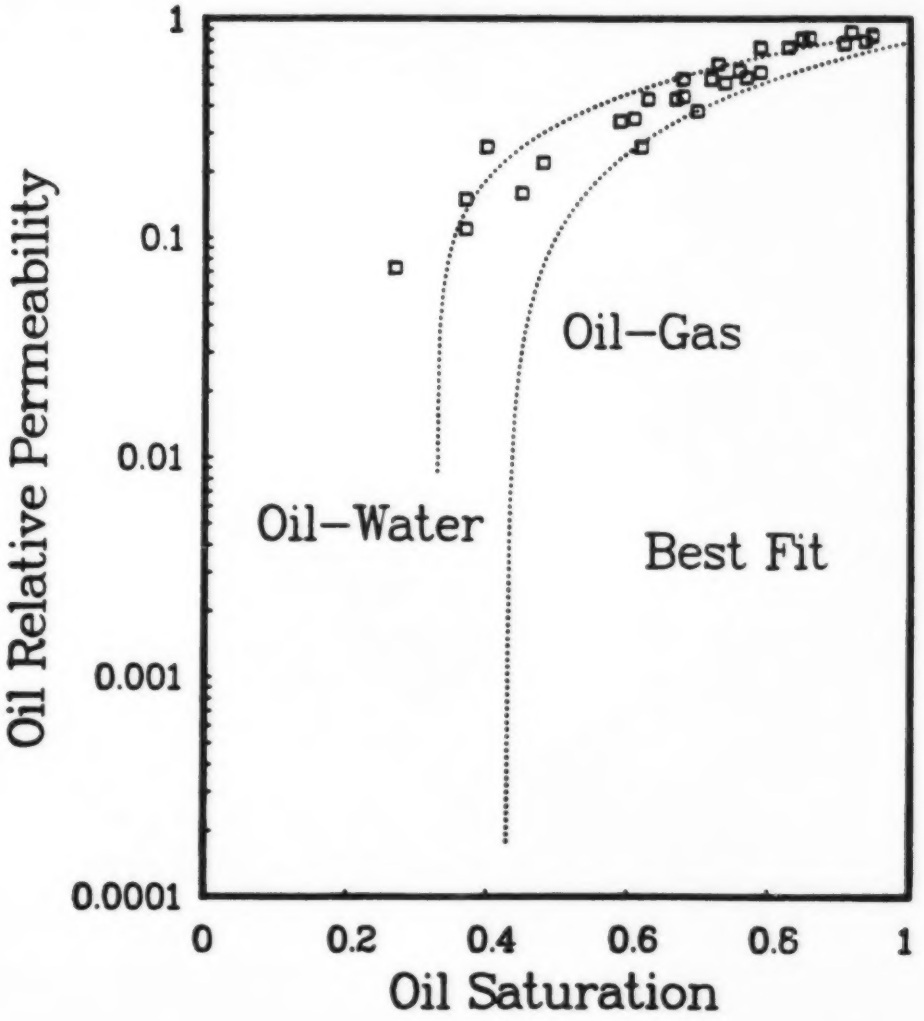

FIGURE 10

Three Phase Oil Relative Permeability

New Experimental Data

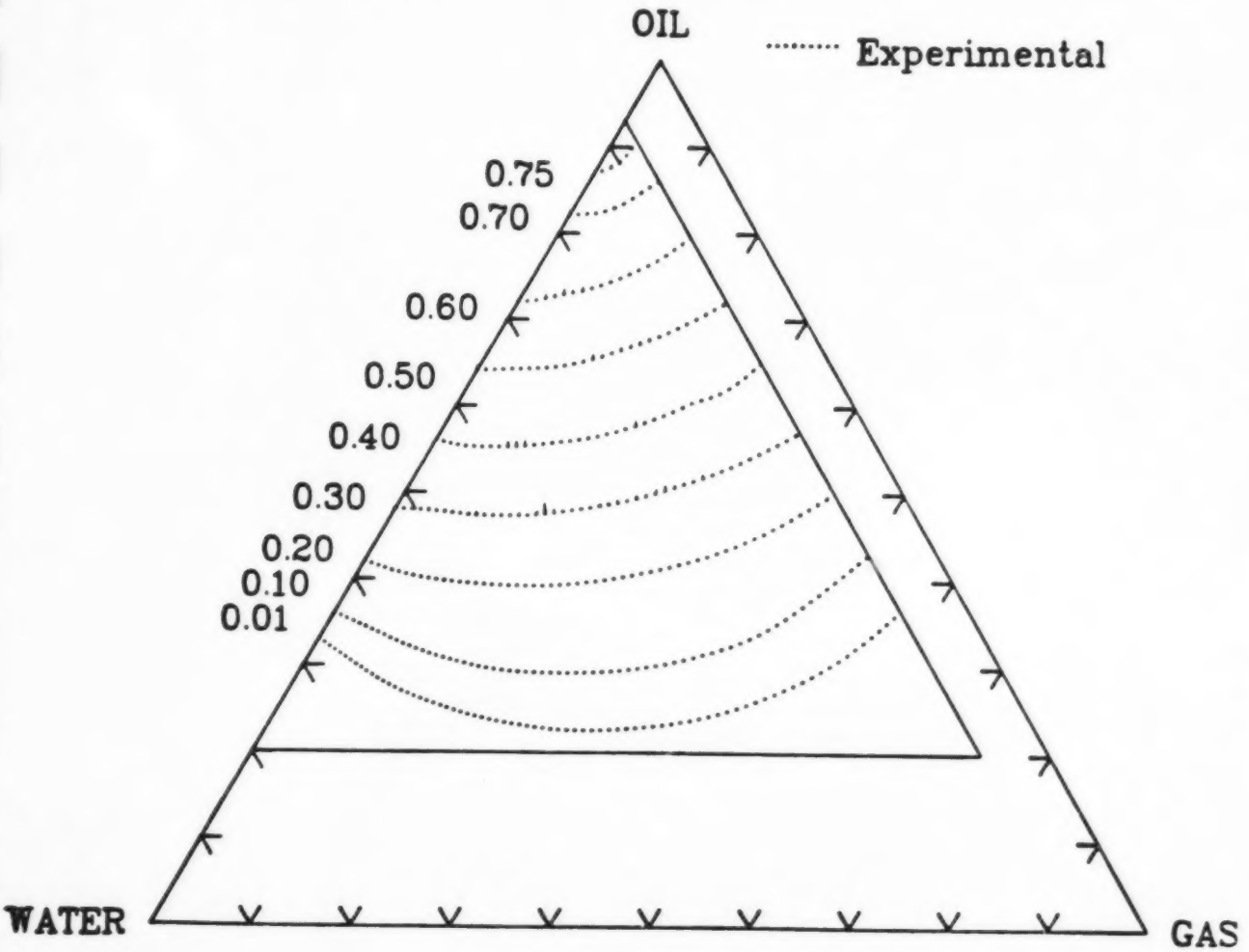

FIGURE 11

Three Phase Oil Relative Permeability
using Stone I model with
New Experimental Data

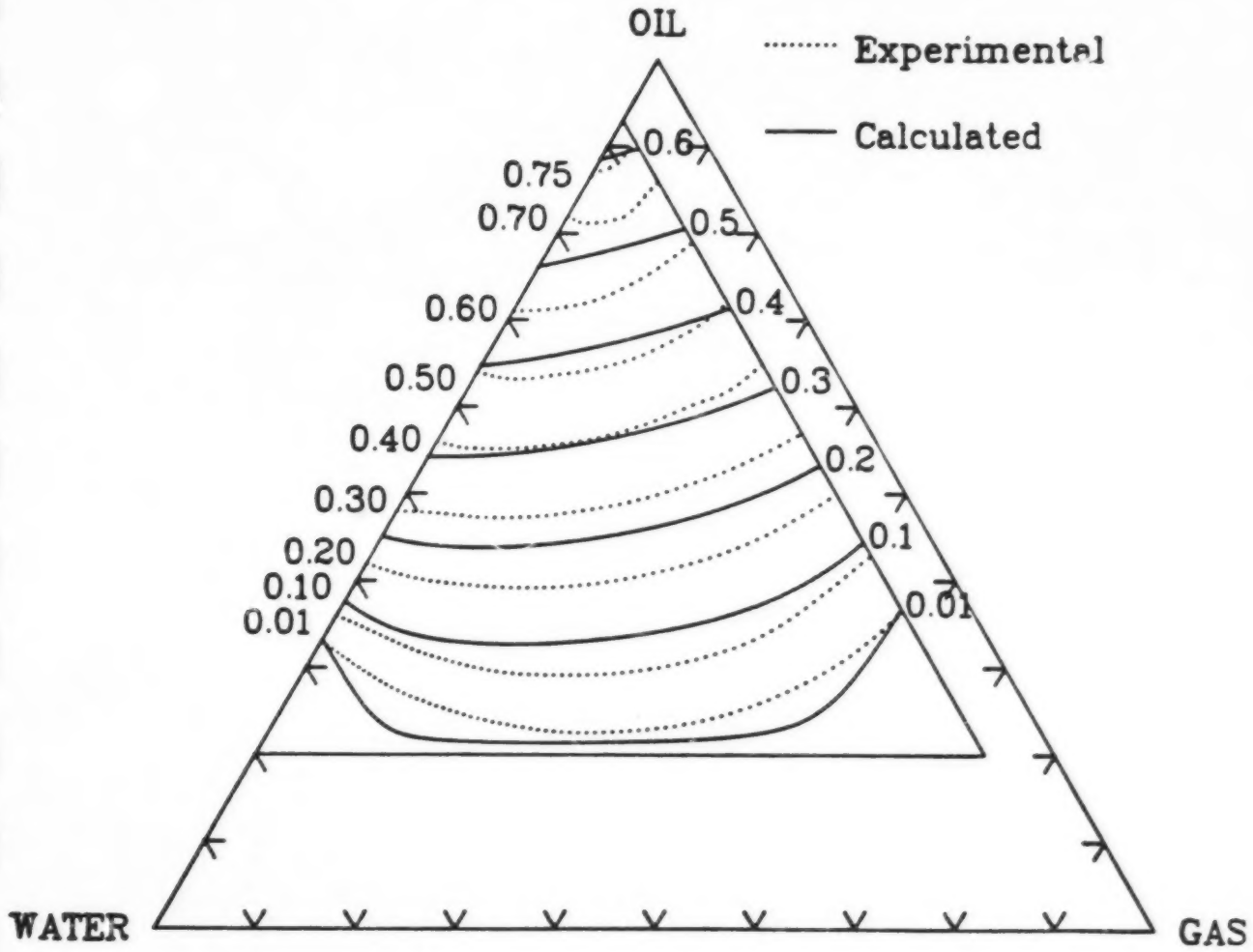

FIGURE 12

Three Phase Oil Relative Permeability
using Stone II model with
New Experimental Data

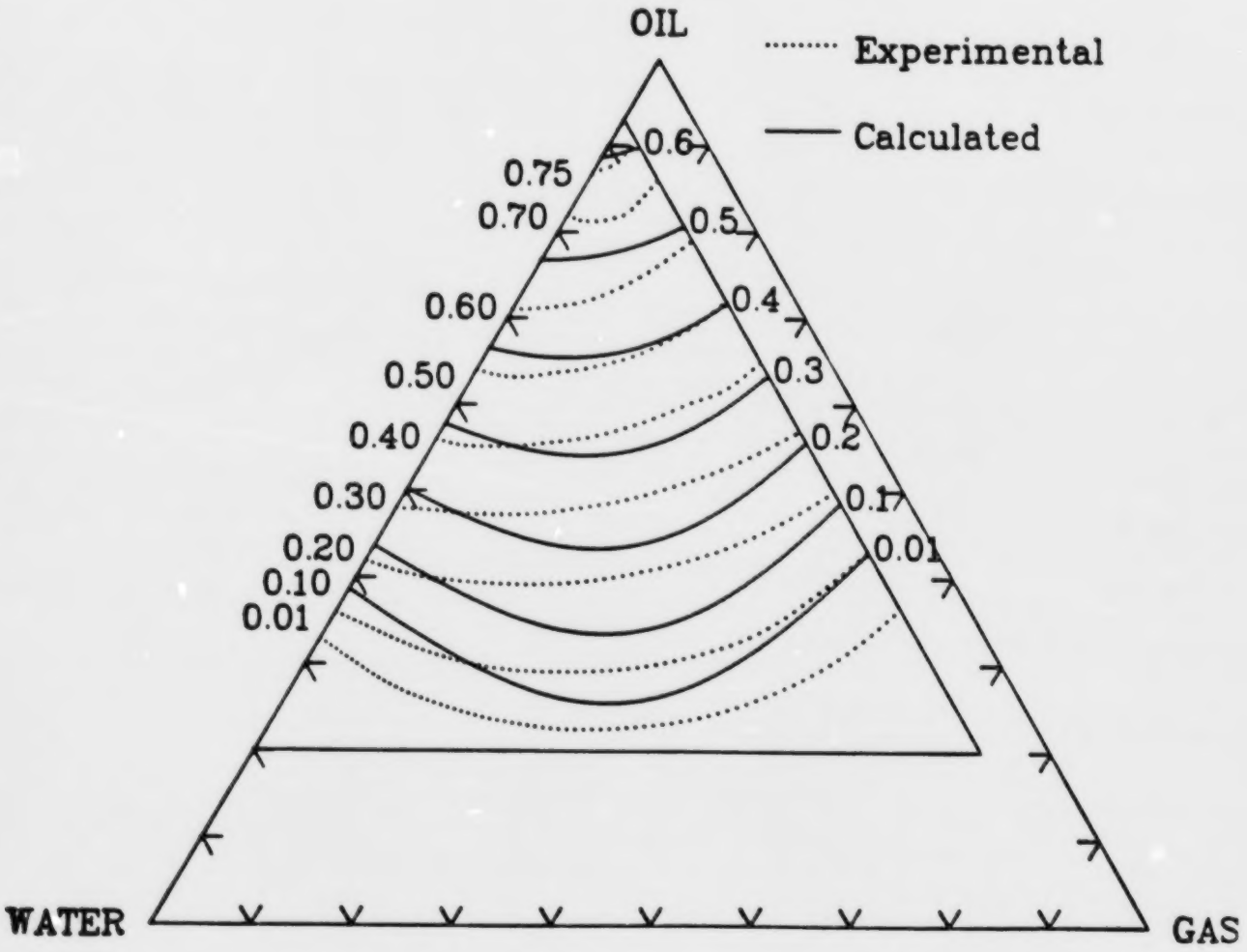

FIGURE 13

Three Phase Oil Relative Permeability
using Modified Stone I model with
New Experimental Data

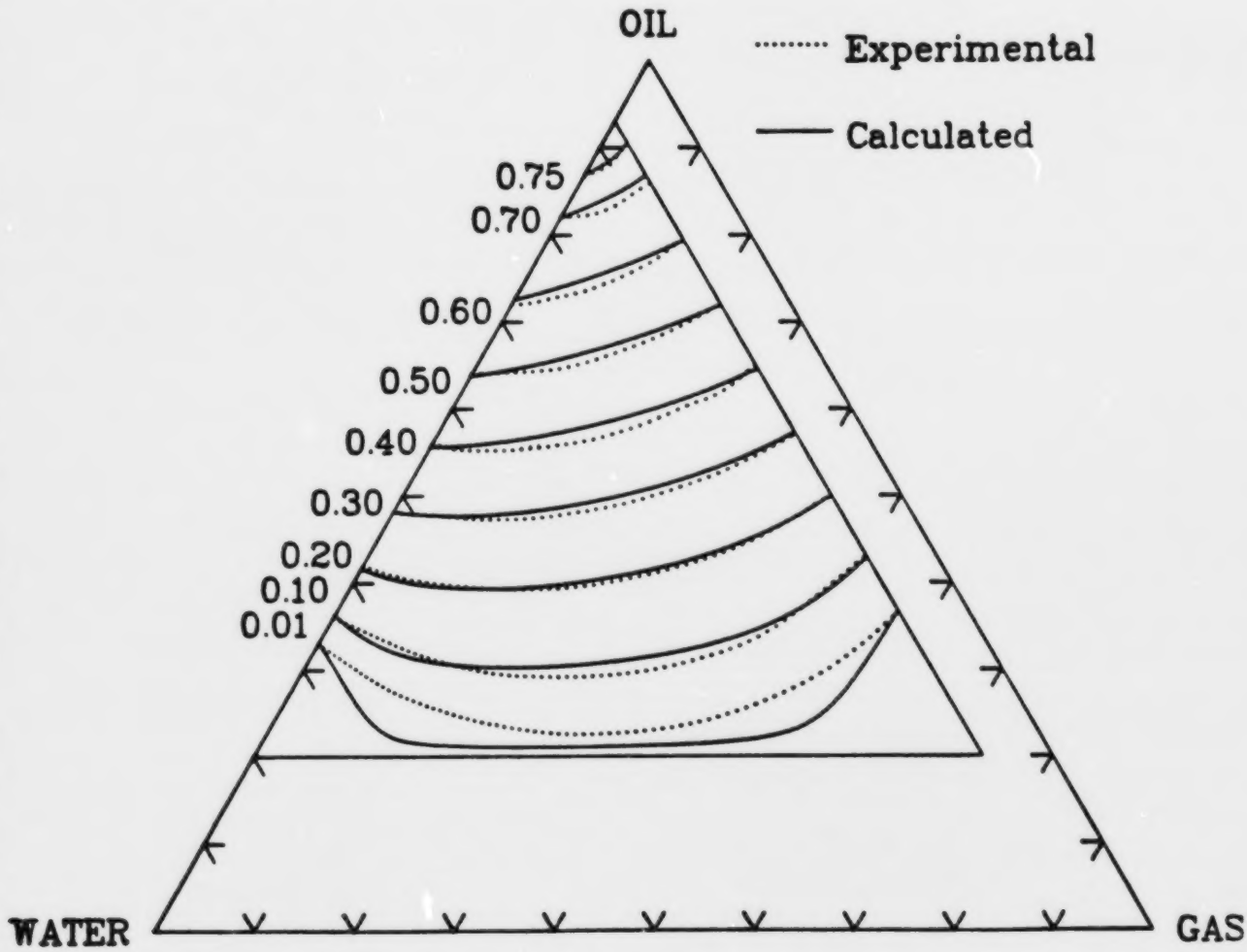

FIGURE 14

Three Phase Oil Relative Permeability
using Modified Stone I Model with
Data of Corey et al. (1956)

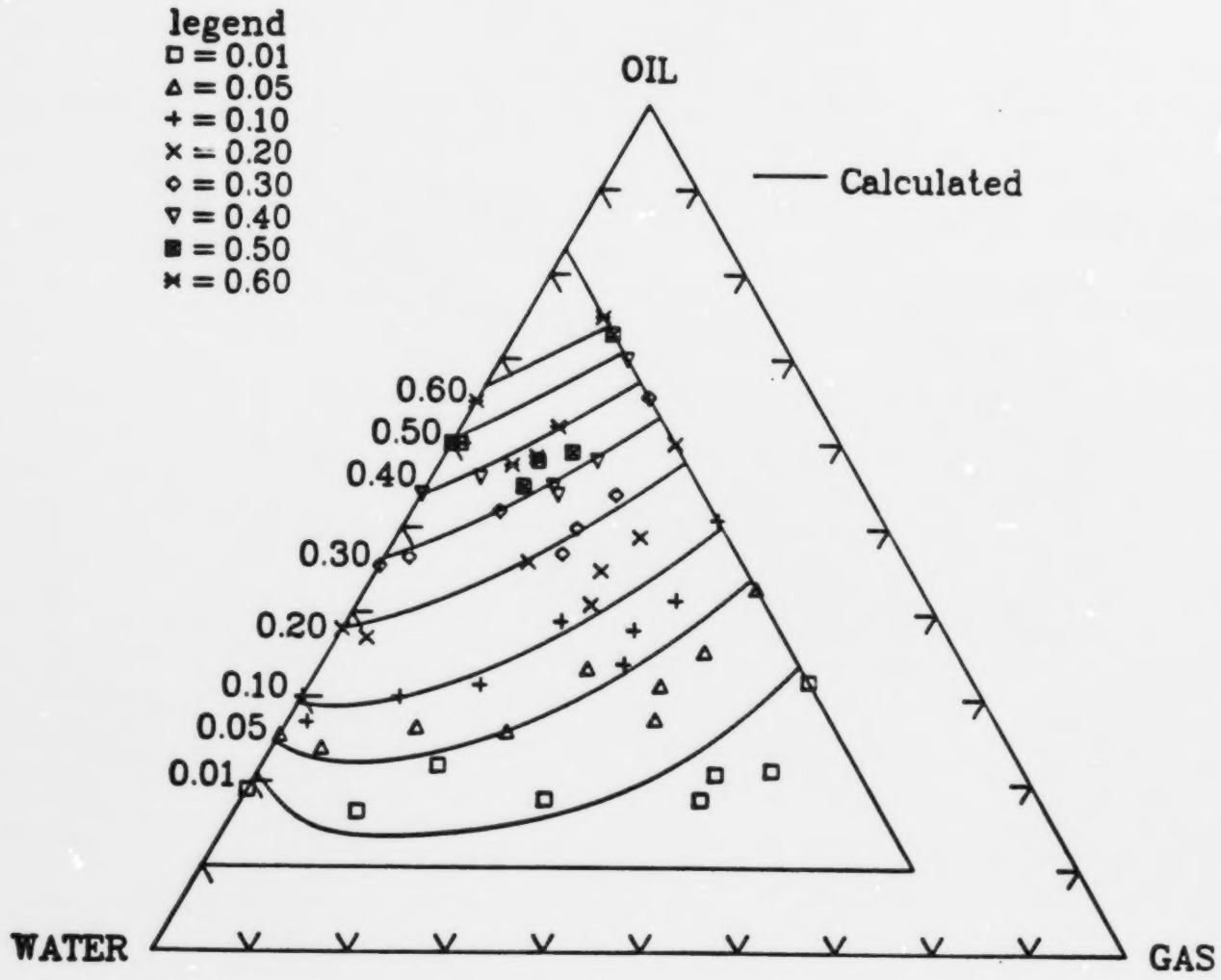

FIGURE 15

Three Phase Water Relative Permeability

Data of Corey et al. (1956)

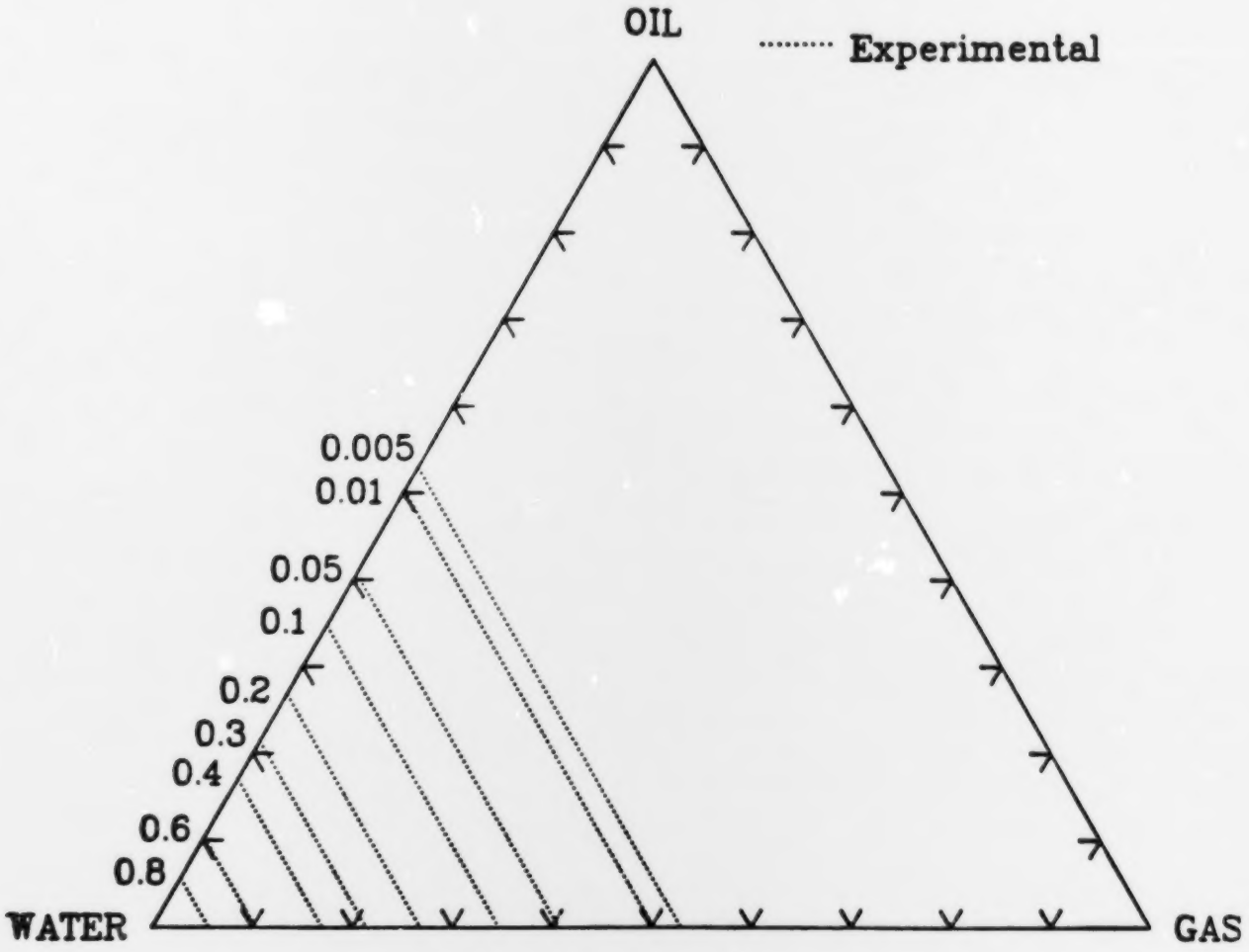

FIGURE 16

Three Phase Gas Relative Permeability

Data of Corey et al. (1956)

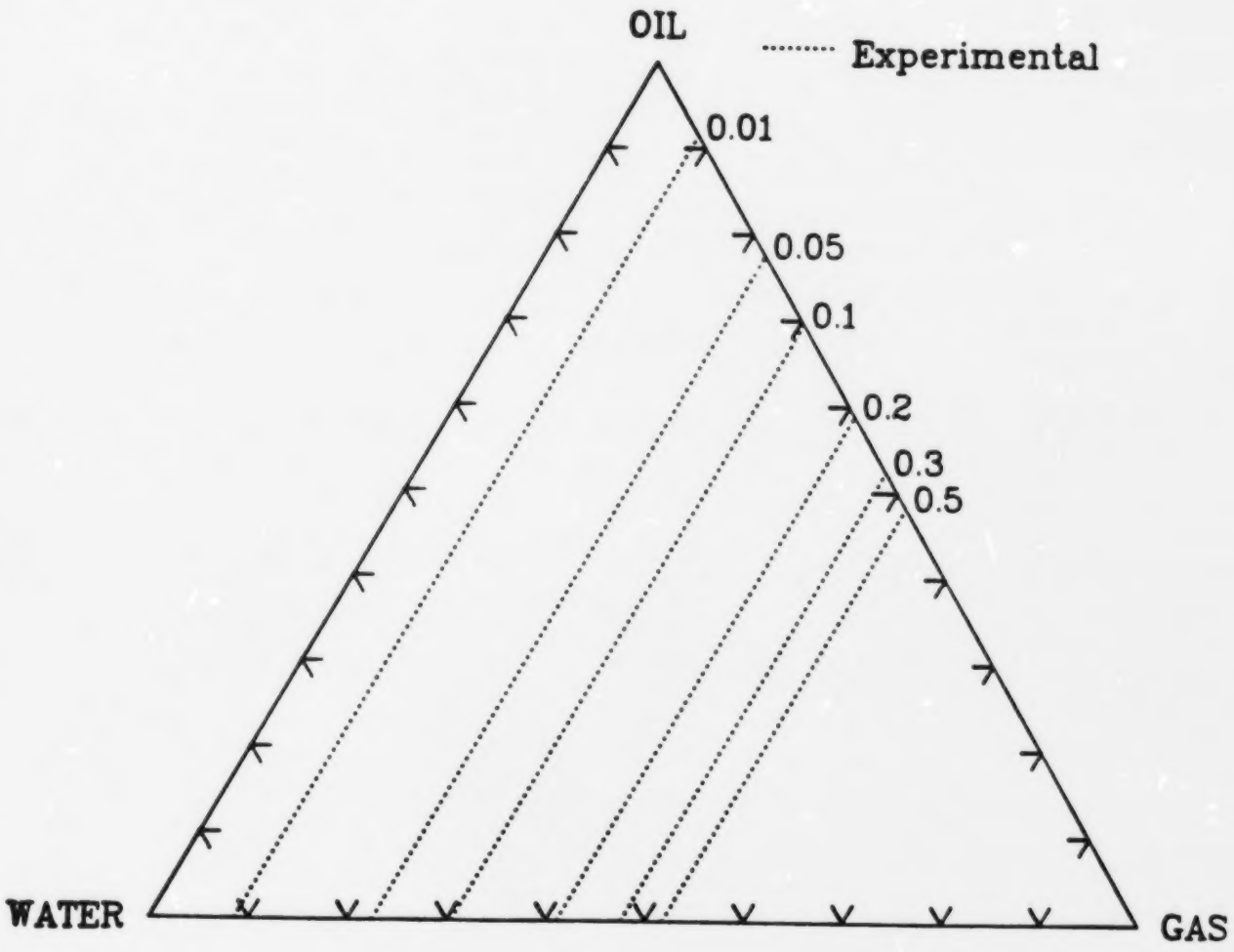

FIGURE 17

Three Phase Oil Relative Permeability
using Modified Stone I Model with
Data of Donaldson & Dean (1966)

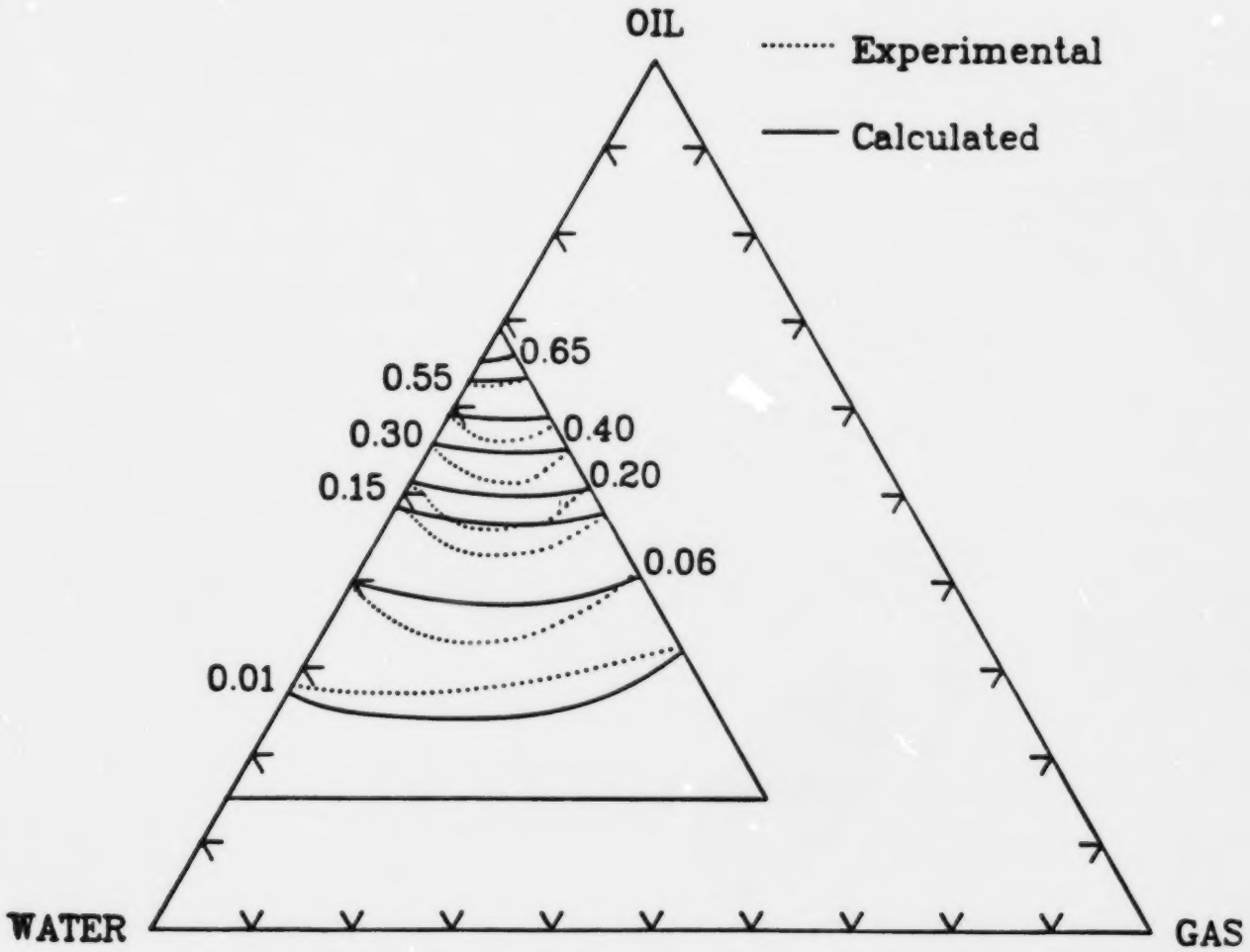

FIGURE 18

Three Phase Water Relative Permeability

Data of Donaldson & Dean (1966)

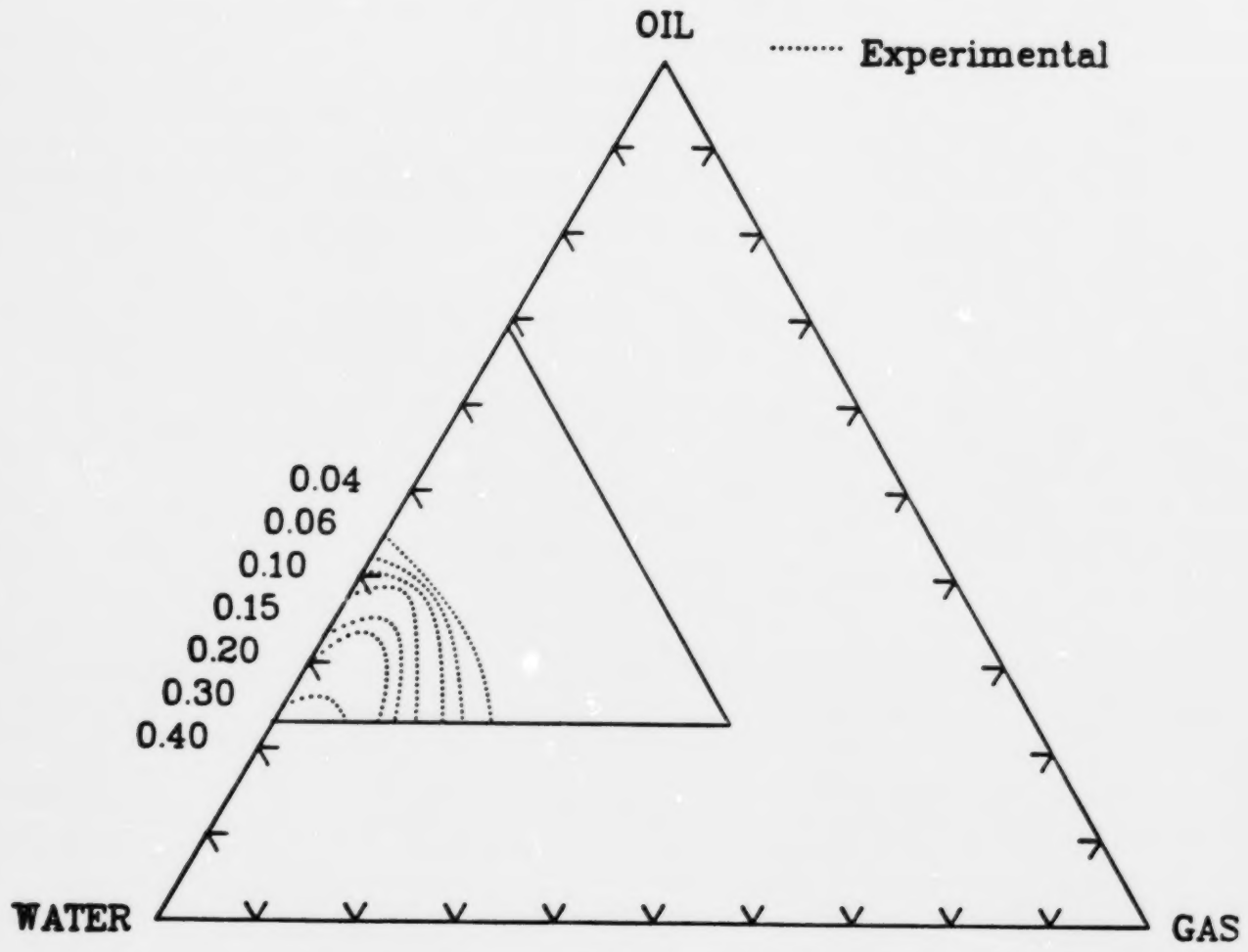

FIGURE 19

Three Phase Gas Relative Permeability

Data of Donaldson and Dean (1966)

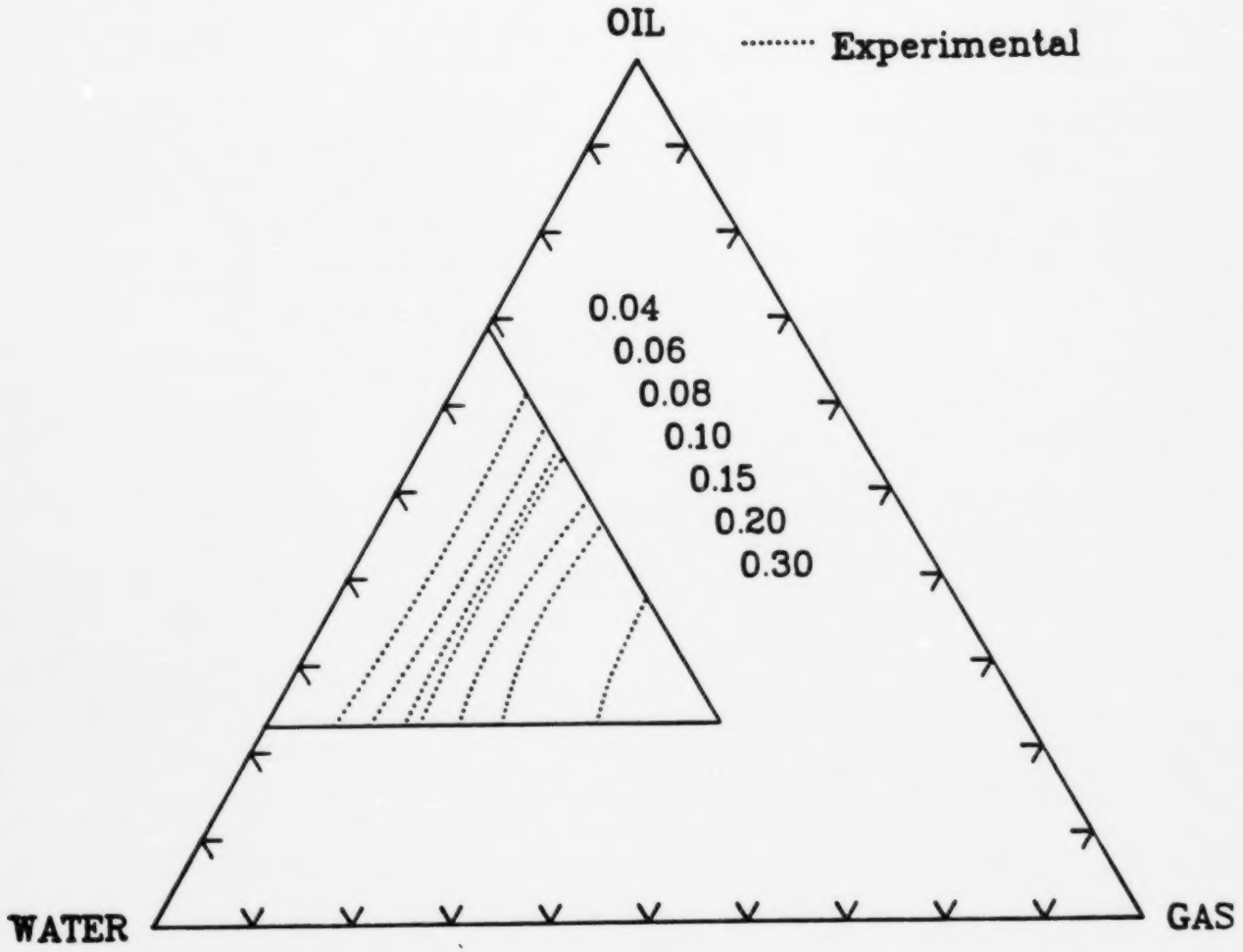

FIGURE 20

Three Phase Oil Relative Permeability
using Modified Stone I Model with
Data of Saraf and Fatt (1967)

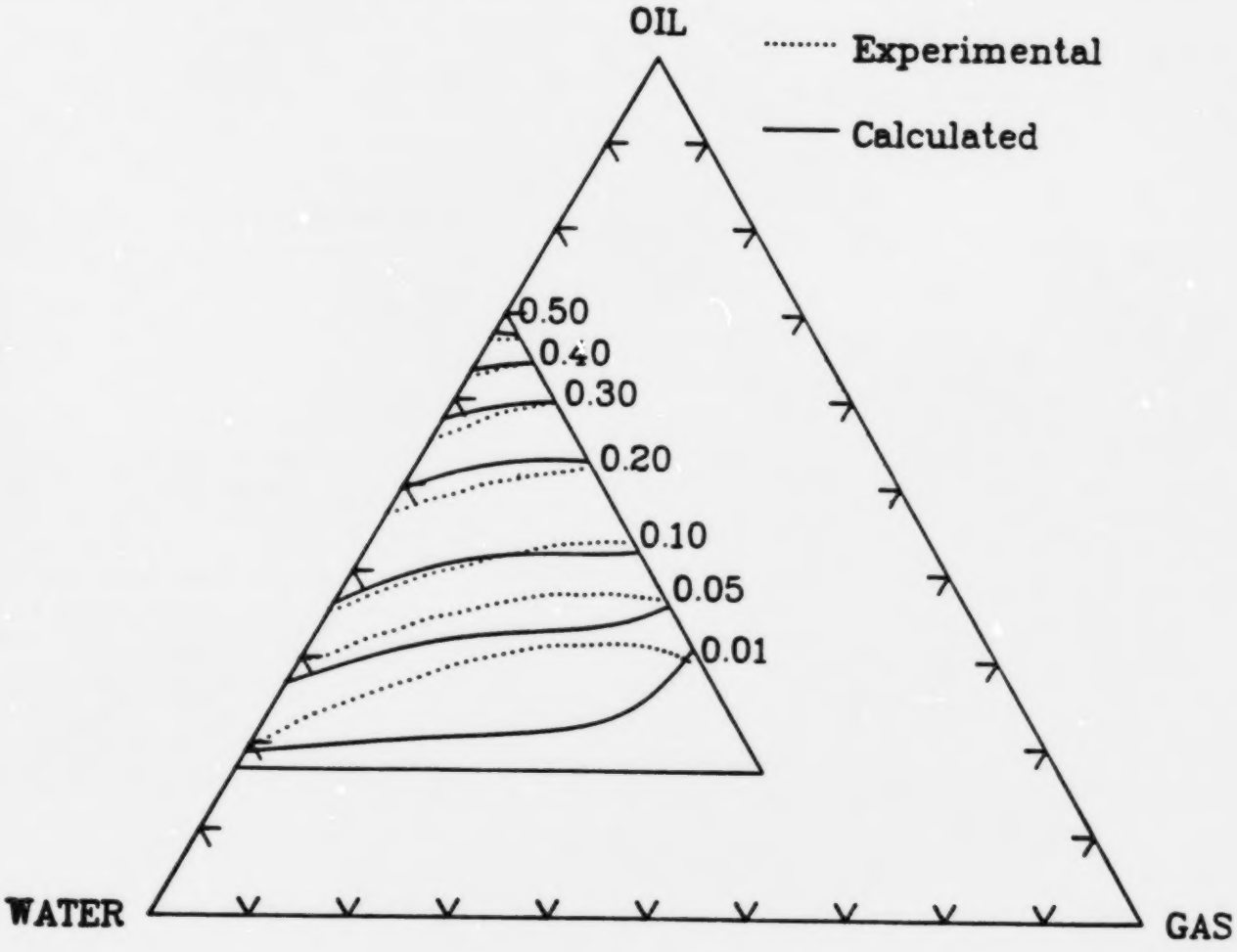

FIGURE 21

Three Phase Water Relative Permeability

Data of Saraf and Fatt (1967)

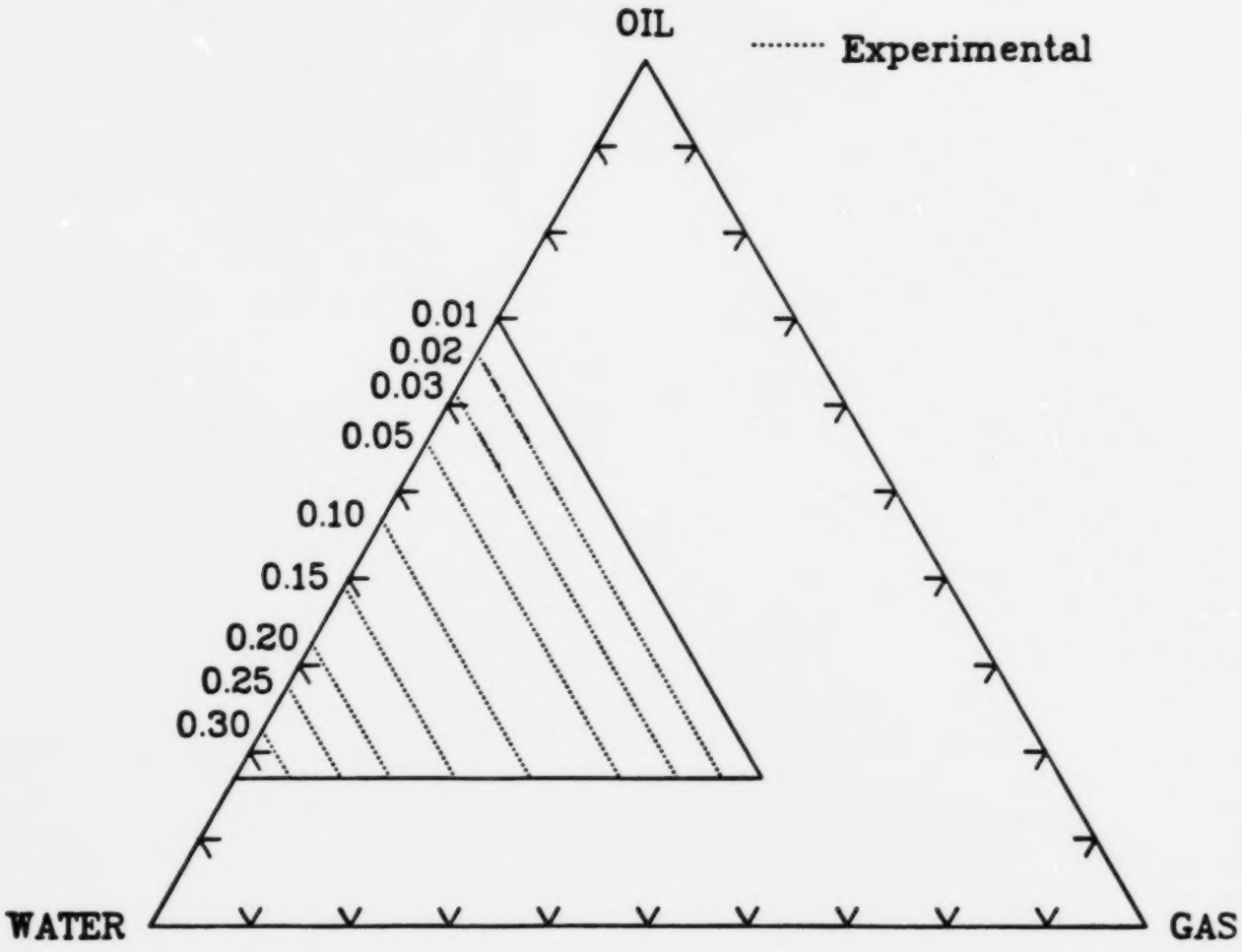

FIGURE 22

Three Phase Gas Relative Permeability

Data of Saraf and Fatt (1967)

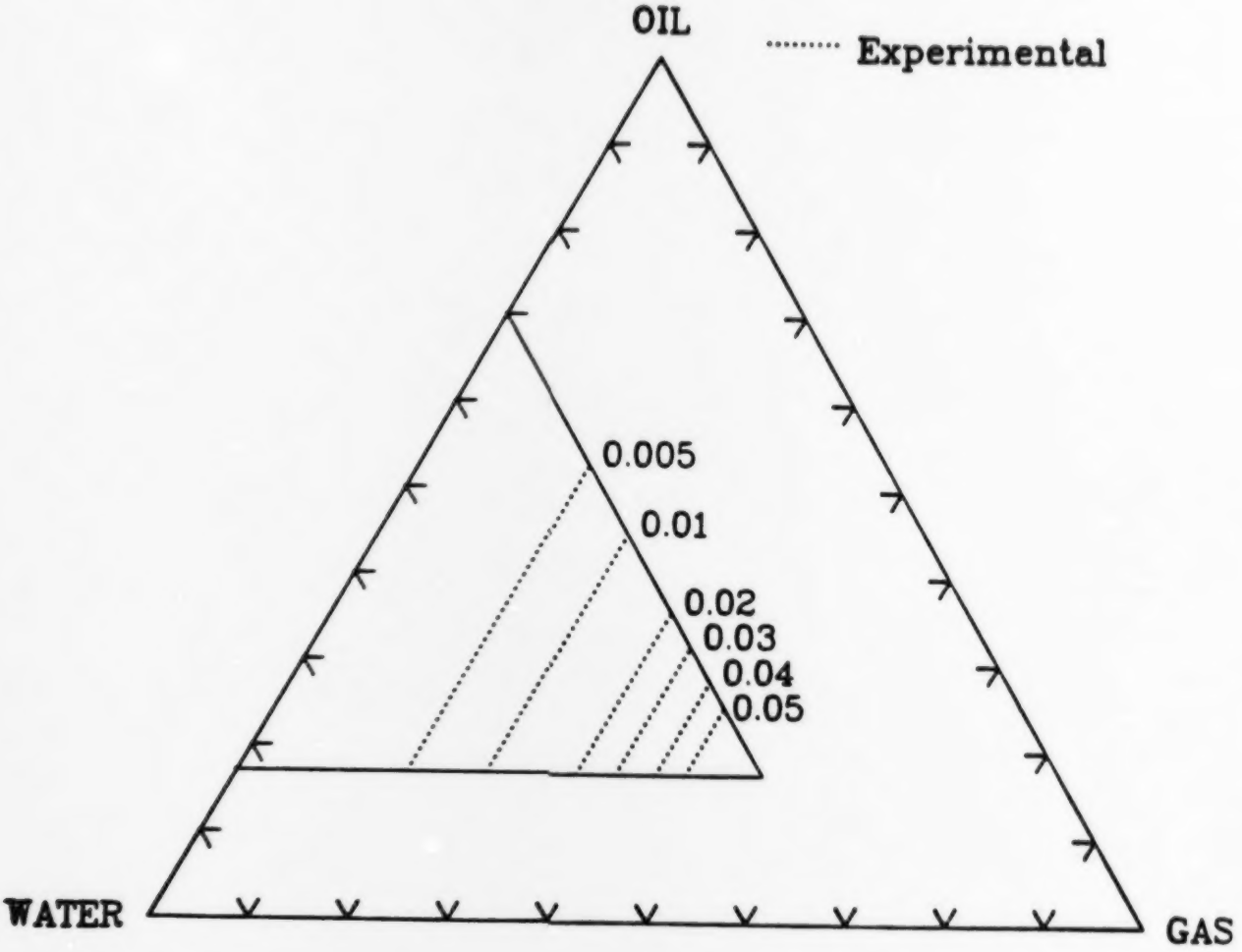

FIGURE 23

Three Phase Oil Relative Permeability
using Modified Stone I model with
Data of Dalton et al. (1970)

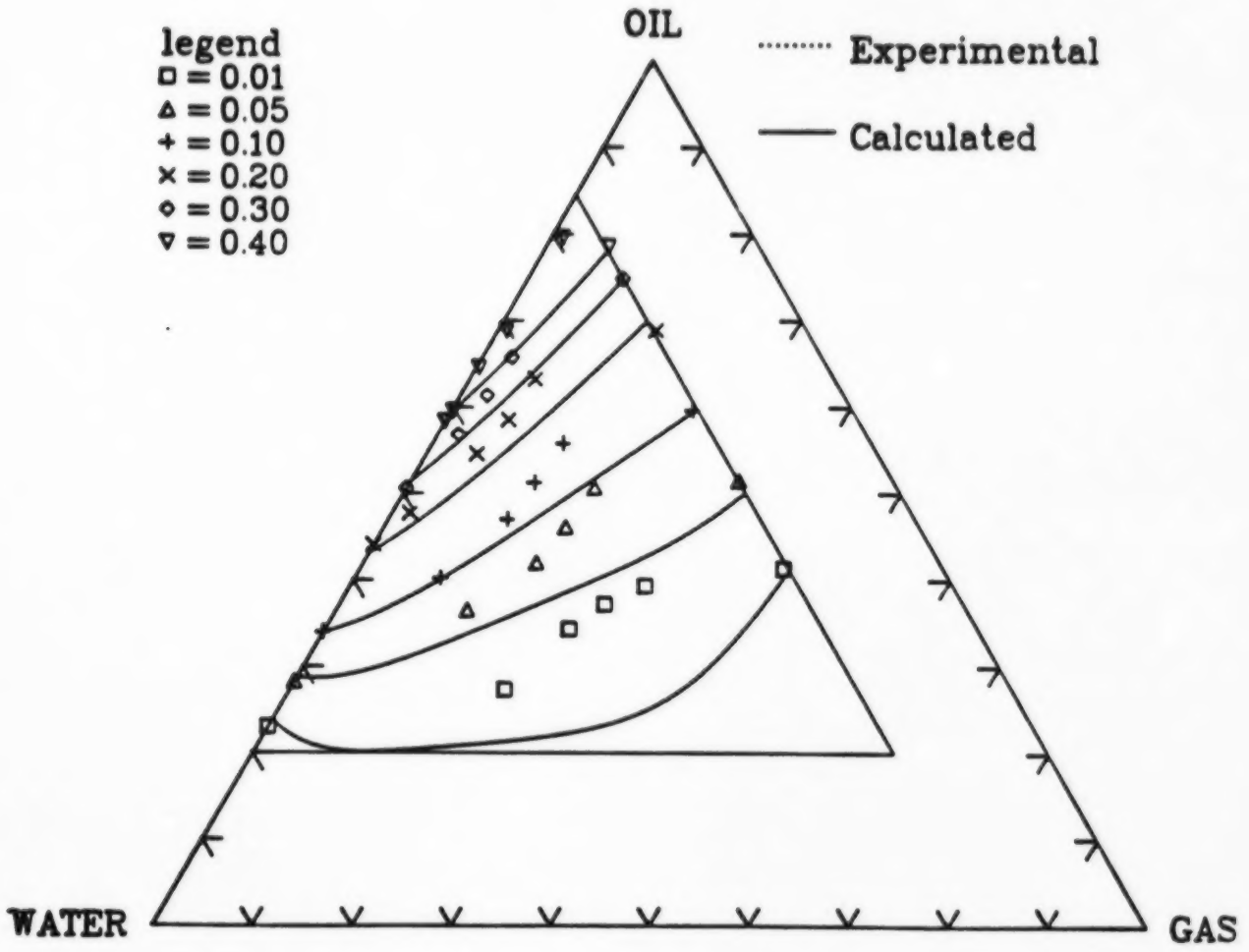

FIGURE 24

Three Phase Oil Relative Permeability
using Modified Stone I Model with
Data of Saraf et al. (1981)

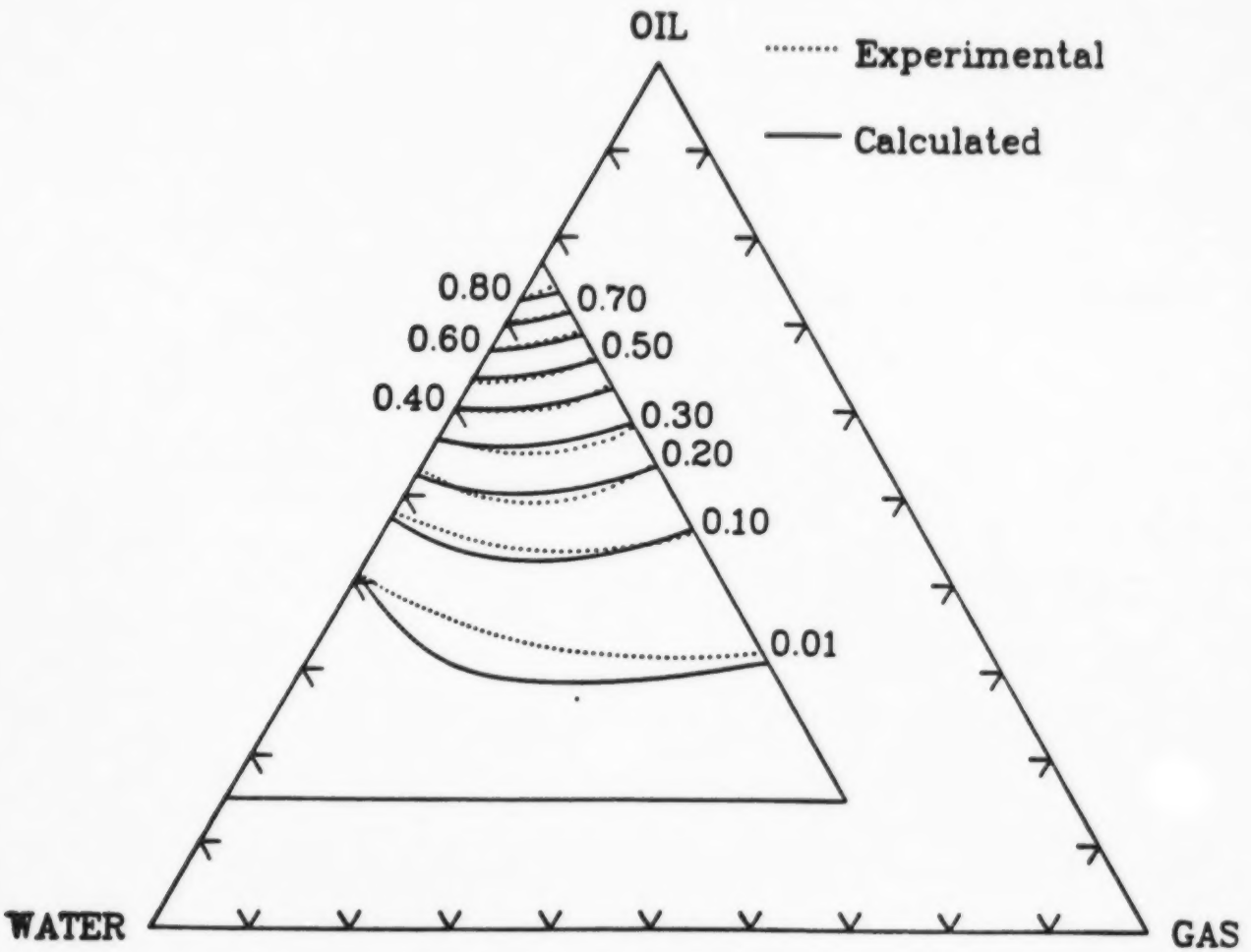

FIGURE 25

Three Phase Water Relative Permeability

Data of Saraf et al. (1982)

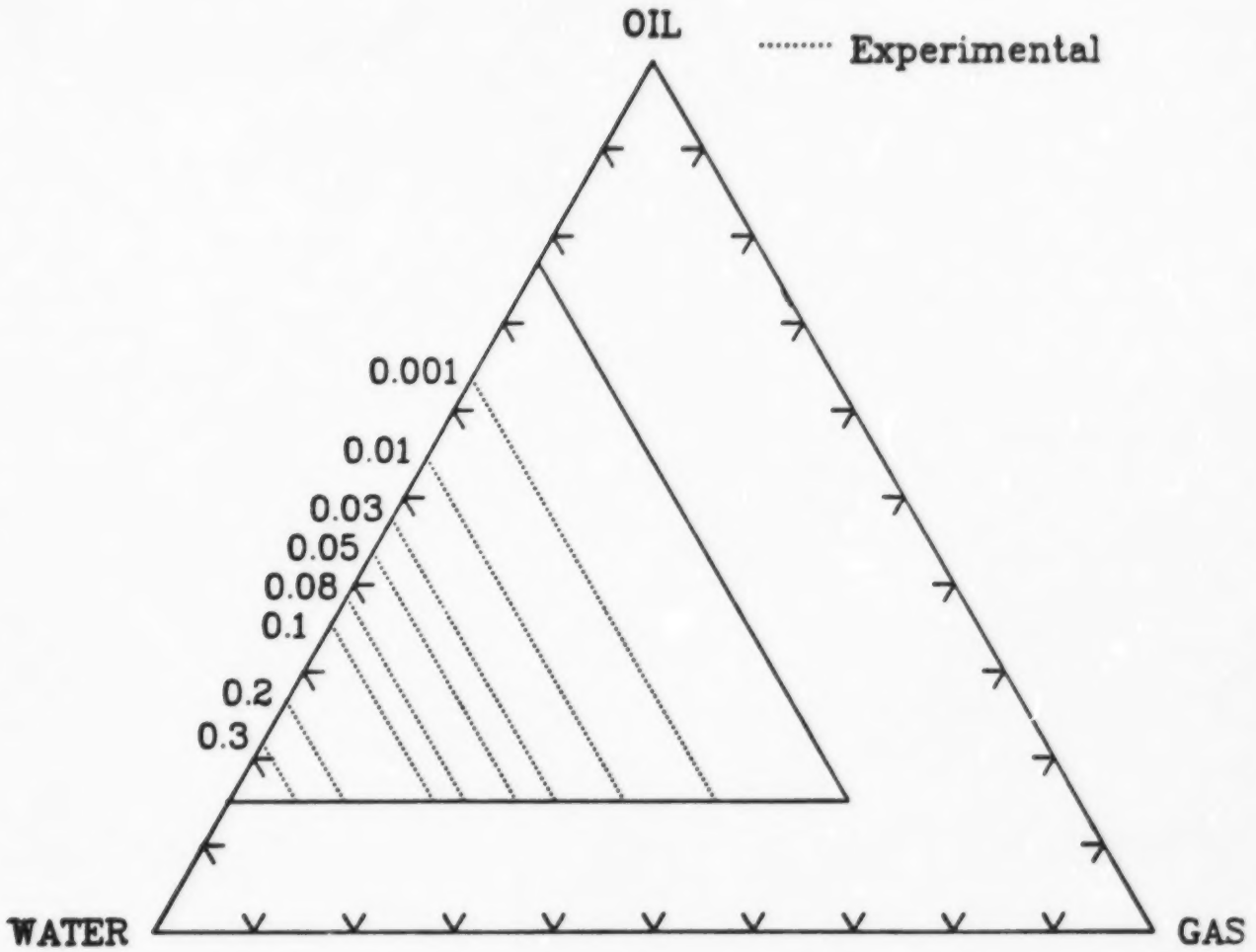

FIGURE 26

Three Phase Gas Relative Permeability

Data of Saraf et al. (1981)

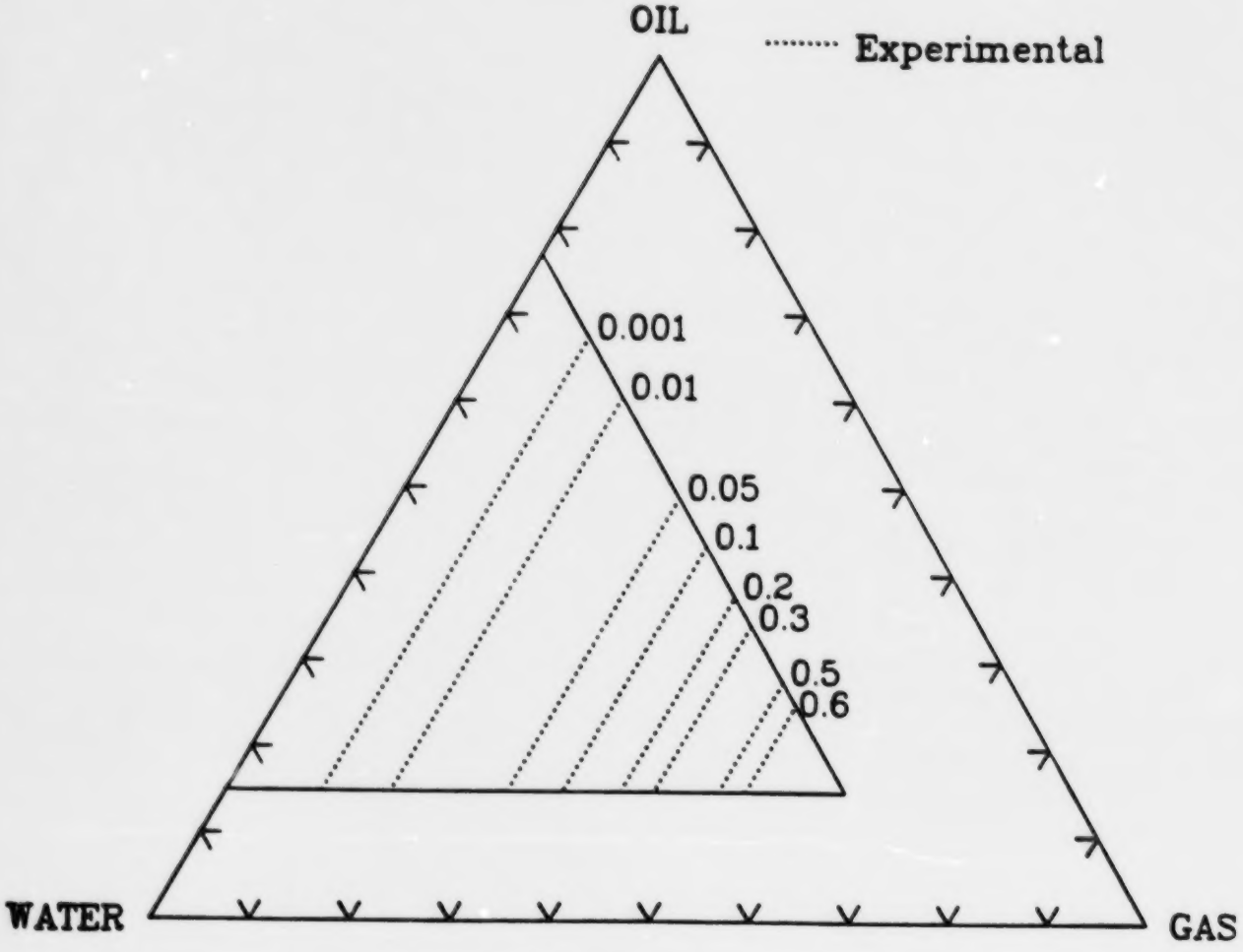

FIGURE 27

Three Phase Oil Relative Permeability
using Modified Stone I model with
Data of Oak et al. (1988)

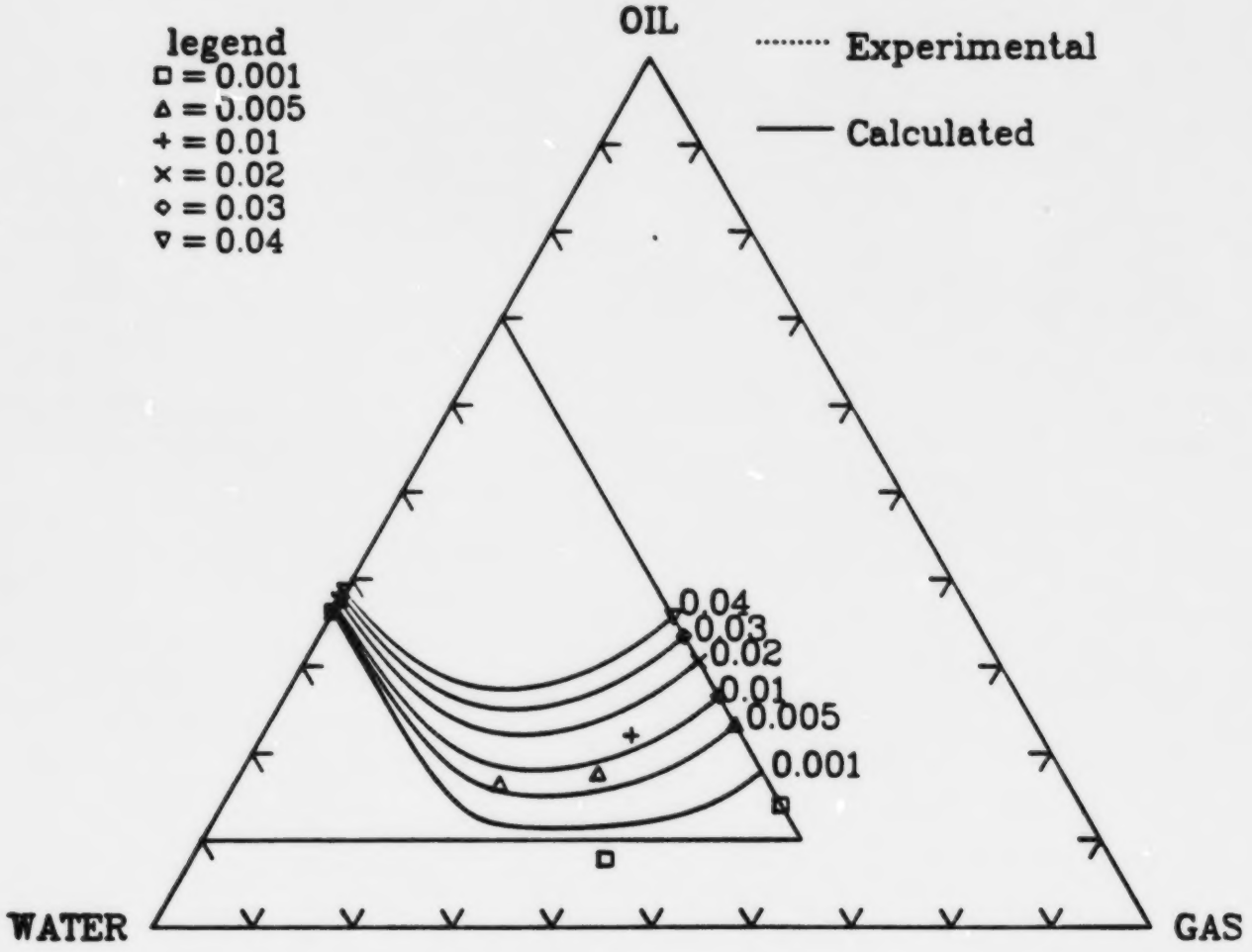

FIGURE 28

Three Phase Water Relative Permeability

Data of Oak et al. (1988)

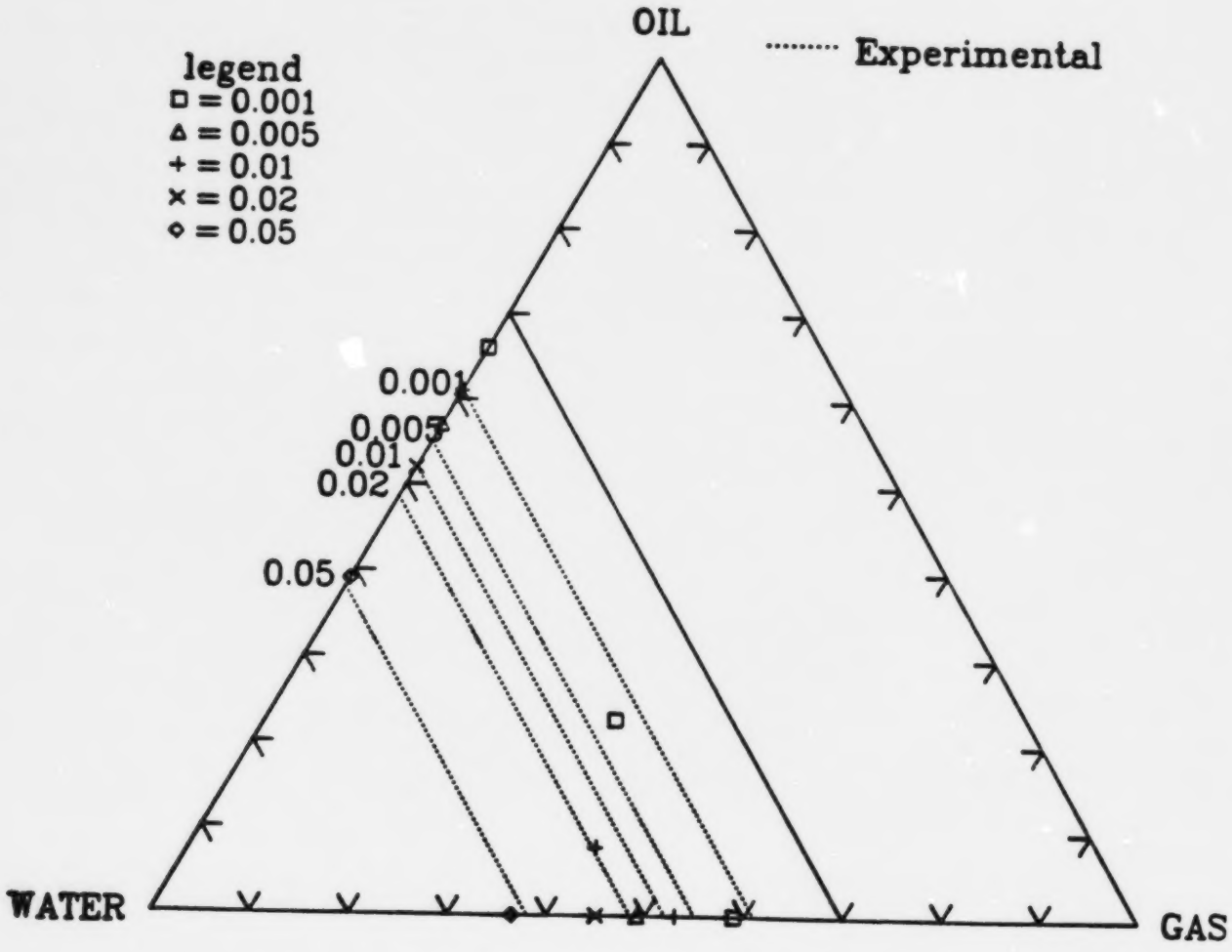

FIGURE 29

Three Phase Gas Relative Permeability

Data of Oak et al. (1988)

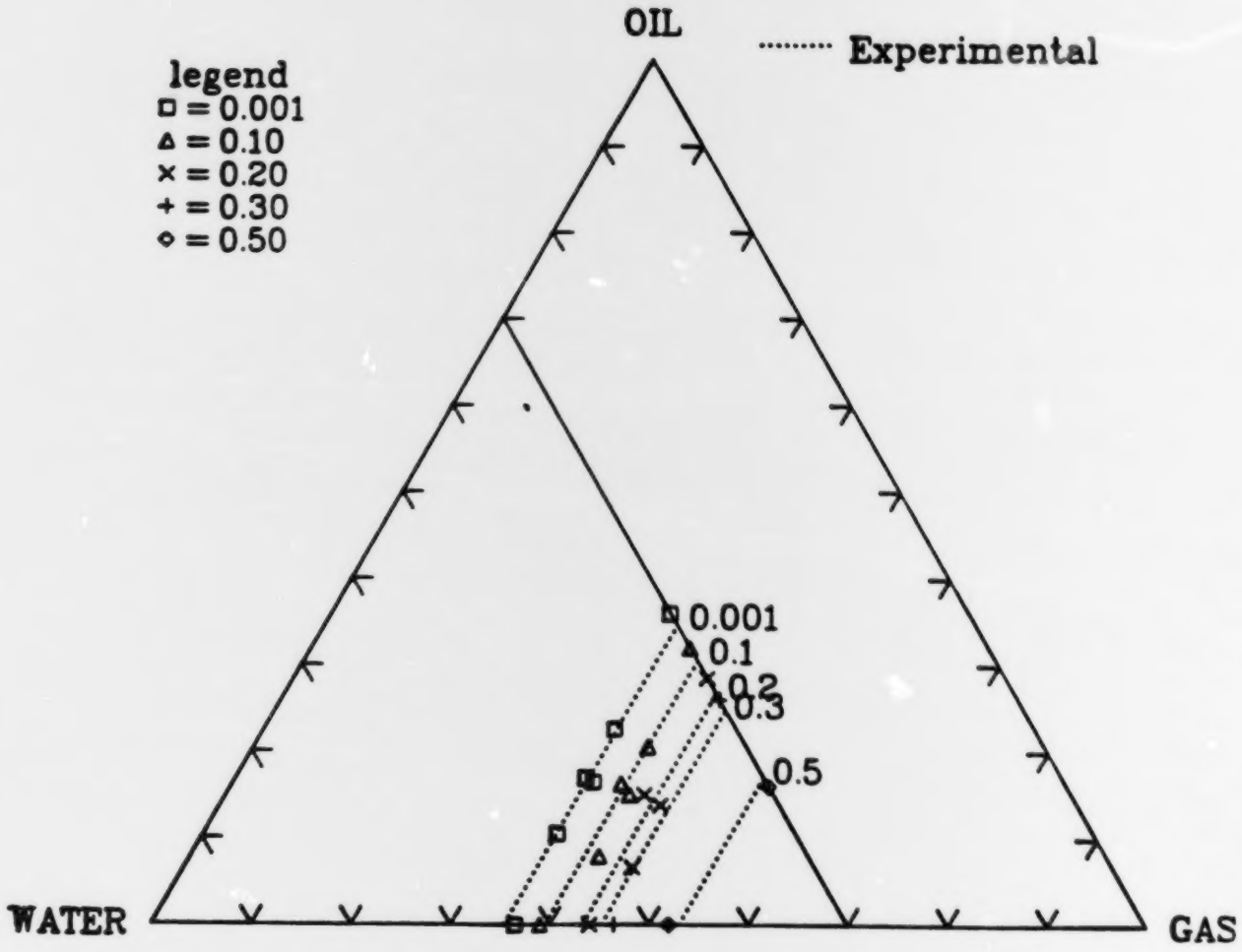

FIGURE 30